Characterizing the effect of menin early deletion in the osteoblast lineage using conditional knockout mice

By: Ildi Troka

Division of Experimental Medicine
McGill University, Montreal

May, 2018

A thesis submitted to McGill University in partial fulfillment of the requirements of the degree of Master of Science

TABLE OF CONTENTS

TABLE OF CONTENTS I

ABSTRACT IV

RÉSUMÉ VI

ACKNOWLEDGMENTS VIII

CONTRIBUTION OF AUTHORS IX

LIST OF FIGURES X

LIST OF TABLES XI

ABBREVIATIONS XII

CHAPTER 1: INTRODUCTION 1

1.1 Bone biology 2

1.1.1 Bone development 3

1.1.3 Bone composition 5

1.1.4 Bone cells 7

1.1.4.1 Mesenchymal stem cells 7

1.1.4.2 Osteoblasts 8

1.1.4.3 Osteoclasts 9

1.1.4.4 Osteocytes 9

1.2 Mechanisms of bone formation 10

1.2.1 Osteoblast differentiation 10

1.2.2 Osteoclast differentiation 11

1.2.3 Bone mineralization 12

1.3 Bone modeling & remodeling 13

1.3.1 Bone disorders 15

1.3.2 Osteoporosis and treatments 16

1.4 Role of bone in whole-body homeostasis 18

1.5 Regulatory pathways of osteoblast differentiation 20

1.5.1 Wnt/β-catenin signaling in bone 20

1.5.1.1 Regulators of the Wnt/*β*-catenin signaling 22

1.5.2 TGF-β and BMP signaling in bone....22
1.5.2.1 TGF-β signalling in osteoblasts....23
1.5.2.2 BMP signalling in osteoblasts....24
1.5.2.3 Regulators of TGF-β/BMP signaling....24
1.6 Multiple Endocrine Neoplasia Type-1 (MEN1) & menin....25
1.7 Cellular functions of menin....27
1.8 Menin interacting partners & functions....28
1.8.1 AP-1 transcription factor....28
1.8.2 MLL complex....28
1.8.3 β-catenin....29
1.8.4 TGF-β superfamily....29
1.8.5 Menin and other protein partners....30
1.9 Role of menin in myogenesis & adipogenesis....31
1.10 Functions of menin in bone homeostasis....33
1.10.1 Menin & TGF-β/BMP signaling in bone....34
1.10.2 Menin & JunD in osteoblastogenesis....36
1.10.3 Menin & β-catenin in osteoblastogenesis....36
1.10.4 Animal studies of menin and bone....37
1.10.5 Role of menin in mature osteoblast *in vivo*....39
1.10.6 Role of menin in osteoprogenitors *in vivo*....42
CHAPTER 2: RATIONALE AND OBJECTIVES....45
CHAPTER 3: MATERIALS & METHODS....48
3.1 Mice breeding....49
3.2 Animals....49
3.3 Genotyping....50
3.4 Primary calvarial osteoblast isolation....51
3.5 Bone marrow stromal cell isolation....52
3.6 RNA isolation, RT-qPCR....53
3.7 Differentiation and mineralization assays of primary cell cultures....56
3.8 Methyl Thiazolyl Tetrazolium (MTT) viability assay:....57
3.9 3D Collagen scaffolds preparation....57
3.10 Alamar blue assay....58
3.11 Scanning Electron Microscopy (SEM)....59

3.12 Fourier Transform Infrared Spectroscopy (FTIR) 59
3.13 Energy-Dispersive X-ray spectroscopy (EDS) 60
3.14 Forelimb grip strength test 60
3.15 Three-point bending test 61
3.16 Echo-MRI 61
3.17 Tissue Analysis 62
3.18 Statistical analysis 62

CHAPTER 4: RESULTS 63

4.1 Deletion of the *Men1* gene is specific to bone 64
4.2 Mice deficient for menin early in the osteoblast lineage have a reduced body size and show differences in whole body composition 64
4.3 Menin deletion in mesenchyme-derived progenitor cells alters brown adipose tissue activity 70
4.4 *Men1* knockout mice demonstrate altered forelimb grip strength abilities. 73
4.5 Reduced femur length & bone strength are observed in *Men1* knockout femurs. 76
4.6 Primary calvarial osteoblasts and BMSCs of the earlier menin knockout mice models demonstrate no changes in proliferation. 78
4.7 *In vitro* analysis of primary calvarial osteoblasts and BMSCs of *Men1* knockout mice shows altered mineralization capabilities but no change in alkaline phosphatase intensity. 80
4.8 Disruption of the *Men1* gene early in the osteoblast lineage alters the *RANKL/OPG* ratio *in vitro*. 84
4.9 Osteoblast-specific early deletion of the *Men1* gene results in the increase of the *RANKL/OPG* ratio from bone RNA favoring osteoclastogenesis. 87
4.10 Primary calvarial osteoblasts of the early *Men1* knockout mice seeded within dense collagen gels show defective mineralization mediated processes. 90

CHAPTER 5: DISCUSSION 96

5.1 General discussion 97
5.2 Future work and perspectives 114
5.3 Conclusion 118

REFERENCES 119

ABSTRACT

Menin, the product of the Multiple Endocrine Neoplasia Type 1 (*MEN1*) gene, is a widely expressed, predominantly nuclear protein that facilitates cell proliferation and differentiation control. In osteoblasts, menin has been shown to modulate osteoblast differentiation, an essential process for bone homeostasis. Our laboratory has initially established *in vivo* the importance of menin for proper functioning of the mature osteoblast and maintenance of bone mass in adult mice. In the current study, we seek to better understand the role that menin plays *in vivo* when expressed at earlier stages of the osteoblast lineage. To achieve this, conditional knockout mice in which the *Men1* gene is specifically deleted early in the osteoblast lineage were generated by using the Cre-LoxP recombination system. *Prx1-Cre; Men1f/f* and *Osx-Cre; Men1f/f* mice represent knockout of the *Men1* gene at the level of the pluripotent mesenchymal stem cell and preosteoblast, respectively. Proceeding with the gross phenotypic characterization, the bodyweights of knockout mice were decreased in comparison to control *Men1f/f* mice. Adult animals between 10-14 month-old from both knockout strains revealed changes in fat and lean mass content. Brown adipose tissue activity was also affected, with the relative expression of *Ucp1* being significantly higher in *Prx1-Cre; Men1f/f* mice. By 3-dimensional micro-computed tomography imaging of the femur, both strains of *Men1* knockout mice had decreased trabecular bone volume with altered trabecular structure. Bone mass and femur length were also significantly reduced in both knockout mice models. Three-point bending test showed a reduction in femur strength and stiffness in knockout animals. The forelimb grip strength of *Prx1-Cre; Men1f/f* mice was reduced and that of *Osx-Cre; Men1f/f* increased in comparison to wild-type mice. Proliferative capabilities of calvarial osteoblasts and bone marrow stromal cells (BMSCs) of *Prx1-Cre; Men1f/f* and *Osx-Cre; Men1f/f* animals were unaltered. Mineralization capabilities of primary calvarial osteoblasts in the knockout mice were however deficient relative to those of wild-type mice as assessed by alizarin red staining. The gene expression profiles of primary calvarial osteoblasts and BMSCs of *Prx1-Cre; Men1f/f* mice were also altered. Culturing primary calvarial osteoblasts via a new method using dense collagen gels, which better mimic the physiological bone microenvironment, revealed defective mineralization capabilities in *Prx1-Cre; Men1f/f* mice. The RANKL/OPG ratio from bone RNA was also found to be higher in *Prx1-Cre; Men1f/f* animals, which is consistent with *in*

vivo histomorphometric analysis that demonstrates an increase in osteoclast number and activity in *Prx1-Cre; Men1f/f* and *Osx-Cre; Men1f/f* mice. In conclusion, these studies demonstrate the essential role that osteoblast menin plays in bone homeostasis and show the potential of menin as a molecular therapeutic target for treating disorders of low bone mass such as osteoporosis.

RÉSUMÉ

La ménine, le produit du gène de la néoplasie endocrinienne multiple de type 1 (*MEN1*), est une protéine principalement exprimée dans le noyau qui joue un rôle dans le contrôle de la prolifération et de la différenciation cellulaire. Dans les ostéoblastes, il a été montré que la ménine régularise l'ostéoblastogenèse, un processus essentiel au cours de l'homéostasie osseuse. Notre laboratoire a aussi initialement établi *in vivo* l'importance de la ménine pour le bon fonctionnement des ostéoblastes matures et pour le maintien de la masse osseuse chez les souris adultes. Dans l'étude présente, nous cherchons à mieux comprendre le rôle que joue la ménine *in vivo* lorsqu'elle est exprimée à des stades précoces de la lignée ostéoblastique. Pour atteindre cet objectif, des souris knock-out conditionnelles dans lesquelles le gène *Men1* est spécifiquement supprimé au début de la lignée ostéoblastique ont été générées, et ceci en utilisant le système de recombinaison Cre-LoxP. Les souris *Prx1-Cre ; Men1f/f* et *Osx-Cre ; Men1f/f* représentent à cet effet l'invalidation du gène *Men1* au niveau de la cellule souche mésenchymateuse pluripotente et des préostéoblastes, respectivement. En procédant à la caractérisation phénotypique des souris transgéniques, les poids des souris knock-out sont réduits par rapport aux souris *Men1f/f* servant de contrôles. Les animaux adultes âgés entre 10 à 14 mois provenant des deux souches knock-out révèlent des changements en termes de la teneur en gras et en masse maigre. L'activité du tissu adipeux brun est également affectée par le fait que l'expression relative de *Ucp1* est plus élevée dans les souris *Prx1-Cre ; Men1f/f*. Par micro-tomographie tridimensionnelle du fémur, nous percevons une diminution du volume trabéculaire osseux et une structure trabéculaire aberrante dans les deux souches de souris knock-out. La masse osseuse et la longueur des fémurs sont également significativement réduites dans les deux modèles de souris knock-out. Le test de flexion en trois points démontre aussi une réduction en termes de force et de raideur du fémur chez les animaux knock-out. La force de pré-adhérence des membres antérieurs des souris *Prx1-Cre ; Men1f/f* est réduite et celle des souris *Osx-Cre; Men1f/f* élevée par rapport aux souris de type sauvage. Les capacités prolifératives des ostéoblastes issues de la calvaria et des cellules stromales de la moelle osseuse (BMSCs) des souris *Prx1-Cre ; Men1f/f* et *Osx-Cre ; Men1f/f* ne sont pas affectées. Le degré de minéralisation des ostéoblastes primaires issues de la calvaria chez les souris knock-out est cependant réduit par rapport aux cellules provenant des souris de type sauvage, tel qu'évalué par coloration alizarine rouge. Les profils d'expression géniques des ostéoblastes primaires et des BMSCs des souris *Prx1-Cre; Men1f/f* sont également altérés. Cultiver les cellules ostéoblastiques issues de la calvaria par

une nouvelle méthode consistant à utiliser des gels de collagène dense, qui imitent mieux le microenvironnement osseux physiologique, révèle des capacités de minéralisation défectueuses au niveau des cellules ostéoblastiques issues des souris *Prx1-Cre; Men1f/f*. Le ratio RANKL/OPG de l'ARN osseux est également plus élevé dans les animaux *Prx1-Cre; Men1f/f*, ce qui est concorde avec l'analyse histomorphométrique *in vivo* qui démontre également une augmentation au niveau du nombre et de l'activité des ostéoclastes dans les souris *Prx1-Cre; Men1f/f* et *Osx-Cre; Men1f/f*. En conclusion, ces études illustrent le rôle essentiel que joue la ménine ostéoblastique dans l'homéostasie osseuse et soulignent également le potentiel de la ménine ostéoblastique comme cible thérapeutique moléculaire pour le traitement des troubles de faible masse osseuse comme l'ostéoporose.

ACKNOWLEDGMENTS

I would like to begin by thanking all the current and past members of the Hendy lab. First, my supervisor Dr. Geoffrey N. Hendy for providing me with all the means to pursue my research and encouraging me to exceed myself in becoming an overall better scientist. Dr. Hendy, I thank you for your valuable mentorship during my thesis. Dr. Lucie Canaff, I want to thank you for all the help and technical assistance you provided me with throughout my thesis. To Jad-Abi-Rafeh, thank you for your friendship, it was a pleasure working with you.

I would also like to express my sincere thanks to the people that have helped me with the realization of certain experiments. Dr. Iris Boraschi-Diaz I thank you for your assistance and helpful technical advice for some of my experiments. Dr. Martin Pellicli thank you for teaching me how to use the three point-bending machine and Dr. Ken-Ichiro Tanaka thank you for showing me how to perform the grip strength experiment. I want to thank Dr. Showan Nazhat for sharing his method and providing certain reagents for the preparation of dense collagen gels presented in this thesis. Gabriele Griffanti I thank you for showing me how to prepare the 3D collagen gels.

I would like to thank the members of my thesis committee Dr. Elena Torban, Dr. Louise Larose and Dr. Peter Siegel for their insightful comments and suggestions.

I also want to give a special thanks to all the new friends I made during my journey as a master student. I hope you recognize yourselves and a huge thank you for your support and for being there for me in every moment.

Finally, I would like to thank all my entire family for their unconditional love and encouragement. I want to dedicate this thesis to my mom and dad who have made a lot of sacrifices for the wellbeing of my sister and I. Mom, Dad and Sara, I love you all very much!

CONTRIBUTION OF AUTHORS

Ildi Troka designed and performed experiments presented in chapter 4 of this thesis, collected and analyzed results, and wrote the thesis.

Dr. Geoffrey N. Hendy provided contribution in terms of the overall project, supervision, review of results and thesis editing.

Dr. Lucie Canaff provided training and technical help for some of the experiments.

Gabriele Griffanti provided training for the preparation of dense collagen gels, and performed the SEM and FTIR experiments.

LIST OF FIGURES

Figure 1.1: Process of intramembranous ossification……3

Figure 1.2: Process of endochondral ossification……4

Figure 1.3: Illustration of the hierarchical structure of bone……6

Figure 1.4: Bone remodeling cycles initiated within BMUs……15

Figure 1.5: The multifactorial roles of osteocalcin in whole-body metabolism……19

Figure 1.6: Wnt/β-catenin signaling in bone homeostasis……21

Figure 1.7: Menin interacting partners in the nucleus……27

Figure 1.8: Role of menin in myogenesis and osteogenesis……32

Figure 1.9: Role of menin during osteoblast commitment and differentiation……35

Figure 1.10: Effect of *Men1*$^{-/-}$ in mice embryos……38

Figure 1.11: Effect of menin deletion and overexpression in mature osteoblast……41

Figure 1.12: Representative images of micro-CT analysis of the femurs of knockout mice……43

Figure 3.1: Schematic representation of 3D collagen scaffolds preparation……58

Figure 4.1: Growth curves of *Prx1-Cre; Men1f/f* and *Osx-Cre; Men1f/f* mice during postnatal development……67

Figure 4.2: Body composition analysis of adult *Prx1-Cre; Men1f/f* and *Osx-Cre; Men1f/f* mice……68-69

Figure 4.3: BAT & WAT fat analysis……71-72

Figure 4.4: Forelimb grip strength test of *Prx1-Cre; Men1f/f* and *Osx-Cre; Men1f/f* mice…..74-75

Figure 4.5: Reduced femur length and bone biomechanical parameters in *Prx1-Cre; Men1f/f* and *Osx-Cre; Men1f/f* mice……77

Figure 4.6: Morphological appearances and proliferative capabilities of calvarial osteoblasts and BMSCs…79

Figure 4.7: Differentiation and mineralization assays for calvarial osteoblasts and BMSCs…81-83

Figure 4.8: Gene expression profiles of isolated calvarial osteoblasts and BMSCs of *Prx1-Cre; Men1f/f* and *Men1f/f* mice……...86

Figure 4.9: Gene expression profiles of bone RNA of femurs and tibia of *Prx1-Cre; Men1f/f* and *Men1f/f* mice…….……...……...89

Figure 4.10: Viability and microscopic analysis of primary calvarial osteoblast in dense collagen scaffolds under osteogenic conditions…….....93-94

Figure 4.11: FTIR analyses of mineralization of calvarial osteoblast-seeded dense collagen scaffolds under osteogenic differentiation……...……...95

LIST OF TABLES

Table 1.1: Dynamic and static histomorphometric analysis of the femurs of knockout mice.....44

Table 5.1: *Men1* mouse models illustrating the role of menin in bone development ……...…113

ABBREVIATIONS

ALP: alkaline phosphatase

AP-1: activator protein - 1

ATF: activating transcription factor

BAT: brown adipose tissue

bp: base pairs

BGLAP: bone gamma-carboxyglutamate protein

BMD: bone mineral density

BMP: bone morphogenetic protein

BMSC: bone marrow stromal cell

BMU: basic multicellular unit

BSP: bone sialoprotein

Ca^{2+}: calcium

CDK: cyclin-dependent kinase

cDNA: complementary deoxyribonucleic acid

cFMS: colony stimulating factor 1 receptor

COL1α1: collagen type 1 alpha 1

Ctnb1: catenin beta 1

CXCL10: C-X-C motif chemokine 10

Dkk: dickkopf

DMP1: dentin matrix acidic phosphoprotein 1

DNA: deoxyribonucleic acid

DXA: dual X-ray absorptiometry

ECM: extracellular matrix

EDS: energy dispersive X-ray spectroscopy

ERα: estrogen receptor alpha

F-actin: filamentous actin

FANCD2: fanconi anemia complementation group D2

FBS: fetal bovine serum

FOXN3: forkhead box N3

FTIR: fourier transform infrared spectroscopy

FZD: frizzled

GAPDH: glyceraldehyde-3-phosphate dehydrogenase

GFAP: glial fibrillary acidic protein

GPRC6A: G protein-coupled receptor family C group 6 member A

GSK3β: glycogen synthase kinase 3 beta

H3K4me3: trimethylation of lysine 4 of histone 3

IGF-1: insulin like growth factor 1

ISCT: International Society for Cellular Therapy

JunD: transcription factor JunD

LRP: LDL receptor related protein

LEF: lymphoid enhancer binding factor

loxP: locus of X-over P1

MAPK: mitogen-activated protein kinase

M-CSF: macrophage-colony stimulating factor

MEN1: multiple endocrine neoplasia type 1

MLL: mixed-lineage leukemia transcription factor

mRNA: messenger ribonucleic acid

MSC: mesenchymal stem cell

MTT: methyl thiazolyl tetrazolium

MyoD: myoblast determination protein

μCT: micro-computed tomography

NFATc1: nuclear factor of activated T-cells cytoplasmic 1

NLS: nuclear localization signal

NMHCII-A: nonmuscle myosin II-A heavy chain

NPY: hypothalamic neuropeptide

OCN: osteocalcin

OPG: osteoprotegerin

OPN: osteopontin

OSX: osterix

Pax-3: paired box 3

PCR: polymerase chain reaction

PGC1α: peroxisome proliferator-activated receptor gamma coactivator 1-alpha

Pi: phosphate

P1NP: procollagen type 1 amino-terminal propeptide

pNETS: pancreatic neuroendocrine tumors

PPAR: peroxisome proliferator activated receptor

PPARG: peroxisome proliferator activated receptor gamma

PRX1: paired related homeobox 1

PTH: parathyroid hormone

PTHrP: parathyroid hormone-related protein

PU.1: transcription factor PU.1

RANK: receptor activator of nuclear factor kappa-B

RANKL: receptor activator of nuclear factor kappa-B ligand

RNA: ribonucleic acid

RT-qPCR: quantitative reverse transcription polymerase chain reaction

Runx2: runt-related transcription factor 2

RXR: retinoid X receptors

SEM: scanning electron microscopy

sFRP: secreted frizzled-related proteins

SMAD: transcription factor smad

SNS: sympathetic nervous system

SOST: sclerostin

TCF: T-cell specific transcription factor

TG: transgenic

TGFβ: transforming growth factor beta

TRAP: tartrate-resistant acid phosphatase

UCP1: uncoupling protein 1

UV: ultraviolet

VDR: vitamin-D receptor

WAT: white adipose tissue

Wnt: wingless-type

CHAPTER 1: INTRODUCTION

1.1 Bone biology

The human skeleton is a specialized supporting structure of the body characterized by its rigid framework and its capacity to regenerate and repair itself. It is primarily composed of cartilage and bone connective tissues, both of which subserve important functions in the body. Cartilage is a much more elastic connective tissue than bone which provides flexibility in engaging various forms of movements and helps to maintain the elasticity and shape of organs. On the other hand, bone, which is more rigid, plays essential roles in protecting and supporting the entire body as well as acting as an important mineral reservoir for calcium and phosphate ions (1,2). Growth factors, cytokines and proteins within the bone matrix take part in another crucial function of bone, that of a regulator of body metabolism (1,2). The marrow of bones also serves as a site of hematopoiesis. Bone development and homeostasis are thus crucial processes which ensure that the skeletal functions are adequately maintained. While bone development takes place early in life, bone homeostasis is a lifelong process which relies on the highly-coordinated and regulated mechanisms of bone formation, mediated by cells which deposit new bone matrix called osteoblasts, and bone resorption, achieved through cells that degrade bone called osteoclasts (1,2). The maintenance of a balance between bone formation and resorption is critical in preventing the occurrence of bone disorders which are generally classified through gain or loss of bone mass. Improvement of our knowledge of the skeletal system components and of factors affecting bone homeostasis is essential to design new and better therapeutics for treating bone disorders.

1.1.1 Bone development

Bone is formed through two different processes: intramembranous ossification, which involves the direct conversion of mesenchymal cells into bone tissue and endochondral ossification whereby a cartilage model is first formed and then replaced by bone cells (3,4,5). Both processes are characterized by the formation of primary and secondary ossification centres which allow for bones to grow and assume their normal shape. While primary ossification takes places in prenatal development, secondary ossification occurs mainly during postnatal development (4,5).

Flat bones of the skull and certain parts of the clavicles are formed via intramembranous ossification (figure 1.1) (3-5). This process is initiated when a group of mesenchymal stem cells (MSCs) derived from the neural crest proliferate and differentiate into osteoblasts that secrete a collagen-proteoglycan matrix which will bind calcium salts and produce a calcified osteoid matrix that will form the ossification center (3). As the mineralization process continues, osteoblasts that become trapped within the bone matrix become osteocytes, while the surrounding osteoprogenitors differentiate to become new osteoblasts. At the same time, blood vessels will start invading the ossification center and mineralization that takes place on the surrounding capillaries will form trabecular, or spongy, bone. In this process bone is formed without a cartilage intermediate (3-5).

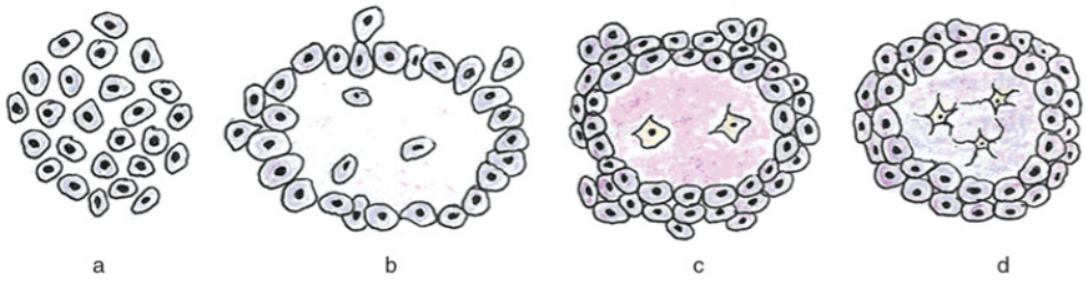

Figure 1.1 : **Process of intramembranous ossification.** (a) A group of osteoprogenitor cells derived from MSCs aggregate together, (b) producing a collagen matrix in the center and in between cells. (c) Differentiated osteoblast secrete osteoid which will become calcified. (d) Bone tissue is formed and osteoblasts that become trapped within the osteoid matrix become osteocytes. Reproduced with permission from Kini U. & Nandeesh BN. Physiology of bone formation, remodeling, and metabolism. In: *Radionuclide and Hybrid Bone Imaging*. 2012. I. Fogelman, G. Gnanasegaran, H. van der Wall (Eds). pp. 29-57.

Endochondral ossification (figure 1.2) involves the formation of long bones and those at the base of the skull (3-6). This process can be divided into five stages. In the first three stages, MSCs condense and differentiate into chondrocytes which then rapidly proliferate to form a cartilaginous model for the bone. During the proliferation and growth of chondrocytes, longitudinal growth of the bone also concurrently takes place. The fourth phase is characterized by chondrocytes stopping to divide and a zone of hypertrophy being formed whereby chondrocytes increase in volume and produce a matrix that becomes mineralized by calcium carbonate. In the last stage, hypertrophic chondrocytes die by apoptosis (3-6). This then creates a bone marrow space which enables blood vessels to enter and bring in osteoblast precursors that will differentiate and deposit new bone matrix that will serve as the primary ossification center. With time this ossification center shifts to the epiphyseal edges of bones, forming the secondary zones of ossification (4-6).

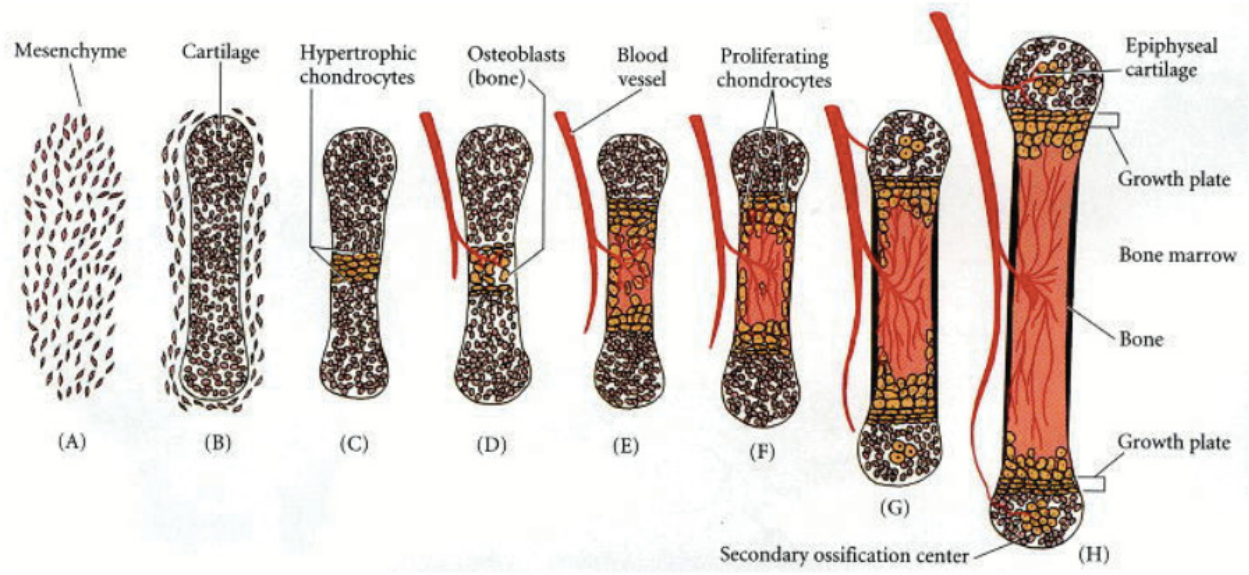

Figure 1.2: Process of endochondral ossification. (A-B) A pool of MSCs differentiate into chondrocytes to form a cartilaginous template. (C) Hypertrophic chondrocytes at the center of the bone enter apoptosis, creating a space which allows (D-E) blood vessels to enter and bring in osteoblasts which will form a primary ossification center. (F-H) With time, this overall process is repeated, allowing bones to grow in size and become calcified. This last step is also characterized by secondary ossification centers being formed near the epiphyseal edges of bone. Reproduced with permission from Gilbert S.F. Osteogenesis: The development of bones. *Developmental Biology*. 2000. 6th edition.

1.1.2 Skeleton components

The adult human skeleton is composed of a total of 206 bones, 126 of which form the appendicular skeleton and 80 the axial skeleton (7). Bones located at the central part of the body such as the skull, rib and spine form the axial skeleton, whereas long bones of the arms and legs along with shoulder and pelvic girdles constitute the appendicular skeleton. The axial skeleton provides support for the main organs of the body whereas the appendicular skeleton facilitates movement (7).

Two types of bone normally compose both the appendicular and axial skeleton: compact and trabecular, or cancellous, bones (1,2,7,8). Compact bone also called cortical bone is denser and more solid than trabecular bone which is characterized by more laminar and polygonal structures called trabeculae (1,2,8). Compact bone constitutes the cortical shell of bones and generally represents 80% of the total skeletal mass, whereas trabecular bone constitutes the core, or inside space of bones, and represents 20% of the skeletal mass (figure 1.3). Because it is less dense than compact bone, trabecular bone also has a higher surface-area-to-volume ratio which makes it weaker. The functions and mechanical properties of both types of bone are different, but generally speaking trabecular bone is more flexible and has a higher turnover rate than compact bone whose strong structure supports the body. Trabecular bone is also more vascularized and comprises the bone marrow where hematopoiesis takes place (1,2,7,8).

1.1.3 Bone composition

Bone is a heterogeneous tissue composed of both organic and inorganic constituents as well as water which makes up to 10% of bone (9,10). Type 1 collagen and small quantities of noncollageneous proteins (e.g. bone sialoprotein (BSP)) form the organic matrix of bone, or

osteoid, while mineral hydroxyapatite ($Ca_{10}(PO_4)_6(OH)_2$), composed of calcium and phosphate, forms predominantly the inorganic matrix that constitutes 60-70% of total bone (9,10). Structural proteins of the bone matrix like collagen play crucial roles in providing elasticity, supporting the extracellular matrix and regulating the mineralization process. The organic matrix of bone is also composed of small amounts of accessory proteins, such as osteopontin (OPN) and osteocalcin (OCN) that are involved in bone mineralization (11). The coordinated alignment of organic and inorganic constituents is regulated by the expression of various genes and signaling factors. Any alteration in either the bone mineral and protein compositions can lead to bone diseases generally associated with high risk of fracture, such as osteoporosis (10).

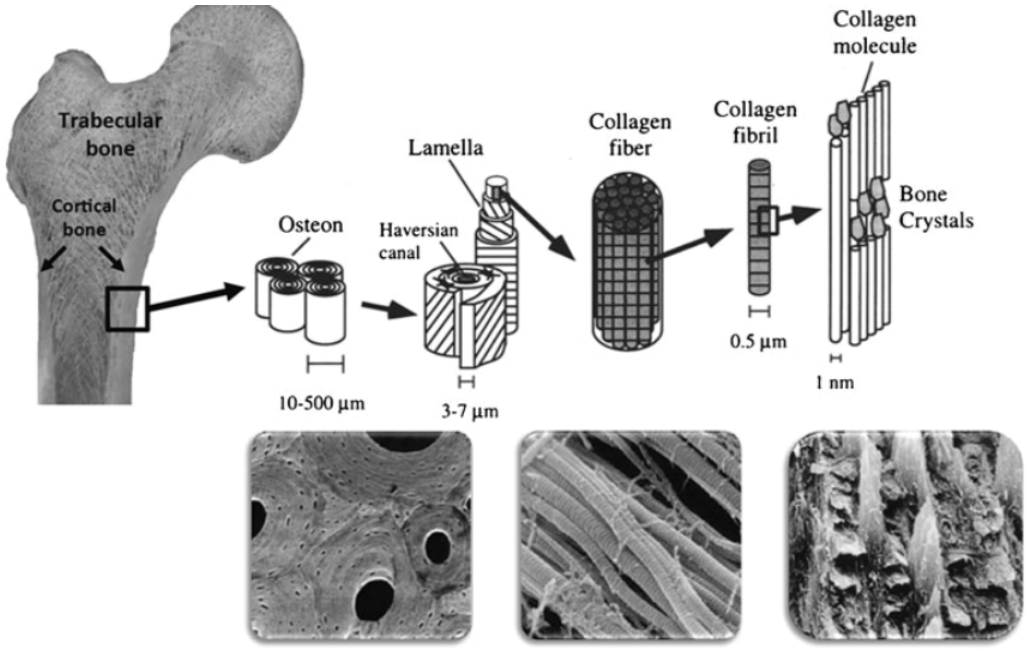

Figure 1.3 : Illustration of the hierarchical structure of bone. At the macroscopic level, dense cortical bone and cancellous (trabecular) bone comprise the outside shell and inside structure of bone, respectively. At a microscopic scale, cortical bone is formed of many anatomical units called osteons. Each osteon is composed of a haversian canal which carries blood vessels and nerves surrounded by layers of lamella. At the nanoscopic level, bone is composed of type 1 collagen fibrils which provide an essential framework for the deposition of mineral crystals. Reproduced with permission from Bala Y, Farlay D, Boivin G. Bone mineralization: from tissue to crystal in normal and pathological contexts. *Osteoporosis International*. 2013;24(8):2153-66.

1.1.4 Bone cells

Bone is primarily composed of three types of cells: osteoblasts, osteoclasts and osteocytes. Each cell plays an important and unique function in bone homeostasis and can be characterized by a distinctive shape. Bone cells have the ability to communicate with each through different factors that they release. This feature enables them to mediate and regulate bone formation and resorption processes which are essential for bone homeostasis (12).

1.1.4.1 Mesenchymal stem cells

MSCs are multipotent cells with the ability to self-renew and to differentiate into a variety of cell types, which include but are not limited to osteoblasts, chondrocytes, adipocytes and myocytes (13). Adult MSCs can be found and isolated from many tissues, but the major sources include the bone marrow, adipose tissue and umbilical blood (14). The biological properties of MCSs differ depending on the tissue type in which they are found (14). Nonetheless, morphologically, all MSCs have a characteristic elongated fibroblastic-like appearance (13). In *ex vivo* cell studies, the bone marrow remains the most used site for the isolation of MSCs. The bone marrow is also the preferred site in bone studies as MSC populations derived from there can more easily be committed to become bone cells (13). Because they are mostly derived from the stroma of the bone marrow, MSCs are often also referred to as mesenchymal stromal cells. The International Society for Cellular Therapy (ISCT) recommends the general use of the term mesenchymal stromal cells, and only if the stemness property of the mesenchymal cells is established, can the term mesenchymal stem cell be used (15). In cell culture, MSCs are also known for their ability to adhere to plastic surfaces, and this special feature of MSCs has been established as one of the first criteria for their identification (13,16). As proposed by the ISCT,

MSCs can generally be further characterized by the presence of positive surface markers, such as CD105 and CD90, and negative markers like CD34 (17). *Ex vivo*, isolated populations of MSCs have the ability to differentiate into different cell lineages. However, successful differentiation into the cell lineage of interest relies on the special additives of the cell medium used (13,16). For instance, in order to induce osteogenesis of MSCs, differentiation with cell medium containing L-ascorbic acid and β-glycerophosphate is generally used. Therapeutically, MSCs also offer many benefits, including but not limited to their use in tissue regeneration and in graft versus host diseases (18).

1.1.4.2 Osteoblasts

Osteoblasts are essential bone forming cells that are found on the surface of newly synthetized bone. They are singly nucleated, have a cuboidal appearance and comprise 4-6% of total bone cells (12). Osteoblasts originate from multipotent MSCs of the bone marrow stroma and as they differentiate and become mature, they produce an extracellular matrix which then becomes mineralized (12,19). Differentiated and mature osteoblasts can be characterized by the high expression levels of collagen type 1 alpha 1 (COL1α1), OCN and alkaline phosphatase (ALP) that represent the three main bone matrix proteins that they secrete (20). Once mature, osteoblasts that become entrapped within the bone matrix eventually differentiate into osteocytes, whereas those that remain on the surface of bone can either undergo apoptosis or become bone lining cells (12,19).

1.1.4.3 Osteoclasts

Osteoclasts are multinucleated giant cells that originate from monocyte precursors of the hematopoietic stem cell lineage. They are found on the bone surface and are involved in the decalcification and degradation of the bone matrix (12). The proliferation and differentiation of osteoclast precursors leads to the maturation of osteoclasts where these cells can achieve their bone resorption role (21). Fully differentiated osteoclasts are characterized by a sealing zone rich in filamentous actin (F-actin) which allows them to adhere to the surface of the bone matrix (22).When attached to bone, osteoclasts begin the resorption process by secreting acids and protons which make the local pH more acidic leading to demineralization of the inorganic bone matrix. Degradation of the organic component of bone then follows by a lysosomal protease mediated process involving cathepsin K. The liberated products from bone degradation are then endocytosed by the osteoclast and further released (22).

1.1.4.4 Osteocytes

Osteocytes are the most abundant bone cells in the mature skeleton, representing around 95% of total bone cells (23). In humans, their mean half-life of 25 years is the longest out of all bone cells (23). Osteocytes are matured osteoblasts that become embedded within the bone matrix after the bone formation cycle. In contrast to osteoblasts however, osteocytes have a more elongated shape with cytoplasmic processes extending in the bone canaliculi enabling them to communicate with each other (23,24,25). Osteocytes play a crucial role as mechanosensors, detecting changes in external mechanical forces applied to the bone and adapting the bone accordingly by regulating both osteoblast and osteoclast activity (23,24,25).

1.2 Mechanisms of bone formation

1.2.1 Osteoblast differentiation

As previously mentioned, MSCs are multipotent cells that have the ability to differentiate into various cell lineages and give rise to either chondrogenic, myogenic, adipogenic or osteogenic cells. The primary commitment of MSCs is essential in determining their eventual cell type. This is generally controlled through the action of important transcriptional regulators (26). For the myogenic and adipogenic lineages these are MyoD and PPARγ, whereas for the chondrogenic and osteogenic lineages, these are the Sox9 and the runt-related transcription factor 2 (Runx2) transcription factors, respectively (12,26). Once these master genes of differentiation are activated through the action of different factors, cells are generally categorized into a pre-differentiated state (e.g. preadipocyte, preosteoblast, etc.) that is necessary for further differentiation and for these cells to achieve their normal physiological functions.

For osteogenesis, Runx2 activation marks the first step of osteoblast differentiation (27). Further differentiation of the preoteoblasts to mature osteoblasts requires a timely and coordinated expression of osteoblast specific genes which are either unregulated or suppressed in a Runx-dependent manner (12,19,26,27). The first stage of differentiation of the preosteoblast is marked by the stimulation of cell cycle markers (e.g. histones) that leads to an increase in proliferation (e.g. downregulation of cyclin-dependent kinase inhibitors). The preosteoblasts at this step also normally start expressing collagen, OPN, transforming growth factor beta (TGFβ) receptor 1 and fibronectin (26-28). The second stage is characterized by the extracellular matrix maturation, whereby preosteoblasts stop proliferating and start differentiating. This stage is characterized by the increase in expression of extracellular matrix-related proteins, such as ALP and collagen (COL1α1). In the third step, osteoblasts become fully differentiated and matrix mineralization

takes place, with the expression of mineralization proteins, like OCN, increasing (26-28).When osteoblasts become terminally differentiated and when the cellular matrix is mineralized, osteoblasts can undergo apoptosis as a result of cell maturation. This last step of osteoblast differentiation is generally distinguished by the increased expression of proapoptic genes and decreased expression of anti-apoptic genes (e.g. *p53*) (26-28).

1.2.2 Osteoclast differentiation

Osteoclasts are derived from hematopoietic stem cells which have been committed to the monocyte/macrophage lineage. Important transcription factors and cytokines at this stage are needed for coordinating osteoclastogenesis events. Like Runx2 is for osteoblastogenesis, PU.1 is the master transcription factor of osteoclastogenesis responsible for regulating the expression of important genes mediating osteoclast differentiation (21). One key function of PU.1 is to stimulate gene transcription of the receptors of both the receptor activator of nuclear factor kappa-B ligand (RANKL), RANK, and the macrophage-colony stimulating factor (M-CSF), c-FMS, which are essential for osteoclast differentiation (21,29). In the bone microenvironment, M-CSF is produced and secreted by stromal cells of the bone marrow and osteoblasts, whereas RANKL is mainly produced by osteoblasts and osteocytes. Activation of c-FMS by M-CSF on macrophage/osteoclast progenitor cells favors their proliferation and survival, as well as promotes their commitment to become pre-osteoclasts (30). RANKL-RANK interaction in pre-osteoclasts initiates a downstream signaling cascade resulting in the activation and nuclear translocation of the nuclear factor of activated T-cells cytoplasmic 1 (NFATc1) which induces the differentiation of pre-osteoclasts to mature osteoclasts (21). NFATc1 also regulates the expression of osteoclast-specific genes, such as *TRAP* and *cathepsin K*, which mediate important activities in differentiated osteoclasts (31). It

is important to note that the differentiation of osteoclasts is supported by osteoblasts through cell to cell contact with osteoclast precursor cells. While RANKL supports the differentiation and maturation of osteoclasts, another factor called osteoprotegerin (OPG), also released by osteoblasts, acts as a decoy receptor to RANKL preventing its interaction with the RANK and inhibiting osteoclastogenesis. Hence, the RANKL to OPG ratio is generally a strong indicator of osteoclast formation and of the extent of bone resorption. Any alteration in this ratio will result in either an increase or decrease in the degree of osteoclastogenesis (32).

1.2.3 Bone mineralization

Bone mineralization, also termed bone calcification, is an osteoblast-mediated mechanism whereby minerals are deposited in an organized fashion into the organic extracellular matrix of bone (33). This process usually begins 5-10 days after the organic matrix composed of type 1 collagen, proteoglycans and a variety of non-collagenous proteins, like OCN and BSP, is initially deposited by osteoblasts (34). In bone, the extracellular matrix (ECM) is critical for mineralization as it defines the sites of where mineralization will occur and the final size of the mineral crystals formed (8,9,33,34). The principal constituent of the ECM is collagen and it is predominantly found as a fibrillary network in bone. Without the bone ECM, mineral deposition simply cannot occur (33-35).

After osteoid deposition by osteoblasts, mineralization begins following a two-phase process involving vesicular and fibrillar phases (36). The vesicular phase is mediated by matrix vesicles, which are extracellular membrane particles that are located within the bone matrix. These vesicles are released by polarized budding from the apical membrane surface of osteoblasts and serve as the initial site of mineralization (37). The formation of calcium (Ca^{2+}) and inorganic

phosphate (Pi) ions within the matrix vesicles constitutes the first step of mineralization (33). During the vesicular phase, these matrix vesicles are released from osteoblasts into the ECM, where they bind various components of the organic matrix. One such component includes the proteoglycans that can bind to and immobilize Ca^{2+} ions within the matrix vesicles (38). When proteoglycan degrading enzymes (e.g. matrix metalloproteinases) are produced by osteoblasts, this leads to the release of the bound Ca^{2+} ions which can then travel across the vesicular membrane (39). At this same time, ALP secreted by osteoblasts degrades compounds that bind Pi ions, further liberating these ions within the vesicles. Ca^{2+} and Pi ions can then nucleate in the matrix vesicles, resulting in the formation of hydroxyapatite crystals (38). At this stage, certain proteins of the organic matrix, like BSP, can regulate the concentrations of Ca^{2+} and Pi ions needed for the formation of hydroxyapatite crystals (33). The fibrillar phase then follows with the breakdown of the matrix vesicles releasing hydroxyapatite crystals which can migrate to collagen fibrils to initiate the mineralization process (40).

1.3 Bone modeling & remodeling

Bone modeling is a process whereby bones can grow and change their preformed shape in order to adapt to the external mechanical forces that they encounter. Bone modeling permits longitudinal growth of bones which is essential during development in vertebrates. In bone modeling, bone formation, mediated by osteoblasts, and resorption, mediated by osteoclasts, are independently occurring processes taking place at different anatomical sites within the skeleton (1,2,41). Bone modeling is particularly important during early skeletal development throughout childhood, but decreases in frequency during adulthood (42).

On the other hand, bone remodeling is a process which persists throughout life (1,2). As opposed to modeling, bone resorption and formation are not independently occurring processes in bone remodeling. In fact, adequate remodeling relies on a homeostatic equilibrium between bone resorption and formation which are normally two coupled and collaborative mechanisms occurring sequentially within temporary anatomic structures termed basic multicellular units (BMUs) (43, 44, 45). In a normal bone remodeling cycle, mature osteoclasts adhere to the bone surface, become activated and begin the resorption process of the bone matrix by acidification and proteolytic digestion (46). After bone is degraded, osteoclasts undergo apoptosis and the excavated area is filled by osteoblasts which produce new bone matrix that becomes mineralized. At the end of each remodeling cycle, osteoblasts either die by apoptosis or become embedded within the bone matrix as osteocytes (46,47). Figure 1.4 illustrates BMUs that are spread throughout the different bone compartments where remodeling takes place. Normally, precursors of both the osteoclast and osteoblast lineage are supplied to BMUs through the bloodstream and once within the BMU, these are able to differentiate into bone specific cells, osteoblasts and osteoclasts being the two main executive cells of BMUs (43-45). The lifespan of bone executive cells (2 weeks for osteoclasts and 3 months for osteoblasts) is usually shorter than that of the BMU (6-9 months), thus a continuous supply of new osteoclasts and osteoblasts is critical for the BMU (43-45). As a result, the balance between levels of osteoclasts and osteoblasts at any time point within the lifespan of the BMU is a key determinant of the degree of bone being resorbed and formed.

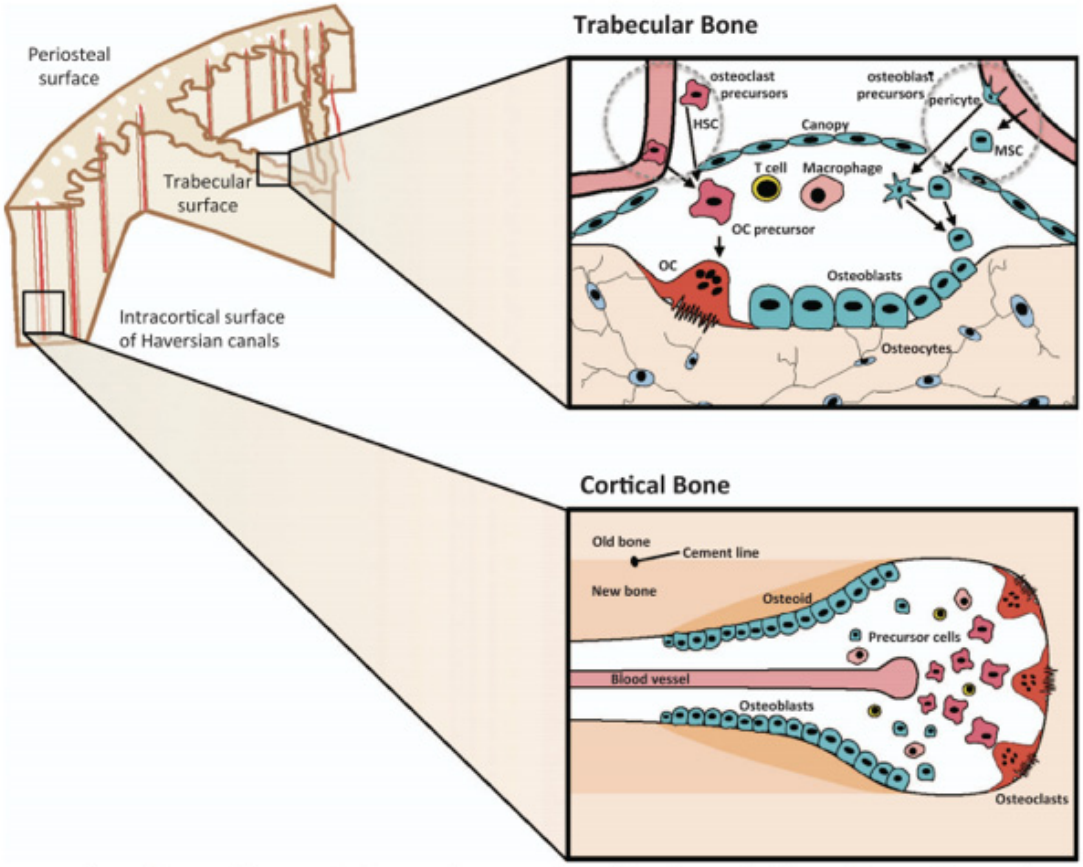

Figure 1.4: Bone remodeling cycles initiated within BMUs. Under the canopy generated by bone lining cells, hemopoietic precursor cells and MSCs are supplied by the marrow and the blood stream to the BMUs. In the BMU, osteoclast and osteoblast precursors derived from hemopoietic precursors and MSCs, respectively, are able to differentiate into fully functional cells necessary to initiate bone remodeling. Reproduced with permission from Sims N.A. & Martin T.J. Coupling the activities of bone formation and resorption a multitude of signals within the basic multicellular unit. *Bonekey Reports*. 2014. 3: 481.

1.3.1 Bone disorders

Bone is a dynamic structure which undergoes constant remodeling throughout an individual's lifetime. The adequate balance between bone formation and resorption is maintained through the tightly-controlled regulation of signaling pathways involved in osteoblast and osteoclast differentiation. Any alteration or imbalance in these processes can lead to a variety of bone diseases which will be classified as disorders of bone remodeling, the most common one being osteoporosis (48).

1.3.2 Osteoporosis and treatments

Osteoporosis is the most prevalent metabolic bone disorder characterized by low bone mass and structural deterioration of bone leading to enhanced bone fragility (49). It is often represented as a clinically silent disease the severity of which progresses with aging resulting in increased risk of fracture of the hip, wrist and spine if untreated (49). In today's population, it is estimated that one in three women and one in five men will suffer from an osteoporotic fracture in their lifetime, with recent reports placing the worldwide number of individuals affected by osteoporosis at 200 million (41,50). Learning more about this disorder is thus important in order to design more effective therapeutic strategies to treat it.

In general terms, osteoporosis is classified into primary and secondary types (51). Primary osteoporosis is the most common type that is caused by genetic and physiological alterations. Age-related and postmenopausal bone loss are classified as type I osteoporosis (48,51). These are often linked with hormonal changes which include, but are not limited to, reduction in levels of sex steroids (e.g. androgen & estrogen), decreased secretion of growth factors (e.g. IGF-1) and increased parathyroid hormone (PTH) release (48). The net effect of these changes is a negative remodeling balance that is characterized by low osteoblast-mediated bone formation and/or high osteoclast-mediated bone resorption, overall leading to bone loss. Secondary osteoporosis, on the other hand refers to osteoporosis that is caused by environmental factors which often include changes in physical activity or secondary adverse results of therapeutic interventions against certain complications (48,51,52). Reduced mechanical loading of the skeleton as a result of reduced muscle mass and inactivity affects mechanosensing pathways involved in promoting bone formation and regulating bone remodeling, overall leading to low bone mass (48). Certain medically used drugs, such as glucocorticoids, which are largely used to treat inflammatory

disorders, can also induce osteoporosis at pharmacological doses. In the case of glucocorticoids, they can cause bone loss by inhibiting osteoblast differentiation and/or promote osteoclastogenesis through the indirect increase of the *RANKL* expression (53).

Given the multifactorial causes of osteoporosis, current pharmacologic agents used to treat this disorder are aimed at either directly stimulating gains in bone mass or decreasing the extent of bone resorption occurring (49,54). Anti-resorptive agents which inhibit osteoclast activity by promoting their apoptosis, like bisphosphonates, are considered as standard of care for treating osteoporosis. However, their clinical use is inefficient in restoring full bone mass and bone architecture (55). In contrast to anti-resorptive pharmaceuticals, anabolic agents are more advantageous as they act by enhancing bone formation, thus increasing bone mass (49,54,56). The first and most used anabolic agent for osteoporosis is teriparatide, a peptide of the 1-34 amino terminal sequence of PTH (56). Although the precise mechanism of action is not known yet, administered intermittently, teriparatide stimulates bone formation by enhancing osteoblast differentiation (56). Abaloparatide is another more recent clinically approved anabolic agent for osteoporosis (57). It is a synthetic 34 amino acid peptide with a modified sequence of parathyroid hormone-related peptide (PTHrP) which acts as an agonist of the PTH type I receptor through which PTH signals (56,57). The key distinctive feature of abaloparatide however is that its 34 amino acid sequence shares more homology to PTHrp 1-34 (76%) than to PTH 1-34 (41%). Hence, most of its bone promoting effects are mediated through similar mechanisms as PTHrp (56,57). Teriparatide and abaloparatide are the only two anabolic agents approved for clinical use for osteoporosis today. The only other anabolic agents currently undergoing phase 3 clinical trial is romosozumab, a monoclonal antibody against sclerostin which stimulates bone formation by enhancing wingless-type (Wnt) signaling (58). Although romosozumab substantially increases the

bone mineral density (BMD) of osteoporotic patients, its use has been linked to a high incidence of cardiovascular problems (56,58). New and more beneficial drug targets aimed at treating osteoporosis and reducing the incidence of adverse events are thus needed.

1.4 Role of bone in whole-body homeostasis

The roles of the skeleton are to support the body and facilitate movement by serving as a scaffold for muscle attachment. Recently, the skeleton has been suggested to act as an endocrine organ, playing important roles in whole-body metabolism (59). One of the main drivers of the functions of bone in regulating metabolic processes is the bone protein hormone OCN (59).

OCN, or bone γ-carboxyglutamic acid (Gla)-containing protein (BGLAP), is a non-collagenous protein encoded by the *BGLAP* gene. It is primarily produced by osteoblasts and deposited in a carboxylated form into the mineralized bone matrix where it can bind hydroxyapatite crystals (60). In osteoblasts, OCN is involved in regulating mineralization as well as mediating osteoblast-osteoclast interactions (60). Increased osteoclast activity acidifies the bone microenvironment which results in OCN being partially decarboxylated at carbon 17 (61). The undercarboxylated Glu13-OCN represents the active hormonal form of OCN (60,61).

Studies using *Ocn*$^{-/-}$ mice, whereby the *OCN* gene is conventionally knockout, have demonstrated that bone OCN is involved in the regulation of various metabolic processes (62). *Ocn*$^{-/-}$ mice show elevated glucose and decreased insulin circulating levels, suggesting a role for OCN in improving insulin release and sensitivity. OCN was in fact shown to bind to the G protein-coupled receptor family C group 6 member A (GPRC6A) receptor expressed in pancreatic β-cells and promote their proliferation as well as the synthesis and release of insulin, overall improving glucose tolerance (62,63). Low OCN levels have also been linked with decreased rates of oxygen consumption and energy expenditure. In this perspective, OCN has been shown to stimulate energy

expenditure by promoting mitochondrial biogenesis in brown adipose tissue and skeletal muscle (62). In terms of the roles that OCN plays in muscle physiology, recent studies have demonstrated that OCN is necessary to maintain muscle mass in older mice and improves the fatty acid oxidation of muscle cells (64). As to the role that OCN plays in adipogenesis, it has been illustrated that OCN can decrease lipid accumulation by stimulating the expression and release of adiponectin by fat cells, which ameliorates glucose tolerance (65). In addition, OCN can also influence male fertility by binding to the GPRC6A receptor and promoting testosterone synthesis in the Leydig cells of the testis (66). With the discovery of the endocrine functions of bone OCN, it has become clear that regulatory pathways affecting bone homeostasis can also influence whole-body metabolism (figure 1.5) and secondary metabolic changes as a result of bone disorders should also be taken into consideration.

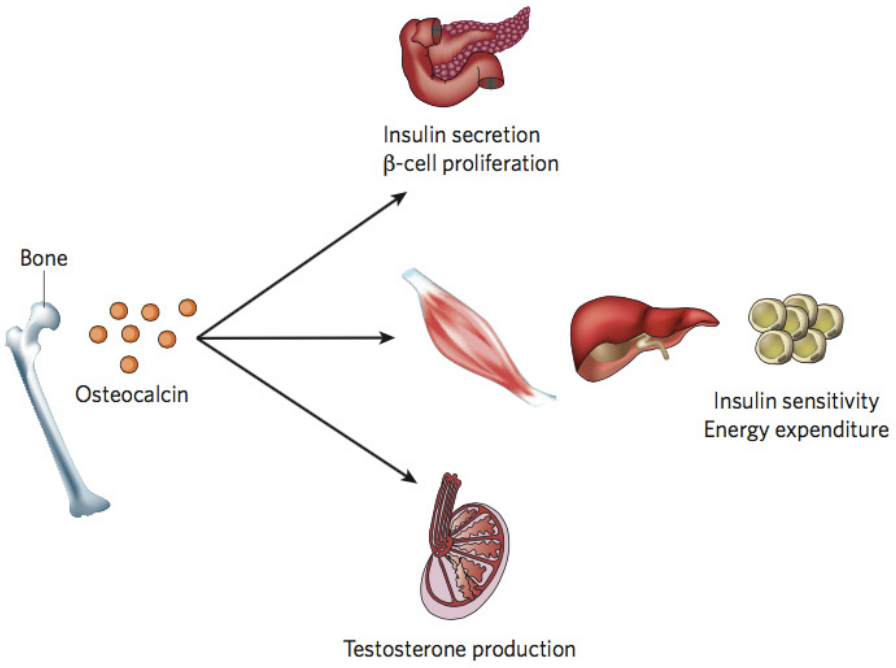

Figure 1.5: The multifactorial roles of osteocalcin in whole-body metabolism. Bone-derived OCN acts as a hormone in the body, stimulating insulin secretion from β-cells of the pancreas, promoting energy expenditure in skeletal muscle, and increasing insulin sensitivity in adipose tissue and liver. OCN can also act on Leydig cells of the testis to stimulate testosterone biosynthesis, promoting male fertility. Reproduced with permission from Karsenty G & Ferron M. The contribution of bone to whole-organism physiology. *Nature*. 2012;481(7381):314-20.

1.5 Regulatory pathways of osteoblast differentiation

Skeletal development and homeostasis are mediated by a number of signaling pathways that regulate osteoblast differentiation. These pathways are crucial for the maintenance of bone mass and for coordinating bone remodeling events involving osteoblasts, osteoclasts and osteocytes. The main regulatory pathways of osteoblast differentiation include the TGF-β/BMP and the Wnt/β-catenin signaling pathways. Each of these individual pathways exerts different functions in bone, but all control important events ranging from the commitment of osteoblasts from MSCs to their proliferation and later differentiation. Importantly, regulators of these pathways have been of interest in many studies as to their potential manipulation and use for treating low bone mass disorders.

1.5.1 Wnt/β-catenin signaling in bone

The canonical Wnt/β signaling is an important signaling pathway for bone metabolism. Binding of the Wnt ligands to the Frizzled (FZD)/LRP5/6 dual receptor complex initiates a downstream signaling cascade which prevents phosphorylation of β-catenin and its subsequent GSK3β-mediated proteosomal degradation. In turn, this leads to β-catenin stabilization and accumulation in the cytoplasm where it can then translocate into the nucleus and associate with members of the TCF/LEF transcription factor family to regulate gene transcription (67).

It is well established that Wnt/β catenin signaling exerts positive effects on bone homeostasis. In osteoblastogenesis, canonical Wnt/β catenin signaling promotes the commitment of MSCs to the osteoblast lineage, while repressing adipogenesis and chondrogenesis (68,69,70). Wnt/β catenin signaling also enhances the expression of *Runx2* and *Osterix (OSX)* genes which are required for osteoblastogenesis, thus facilitating the proliferation of osteoblast progenitor cells

and their subsequent differentiation to become mature osteoblasts (71,72). As such, reports have as well illustrated Wnt/β signaling to have an impact in promoting bone matrix mineralization as well as regulating apoptosis of mature osteoblasts (73). For osteoclastogenesis, Wnt/β catenin signaling indirectly inhibits osteoclast differentiation by increasing the expression of the RANKL decoy receptor, *OPG* from both osteoblasts and osteocytes (74). As such, Wnt/β catenin signaling can simultaneously stimulate bone formation and repress bone resorption, overall positively regulating bone remodeling (figure 1.6).

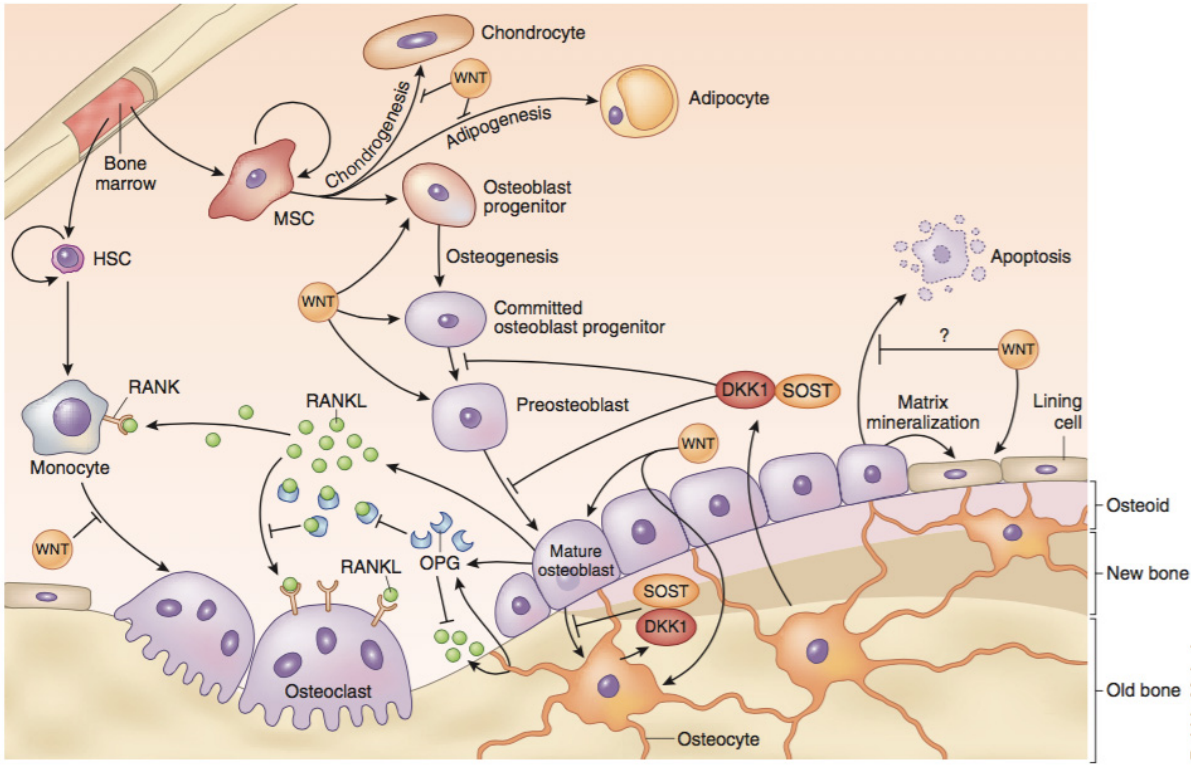

Figure 1.6 : Wnt/β-catenin signaling in bone homeostasis. During osteoblastogenesis, the Wnt/β-catenin signaling is required for the commitment of MSCs to the osteoblast lineage, and for the later differentiation of osteoblast progenitors to mature osteoblast. Wnt/β-catenin signaling can also regulate the apoptosis of osteoblasts. In osteoclastogenesis, Wnt/β-catenin signaling inhibits osteoclastic bone resorption by decreasing the RANKL/OPG ratio from both osteoblasts and osteocytes. The inhibitors of the Wnt/β-catenin signaling, SOST and Dkk1, are released by osteocytes and affect bone remodeling. Reproduced with permission from Baron R, Kneissel M. WNT signaling in bone homeostasis and disease: from human mutations to treatments. *Nature Medicine*. 2013;19(2):179-92.

1.5.1.1 Regulators of the Wnt/β-catenin signaling

Antagonists of the Wnt/β catenin signaling, such as sclerostin (SOST), Dickkopf (Dkk) and secreted frizzled-related proteins (sFRP) offer promising therapeutic targets for the treatment of osteoporosis. All three types of antagonist exert their physiological responses by binding to the Lrp5/6 co-receptor and preventing the activation of Wnt/β-catenin signaling, thus inhibiting bone formation (75). SOST and Dkk are mainly released by osteocytes and are thought to be important in the regulation of bone remodeling. Animal studies have shown that specific deletion of either the *SOST* or the *Dkk* gene greatly enhances bone mass (76,77). A recent study inhibiting sFRP-1 in mice with a small molecule also demonstrated that this enhances bone formation (78). Hence, antagonists of Wnt/β catenin signaling offer potential targets for the development of new anabolic agents for treating osteoporosis.

1.5.2 TGF-β and BMP signaling in bone

TGF-β and bone morphogenetic proteins (BMPs) are essential regulators of osteoblast differentiation, bone formation and remodeling (79,80). Both are primarily synthetized by osteoblasts and belong to the TGF-β ligand superfamily, which signals through type I and type II serine/threonine kinase cell membrane receptors (79,80,81). Types I and II receptors are indispensable for signal transduction. Upon ligand binding, the type I receptor is phosphorylated in a trans manner following activation of the type II receptor (80,81,82). This forms a heterotetrameric-activated receptor complex consisting of both type I and II receptors. The activated type I receptor initiates intracellular signaling by phosphorylating the receptor-regulated Smad proteins (R-Smads). These are Smad-2 and -3 for TGF-β and Smad-1, -5 and -8 for BMPs. These activated Smad proteins then associate with their common partner, Smad4, which creates a

complex that can translocate into the nucleus to mediate transcription of specific genes involved in bone development and remodeling (80-82).

1.5.2.1 TGF-β signalling in osteoblasts

Autocrine and paracrine stimulation by TGF-β is important for the maintenance and expansion of MSCs and osteoblast progenitor cells (80-82). There are three main isoforms of TGF-β : TGF-β1, -β2 and -β3. Deletion of any of these three TGF-β isoforms has been shown to lead to many skeletal defects in mice, in terms of both craniofacial and limb development (79,83). TGF-β1 is however the most abundant isoform found in bone tissue and also the most studied in terms of bone development (79,83). Mechanistically, TGF-β1 stimulates osteoblast proliferation and bone matrix deposition by enhancing the expression of osteoblast-specific genes important during osteoblastogenesis, such as *Runx2* (79,84). Studies have shown that as opposed to its stimulating effect early in the differentiation of osteoblasts, at later stages of osteoblast differentiation TGF-β1 rather suppresses osteoblast maturation. During late stage maturation of osteoblasts, TGF-β signaling in fact inhibits BMP-mediated signaling through the activation of inhibitory Smads and maintains osteoblasts in a differentiated state preventing them from undergoing premature apoptosis (85).

TGF-β signaling is also important for bone remodeling as it links bone formation to bone resorption. In fact, TGF-β stored in the bone matrix in an inactive form can be released by osteoclastic bone resorption and activated in the bone microenvironment. This in turn induces osteoblastic bone formation by stimulating the recruitment and migration of bone MSCs, hence coupling both bone resorption and formation processes (86).

1.5.2.2 BMP signalling in osteoblasts

BMPs were first identified as an activity in the 1960s and later purified from bovine bone in the 1980s, where it was demonstrated that they can induce ectopic bone formation in mice (87,88). Other than skeletal cells, BMPs are also expressed in a variety of cell types where they play a role in development and cell function (89). BMP-2, -4 and -7 are however the most important isoforms whose levels of expression are the highest in osteoblast cultures and whose loss severely impairs osteogenesis (90). An important function of BMPs is to induce the commitment of the early limb bud mesenchymal cells towards both the chondrogenic or osteogenic lineages and to promote their later differentiation and maturation (89, 91). Today, it is widely recognized that BMPs promote bone formation by directly stimulating osteoblastic differentiation through the Smads and mitogen-activated protein kinase (MAPK) pathways, which increase the expression levels of target genes important for osteoblastogenesis like *Runx2*, *OSX* and *ALP* (92). While BMPs promote osteoblast differentiation, studies have showed that they can also induce apoptosis of mature osteoblasts in a Smad1-independent, protein kinase C- dependent pathway (93). Hence, in the early steps of osteoblastogenesis, BMPs (e.g. BMP-2) induce the differentiation of MSCs towards the osteoblast lineage and facilitate osteoblast differentiation, but in the later steps where osteoblast maturate, BMP signaling can lead to osteoblast apoptosis.

1.5.2.3 Regulators of TGF-β/BMP signaling

TGF-β and BMP signaling are modulated by many intracellular and extracellular factors. These include; nonsignaling pseudreceptors, inhibitory smads (e.g. Smad6 & 7), Smad binding and degrading proteins, and extracellular matrix antagonists of TGF-β/BMP ligands (79,89). Each can control TGF-β/BMP signaling and generally results in the extent of osteogenesis being

downregulated. For example, BMP antagonists which consist of a group of secreted polypeptides, such as noggin, inhibit BMP signaling by binding and sequestering BMPs, preventing receptor activation and downstream signaling (89). On the other hand, inhibitory Smads also inhibit TGF-β/BMP but can do so in multiple ways, such as preventing R-Smad complex translocation to the nucleus or promoting R-Smad complex degradation (94). Nonetheless, in most of the animal studies realized to date, the overexpression of these extracellular antagonists and intracellular inhibitors of the TGF-β/BMP signaling leads to a marked reduction in bone formation, whereas their specific deletion in bone tissues generally increases bone mass (89,95). As such, regulators of TGF-β/BMP coordinate important bone remodeling mediated processes and offer advantageous therapeutic treatment strategies for treating bone disorders of low bone mass.

Most of the TGF-β/BMP signaling regulators involved in skeletal development and bone homeostasis so far presented seem to exert negative effects in osteoblast differentiation, but are nonetheless important in regulating bone remodeling and in maintaining overall bone mass when expressed at physiological levels. It is however important to note that other factors also exist which can positively influence and control osteoblast differentiation while still being essential for the maintenance of bone mass (96). One of such factors is the nuclear protein menin, which facilitates R-Smad mediated transcriptional responses.

1.6 Multiple Endocrine Neoplasia Type-1 (MEN1) & menin

Menin is the protein product of the multiple endocrine neoplasia type-1 (*MEN1*) gene, which maps to human chromosome 11q13, that was first identified by Chandrasekharappa and colleagues in 1997 by positional cloning (97,98). Menin is widely expressed in many tissues of the body. Its expression starts early in development and continues postnatally (99).

Over 500 independent germline and somatic mutations scattered throughout the 10 coding exons region of the *MEN1* gene that cause the hereditary autosomal dominant MEN1 disorder have been identified (100). The majority of these mutations have clear inactivating effects and lead to truncated menin products (97,99,100,101). Patients carrying a germline *MEN1* mutation are predisposed to developing tumors in select endocrine and non-endocrine tissues throughout their lifetime. Tumors in patients arise due to the somatic loss of the wild-type *MEN1* allele (the second hit) and these most often occur in the parathyroid, pancreas and pituitary gland (100,101). MEN1 patients however can show a broad phenotype with more than 20 different manifestations occurring in endocrine and non-endocrine tissues (102). Primary hyperparathyroidism as a result of parathyroid tumors is the most common symptom observed in MEN1 patients (103). Other manifestations, such as adrenal adenomas, lipomas, and neuroendocrine tumors of the lungs, thymus or stomach can also occur in MEN1 patients, but the metastatic pancreatic neuroendocrine tumors (pNETs) are the most frequent MEN1-related causes of morbidity and mortality (102,103,104). It is important to note that aside from its definite tumor suppressor role in MEN1 cases, menin may also possess other functions in the tissues in which it is expressed.

1.7 Cellular functions of menin

Human menin consists of a 610 amino-acid sequence and shows no molecular similarities to other known proteins. It possesses two nuclear localization signals (NLS) in its carboxyl-terminal end, both at amino acid positions 479 to 497 and 588 to 608, and hence is primarily located in the nucleus (105). Menin acts as a scaffold protein by interacting with many proteins involved in transcriptional regulation and chromatin modification in order to regulate gene expression as illustrated in figure 1.7 (106). In this model, menin links transcription regulation with chromatin modification, and thus can either act as a repressor or activator of gene transcription depending upon the particular transcription factor involved. Menin also plays important roles in DNA replication, DNA repair and cell cycle progression (107). The crystal structure of menin was recently reported from sea anemone (*N. vectensis*) and human where it was shown that menin contains a deep protein pocket that is covered by a β-sheet motif. This pocket also constitutes the binding site for transcription factors such as JunD and the mixed lineage leukemia (MLL) complex (108,109,110). Some of menin's interacting partners will now be discussed in more detail.

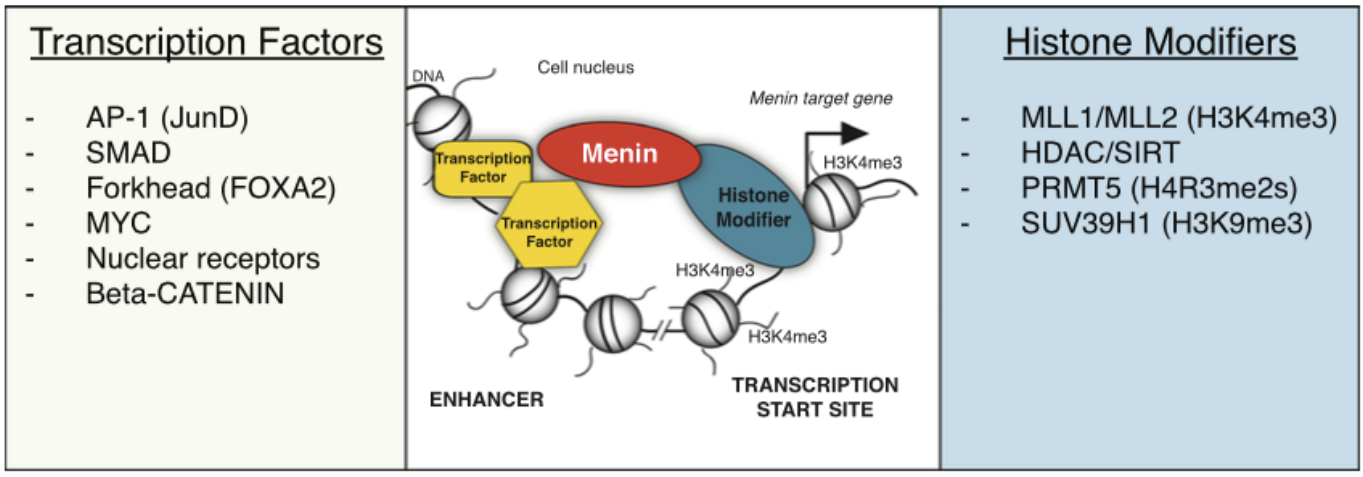

Figure 1.7: **Menin interacting partners in the nucleus.** Menin can interact with many classes of transcription factors (e.g. JunD) and histone-modifying protein complexes (e.g MLL1) in order to link transcriptional regulation with chromatin regulation. Reproduced with permission from Dreijerink KMA, Timmers HTM, Brown M. Twenty years of menin: emerging opportunities for restoration of transcriptional regulation in MEN1. *Endocrine Related Cancer*. 2017;24(10): T135-T45.

1.8 Menin interacting partners & functions

1.8.1 AP-1 transcription factor

The activator protein-1 (AP-1) family of transcription factors are dimeric transcription factors consisting of Jun, Fos and activating transcription factor (ATF) families of proteins (111,112). In response to extracellular stimuli, AP-1 transcription factors bind to a common AP-1 DNA binding site to regulate gene expression and control a variety of cellular processes which include cell proliferation, differentiation and apoptosis (111,112). JunD was the first interacting partner of menin to be identified by in 1999 (113). In that study it was shown that menin represses the transcriptional activation of JunD. It was also demonstrated that menin interacted specifically with the JunD subunit and not with other Jun or Fos family members (113). Other research groups have further demonstrated that menin represses the activity of JunD and this in a histone deacetylase-dependent mechanism, whereby menin has been shown to associate with an mSin3A-histone deacetylase complex. This in turn led to the repression of menin/JunD target genes (114,115). Inactivating mutations occurring in MEN1 patients are thus thought to alter this repression and result in the dysregulation of cellular growth control, ultimately causing tumors in endocrine tissues (113-115).

1.8.2 MLL complex

The MLL complex is a transcriptional co-activator that belongs to the group of histone-modifying enzymes that are important for chromatin remodeling and gene expression regulation (116). Chromosomal rearrangements of the MLL gene are the cause of certain acute leukemias in both children and adults (116). Menin has been reported to be an essential component of a histone methyltransferase complex, such as the MLL complex (MLL1/MLL2), that trimethylates lysine 4

of histone 3 (H3K4me3) (117). Through its interaction with the MLL complex, menin mediates the histone methyltransferase activity, and in doing so has been linked to the transcriptional activation of homeobox Hox genes (e.g. *Hoxc8*) essential for early development and cyclin-dependent kinase (CDK) inhibitors, like *p18* and *p27*, which play determinant roles in cell cycle control and in regulating pancreatic islet growth (117,118,119,120).

1.8.3 β-catenin

Menin has been shown to also physically interact with β-catenin in a number of studies (121,122,123). However, its particular role in the canonical Wnt-β-catenin signaling seems to vary depending on the precise cell type involved. In murine islet cells, menin was reported to stimulate the Wnt signaling by interacting with T-cell factor 3 (TCF3), a transcription factor that β-catenin interacts with (121). Alternatively, in another study using mouse insulinoma cells in which the *Men1* gene was knocked-out, menin was shown to mediate nuclear translocation of β-catenin into the cytoplasm, thus suppressing its transcriptional activity (122). A more recent study using transgenic mouse models where the *Men1* gene and the *Ctnb1* gene (encoding β-catenin) were specifically knockout in pancreatic β-cells demonstrated that the tumorigenesis potential of mice lacking both the *Men1* and *Ctnb1* was less than those lacking only *Men1* (124). These *in vivo* results suggest that menin interaction with β-catenin is required for adequate control of cellular growth and that the loss of this interaction leads to the development of tumors in the pancreas.

1.8.4 TGF-β superfamily

Signals transmitted through members of the TGF-β superfamily are transduced by Smad proteins. In the nucleus, Smad complexes need other partners to facilitate their binding to DNA

and modulate gene transcription in response to cell signaling. Menin has been reported to be one of them. Studies have shown that menin can interact with and co-activate Smad1, Smad3 and Smad5 (125, 126). As previously discussed, Smad3 is a TGF-β specific Smad, whereas Smad1 and Smad5 are BMP specific Smad proteins. *In vitro* studies where menin was inactivated with antisense RNA resulted in the inhibition of the TGF-β signaling due to unsuccessful binding of the Smad3/4 complex at DNA specific transcriptional regulatory sites, resulting in high cell proliferation (127). In that study, menin did not however affect the association between Smad3 and Smad4, nor the nuclear translocation of the Smad3/4 complex, but TGF-β itself did regulate menin's expression in a dose-dependent manner (127). Hence, menin is needed for signaling pathways involving members of the TGF-β superfamily and in this sense also required for controlling the growth of many cell types (e.g. parathyroid & pituitary cells) which TGF-β signaling is known to negatively regulate (128,129,130,131). These observations are consistent with menin's function as a tumor suppressor.

1.8.5 Menin and other protein partners

The studies so far presented on menin and its interacting partners highlight its role as a tumor suppressor, but its functions are not only limited to that. Through its interactions with proteins like FANCD2 and FOXN3, menin is also involved in DNA repair mechanisms (132,133). It can also associate with certain cytoskeletal elements, like nonmuscle myosin II-A heavy chain (NMHC II-A) and glial fibrillary acidic protein (GFAP) to play a role in cytokinesis during the cell-division cycle (134,135). Recent studies have also demonstrated that menin can interact with certain nuclear receptors, which include the estrogen receptor α (ERα), the vitamin D receptor (VDR) and the peroxisome proliferator-activated receptors (PPAR) α and γ (136,137,138). In this

perspective, menin acts as a coactivator of nuclear receptor-mediated transcription and can be implicated in the regulation of certain cellular differentiation processes, like adipogenesis and myogenesis (136,139,140).

Taking all of these findings together, menin is widely expressed in many tissues of the body, but can assume a variety of functions and interact with different molecular elements that regulate a wide range of biological processes. For the purpose of this thesis, the specific implications of menin in bone development as well as in myogenesis and adipogenesis will be explored and discussed in greater detail.

1.9 Role of menin in myogenesis & adipogenesis

Signaling through BMP-2 and TGF-β1 play essential roles during both osteogenesis and myogenesis by regulating the expression of important transcription factors dictating lineage commitment, such as MyoD for muscle differentiation, and Runx2 for osteogenic differentiation (141,142). During myogenesis, BMP-2 and TGF-β1 signaling mediated by R-Smad proteins inhibit MSCs differentiation into muscle cells by mechanisms that are thought to repress MyoD activity (140,142). Because menin is a nuclear protein known to mediate R-Smads transcriptional responses, the role that it has in modulating myogenesis was established in a report which specifically investigated its effects in controlling the commitment and differentiation of muscle cells from MSCs *in* vitro (140). In that study it was demonstrated that menin acts as a molecular rheostat regulating the balance of MSC commitment to both osteogenic lineage and myogenic lineages (figure 1.8). Through its interaction with R-Smads, menin was in fact proposed to potentiate BMP-2/ TGF-β1 mediated inhibition of myogenesis (140).

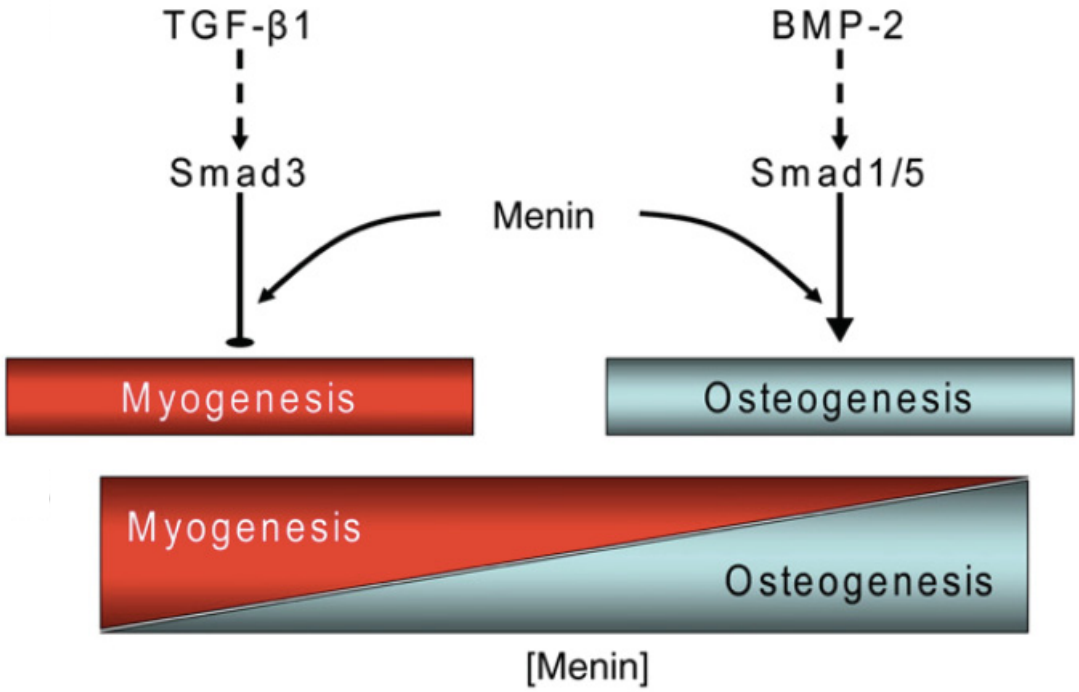

Figure 1.8: Role of menin in myogenesis and osteogenesis. Menin expression level is negatively correlated with MSC commitment to the myogenic lineage. Downstream TGF-β1 signaling, menin interacts with Smad3 and represses myogenesis in MSCs. However, through its interaction with Smad1/5 downstream the BMP-2 signaling, menin promotes osteogenesis. Reproduced with permission from Aziz A, Miyake T, Engleka KA, Epstein JA, McDermott JC. Menin expression modulates mesenchymal cell commitment to the myogenic and osteogenic lineages. *Developmental Biology*. 2009;332(1):116-30.

The clinical presentation of lipomas, which are benign fat-cell tumors, is common in MEN1 cases, occurring in approximately 30% of the affected patients (143). However, their mechanism of formation is at the moment still not fully known. PPARγ is a nuclear receptor which associates with retinoid X receptors (RXRs) in the nucleus in order to regulate the transcription of genes involved in adipocyte differentiation (144). In humans, mutations occurring in the gene encoding PPARγ, *PPARG*, are known to cause partial lipodystrophy, a genetic metabolic condition characterized by the loss of subcutaneous fat (144). Reports have demonstrated that PPARγ is also expressed in many of the MEN1-associated tumors (145,146). Hence, studies have investigated whether menin could interact with PPARγ in order to be a molecular reason causing lipomas. In a

report by Dreijerink *et al*., menin was shown to interact with PPARγ and to act as a transcriptional coactivator (138). Through this interaction, menin was reported to be essential in mediating PPARγ-dependent adipocyte differentiation *in vitro* by regulating the transcription of genes involved in adipogenesis (138). In another *in vitro* study, menin knockdown in MSCs resulted in the increase of the size of fat-cells, revealing another role of menin in the regulation of adipogenesis (139).

1.10 Functions of menin in bone homeostasis

As previously mentioned, in humans, mutations occurring in the *MEN1* gene that encodes menin cause the MEN1 disorder, which is most clinically characterized by the development of tumors in the parathyroid, pancreas and pituitary glands (100,102,103). Germline homozygous inactivation of the *MEN1* gene is predicted to be lethal in patients. Individuals with heterozygous *MEN1* gene mutation however often exhibit parathyroid tumors and have high circulating PTH levels due to overproduction and secretion from the parathyroid cells of the parathyroid gland (100,102,103). As a result, it is difficult to evaluate the direct effects of heterozygous *MEN1* mutations on bone in MEN1 patients, as it is unclear if such effects are due to a direct consequence of the *MEN1* gene disruption within bone cells or to high PTH levels which can also affect bone metabolism, or both. Hence, the analyses of menin's functions in bone homeostasis come mainly from *in vitro* and animal studies. These investigations have provided more information about the role that menin plays downstream of signaling pathways important for osteoblastogenesis.

1.10.1 Menin & TGF-β/BMP signaling in bone

Menin is required for the proper signaling of pathways activated by members of the TGF-β superfamily that are essential for the development and cellular regulation of many organs. However, the implication of menin downstream of these pathways is not only limited to its tumor suppressing role through controlling cellular growth. As previously presented, menin can interact with Smad3, a protein that transduces TGF-β-mediated signaling. As for menin's interaction with other Smad proteins and the implication this has for bone metabolism, our group has shown that menin is needed for both the early differentiation of osteoblasts and inhibition of their later differentiation, by interacting with BMP-2 regulated Smads (Smad-1/5) and Smad3 downstream of TGF-β1 signaling (125). The use of menin antisense oligonucleotides in cultures of C3H10T1/2 mouse pluripotent mesenchymal cell lines revealed significantly reduced ALP activity and expressions of *Col1α1*, *Runx2* and *Ocn* induced by BMP-2. Menin was also shown to physically and functionally interact with Smad1 and Smad5, and its inactivation antagonized BMP-2-induced transcription (125). However, stably inactivating menin in cultures of mouse osteoblastic MC3T3-E1 cells led to an increase in ALP activity and mineralization. Taking together, since C3H10T1/2 cells are MSCs which haven't yet become committed to the osteoblast lineage, this shows that in the early commitment of MSCs to the osteoblast lineage, menin interacts with the Smad1/5 components downstream of the BMP-2 signaling pathway to facilitate commitment (125). On the other hand, after commitment occurs menin seems to retard later osteoblast differentiation. In another study, our group demonstrated this to be due to menin interaction with Smad-3 downstream of the TGF-β signaling pathway (figure 1.9) (126). This study also showed that menin interacts with Runx2 only in uncommitted MSCs, but not in well-differentiated osteoblasts. Hence, as depicted in the schematic figure 1.9, in differentiated osteoblasts menin interacts mostly with

the Smad3 of the TGF-β pathway in order to negatively regulate BMP-2/Smad-1/5 and Runx2-mediated transcriptional activities, inhibiting the later differentiation of committed osteoblasts (126).

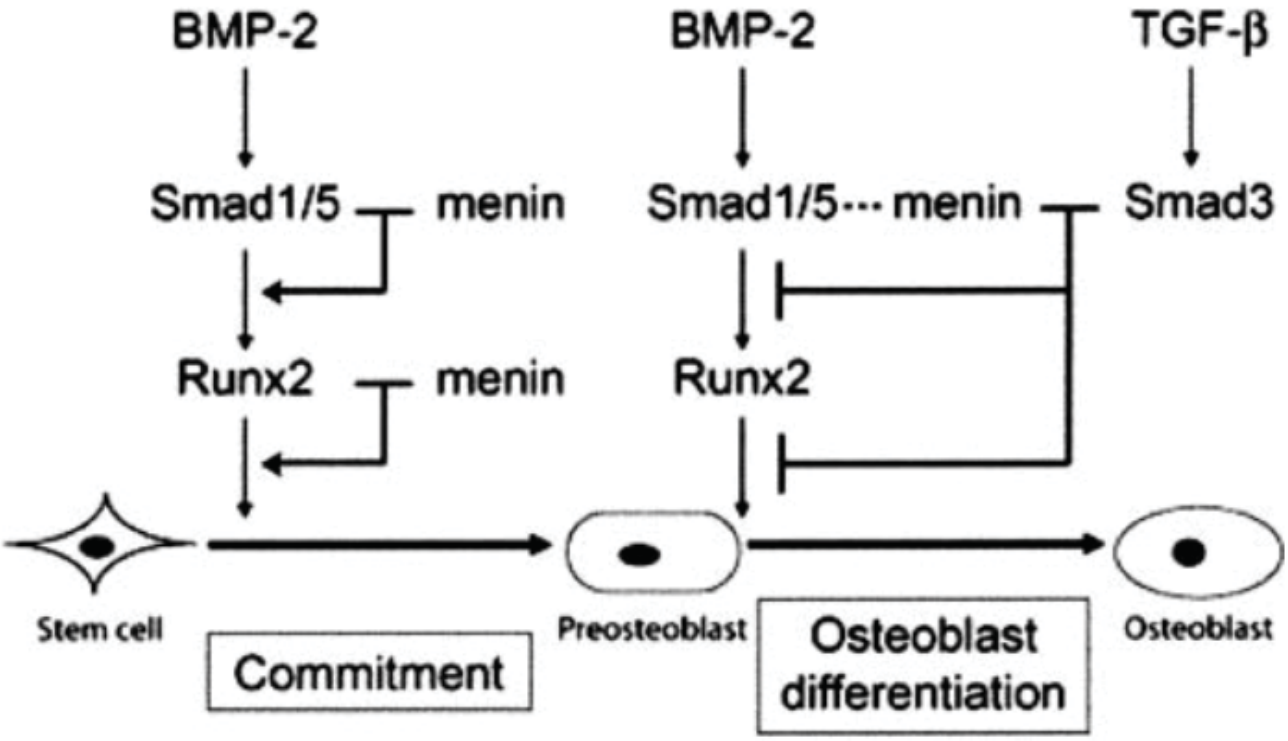

Figure 1.9: Role of menin during osteoblast commitment and differentiation. At the earlier stages of osteoblastogenesis, menin facilitates the commitment of MSCs to the osteoblast lineage by associating with Smad1/5 and Runx2 transcription factors which mediate BMP-2 signaling. At later stages of osteoblast differentiation, menin interacts with Smad3 downstream of TGF-β signaling and suppresses later osteoblast differentiation by negatively regulating BMP-2 signaling mediated by Smad1/5 and Runx2. Reproduced with permission from Sowa H, Kaji H, Hendy GN, Canaff L, Komori T, Sugimoto T, Chihara K. Menin is required for BMP-2 and TGF-β -regulated osteoblastic differentiation through interaction with Smads and Runx2. *Journal of Biological Chemistry*. 2004;279(39):40267-75.

1.10.2 Menin & JunD in osteoblastogenesis

The role of AP-1 family members in bone biology has been investigated by many studies using genetically modified mice which have demonstrated that their loss can affect bone development and growth (147). From the different AP-1 transcription factors studied, only JunD is to date known to bind to menin. A study published by Naito *et al*. in 2005 examined the role that menin-JunD interaction plays in bone through *in vitro* analysis (148). The authors found that menin-JunD interaction occurs in osteoblasts and that JunD is important in promoting osteoblast differentiation (148). Use of antisense oligonucleotides against menin increased JunD levels, whereas overexpression of menin inhibited both transcriptional and ALP activities induced by JunD in the osteoblast cell cultures. This shows that in osteoblasts, menin interacts with JunD and antagonizes its osteoblastic bone promoting activity by suppressing osteoblast differentiation.

1.10.3 Menin & β-catenin in osteoblastogenesis

Wnt proteins regulate many bone biological processes including the commitment of MSCs to the osteogenic and chondrogenic lineages (149). β-catenin is a crucial component of the Wnt signaling pathway that transduces signals in order to regulate gene transcription (149). Menin is known to interact with β-catenin and to control cellular growth of many tissues (121-124). As for bone, our group has revealed that menin can physically and functionally interact with β-catenin and LEF-1 (transcriptional regulator of the Wnt-β-catenin pathway) in both mouse mesenchymal and osteoblastic cells (123). This interaction was found to be important in facilitating the commitment of MSCs to become osteoblasts as well as playing a role in BMP-induced osteoblast differentiation (123).

From the studies presented herein, menin expression and interacting proteins in bone are important for regulating osteoblast differentiation. To sum up menin's implication in osteoblastogenesis, studies involving members of our group have shown that in the early stages of differentiation, menin promotes BMP-2 and Runx2-induced differentiation of MSCs into osteoblasts by interacting with Smad-1/5, Runx2 and β-catenin. However, in the later stages of osteoblast differentiation, menin's role differs and rather suppresses later stage osteoblastic differentiation through its interaction with Smad3 downstream of the TGF-β pathway and JunD. It is important to note that the elucidated functions of menin in bone homeostasis presented so far come mainly from *in vitro* results. *In vivo* studies using transgenic mice have since then been performed and have shed more light onto menin's role in bone.

1.10.4 Animal studies of menin and bone

Menin is expressed in many tissues of the body, including in bone (99). Homozygous constitutional *Men1-/-* deletion in mice is embryonic lethal, with most of the mice dying *in utero* at embryonic day 11.5-13.5 due to developmental deficiencies in multiple organs (150,151). The fetuses of *Men1-/-* are also smaller compared to wild-type *Men1+/+* mice and exhibit craniofacial defects (figure 1.10) (150,151). Because craniofacial bones are formed through intramembranous bone ossification, these were the first studies to show a potential role of menin in the commitment of MSCs to the osteoblast lineage and further differentiation. Heterozygous *Men1+/-* mice however displayed a normal bone phenotype, the same as haploinsufficient humans harboring a germline inactivating mutation in only one *MEN1* allele (150,151, 152,153).

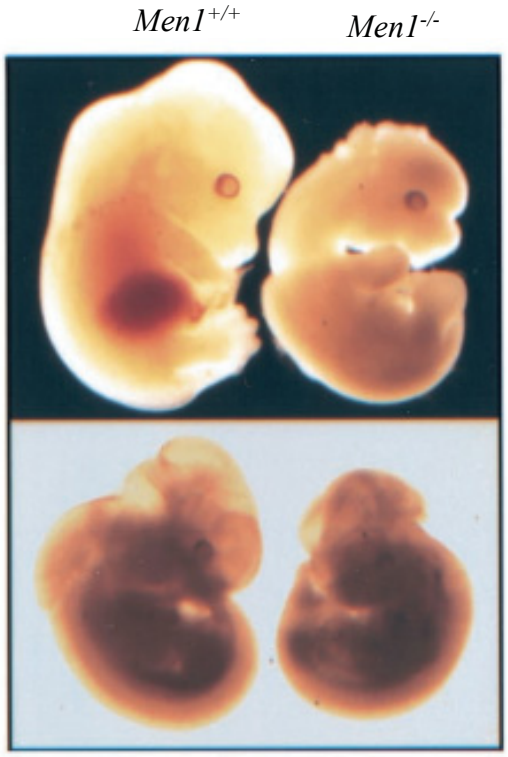

Figure 1.10: Effect of *Men1*$^{-/-}$ in mice embyos. Homozygous *Men1* deletion in mice is embryonically lethal. *Men1*$^{-/-}$ mice also exhibit developmental delay, craniofacial defects as well as neural tube defects, illustrating a potential role of menin in bone development. Reproduced with permission from Crabtree JS, Scacheri PC, Ward JM, Garrett-Beal L, *et al*. A mouse model of multiple endocrine neoplasia, type 1, develops multiple endocrine tumors. *Proceedings of the National Academy of Sciences of the U S A*. 2001;98(3):1118-23.

A study by Engleka *et al*. using mouse models in which menin was conditionally deleted in Pax3- and Wnt1- expressing neural crest cells (that give rise to diverse cell lineages including MSCs that become osteoblasts), reported perinatal death, cleft palate and other cranial bone defects in the transgenic mice (154). It was also shown that menin deletion in Pax3-somite precursors results in patterning defects of rib formation (154). These findings reiterate the crucial role that menin plays in intramembranous ossification and skeletal development *in vivo*.

1.10.5 Role of menin in mature osteoblast *in vivo*

The functions that menin plays in bone development *in vivo* was recently investigated by our group using conditional knockout mice models in which the *Men1* gene was specifically deleted in the mature osteoblast (155). For this study, the Cre-LoxP recombination system was used, whereby osteocalcin (OC)-Cre mice were crossed with *Men1f/f* mice having loxP sites flanking exons 3 and 8 of the *Men1* gene to generate *OC-Cre; Men1f/f* knockout mice. Through dual X-ray absorptiometry (DXA), the bone mineral densities of nine month-old *OC-Cre; Men1f/f* mice were significantly reduced compared to wild-type *Men1f/f* control animals of the same age (155). Micro-computed tomography (μCT) of *OC-Cre; Men1f/f* femurs also showed significant decreases in cortical thickness, trabecular number and bone volume in comparison to control littermates, indicating an overall decrease in bone mass in the knockout animals. Histomorphometric analysis at nine months of age also revealed significant reductions in the bone volume density and mineral apposition rate as well as in the numbers of osteoblasts and osteoclasts. Interestingly, the number of osteocytes was found to be significantly higher in knockout mice. These *in vivo* observations suggest that loss of menin might affect the osteoblast differentiation process causing more osteoblasts to become osteocytes than to remain osteoblasts that create the bone matrix.

In vitro, using primary calvarial osteoblast from age and sex-matched *OC-Cre; Men1f/f* and *Men1f/f* mice*,* the proliferative, differentiation and mineralization capabilities of osteoblasts were all shown to be impaired (155). Alizarin red and von Kossa staining were used to assess extracellular calcium and phosphate deposition, respectively, within the cellular matrix, and intensities were found to both be drastically reduced in menin deficient calvarial osteoblasts. The ALP intensity of the calvarial osteoblasts from knockout mice was as well significantly reduced.

Interestingly, the rate of cellular proliferation of the primary osteoblast from knockout mice was significantly higher than that of control. These results suggest that although the osteoblasts are proliferating at a much faster rate, they could consequently enter apoptosis quicker, hence preventing them from producing an extracellular matrix and expressing *ALP*. This hypothesis was further corroborated through gene expression analysis that revealed significant decreases in osteoblast differentiation markers (e.g. *Runx2*, *ALP*) and in CDK inhibitors (e.g. *p15*, *p21*), as well as significant increases in apoptosis markers (*Bax*, *BAD*). Levels of osteocyte markers, such as *sclerostin*, *phex* and *DMP1* were all found to be significantly elevated in the knockout cells which is consistent with the histomorphometry observations revealing high numbers of osteocytes. Overall, these *in vitro* findings illustrate that the function of menin-deficient osteoblasts is altered, with the cells proliferating more rapidly than normal to either undergo apoptosis or become osteocytes.

The expression of the osteoclast markers, RANKL and OPG, was assessed in cultures of primary calvarial osteoblasts. It was demonstrated that levels of both *RANKL* and *OPG* were significantly decreased. However, the expression of *RANKL* was more reduced than that of *OPG*, resulting in an overall decrease in the *RANKL/OPG* ratio. It is known that the RANKL/OPG ratio is an important determinant of osteoclastogenesis (21,32). In this case, the low RANKL/OPG could explain the significant reduction in the numbers of osteoclast in bone *in vivo*. This was further corroborated with osteoblast-osteoclast co-culture experiments also showing decreases in the osteoclast numbers *in vitro* (155).

This study further investigated whether overexpression of menin ameliorates the bone phenotype of adult mice. For this, transgenic mice, represented as *Col1a1MeninTg*, in which human menin cDNA was overexpressed in differentiated osteoblasts were generated. Histomorphometric and μCT analysis performed at twelve months of age revealed overall increases in bone volume density, trabecular number, mineral apposition rate and osteoblast numbers in the *Col1a1MeninTg* mice. However, the number of osteoclast and osteocytes which were initially decreased and increased in the knockout menin mice, were unchanged in *Col1a1MeninTg*. Overall, the phenotype of transgenic mice overexpressing menin in the differentiated osteoblast was a mirror image to those lacking menin, suggesting that osteoblast menin is important in maintaining bone mass (figure 1.11) (155).

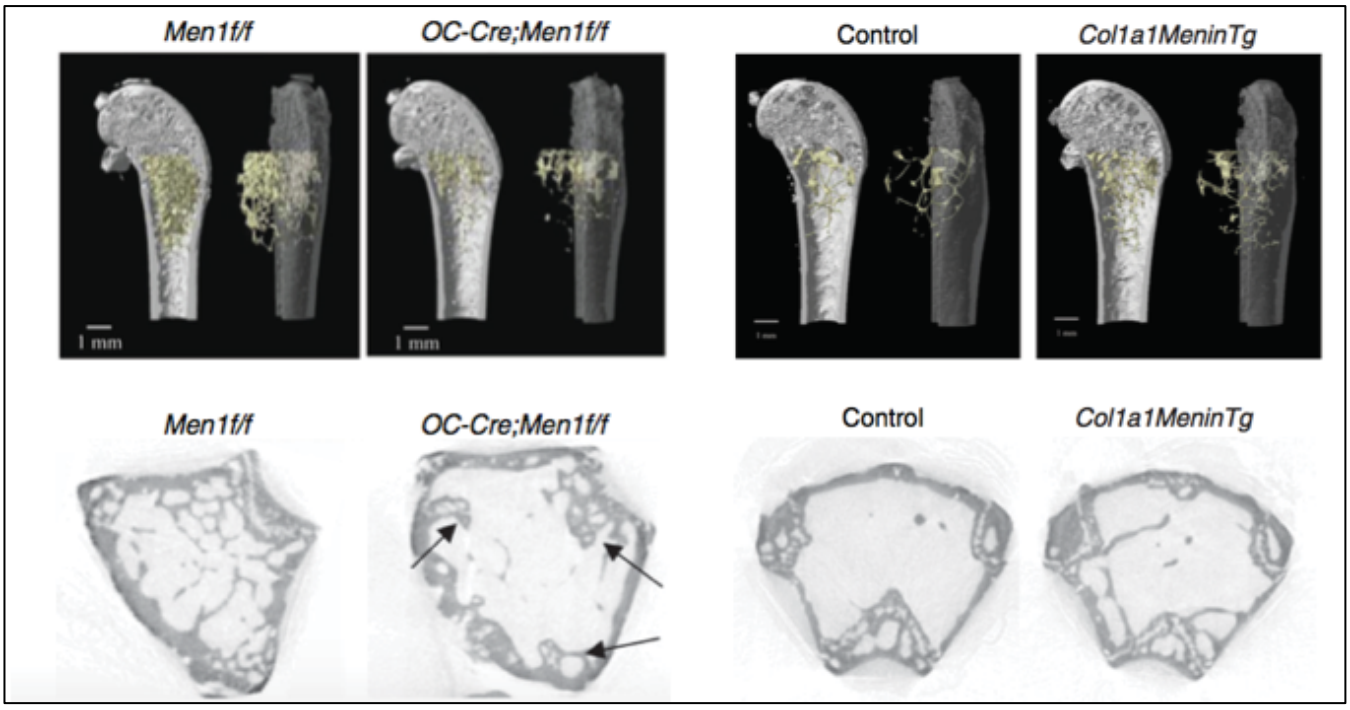

Figure 1.11: Effect of menin deletion and overexpression in mature osteoblasts. μCT analysis of distal femurs of 9 month-old *OC-Cre; Men1f/f* mice revealed marked decreases in total bone and trabecular bone volumes in comparison to control *Men1f/f* mice. Distal femurs of 12 month-old transgenic *Col1a1MeninTg* mice specifically overexpressing menin in the mature osteoblast showed substantial increases in total bone and trabecular bone volumes in comparison to control *Men1f/f* mice. Reproduced with permission from Kanazawa I, Canaff L, Abi Rafeh J, Angrula A, Li J, Riddle RC, Boraschi-Diaz I, Komarova SV, Clemens TL, Murshed M, Hendy GN. Osteoblast menin regulates bone mass in vivo. *Journal of Biological Chemistry*. 2015;290(7):3910-24.

These findings made by our group confirmed the essential role of menin initially established by *in vitro* studies in mediating bone development and maintenance. This also provided strong evidence that menin is playing a functional role in the mature osteoblast *in vivo*, with the bone phenotype being significantly altered in its absence. Further pursuing on these findings, it will be particularly important to investigate the roles that menin plays at earlier stages of osteoblast differentiation, from the commitment of MSCs via osteoprogenitors to the osteoblasts.

1.10.6 Role of menin in osteoprogenitors *in vivo*

To investigate the *in vivo* role that menin plays when it is expressed early in the osteoblast lineage, our group has proceeded to the generation of *Prx1-Cre; Men1f/f* and *Osx-Cre; Men1f/f* conditional knockout mice using the Cre/loxP recombination system. These represent mice which are deficient for menin specifically at the level of the MSC and preosteoblast, respectively. So far, certain *in vivo* results have been obtained by our lab through analysis of the skeletal phenotyping of *Prx1-Cre; Men1f/f* and *Osx-Cre; Men1f/f* mice.

DXA analysis showed that the BMD of femurs was significantly decreased in 6 month-old *Prx1-Cre; Men1 f/f* and *Osx-Cre; Men1f/f* mice in comparison to their control littermates (156). Three-dimensional μCT analysis was performed as well on the distal femurs from both mouse lines and demonstrated significant decreases in bone volume, bone surface and trabecular number in 6 month-old knockout mice in comparison to wild-type littermates (figure 1.12).

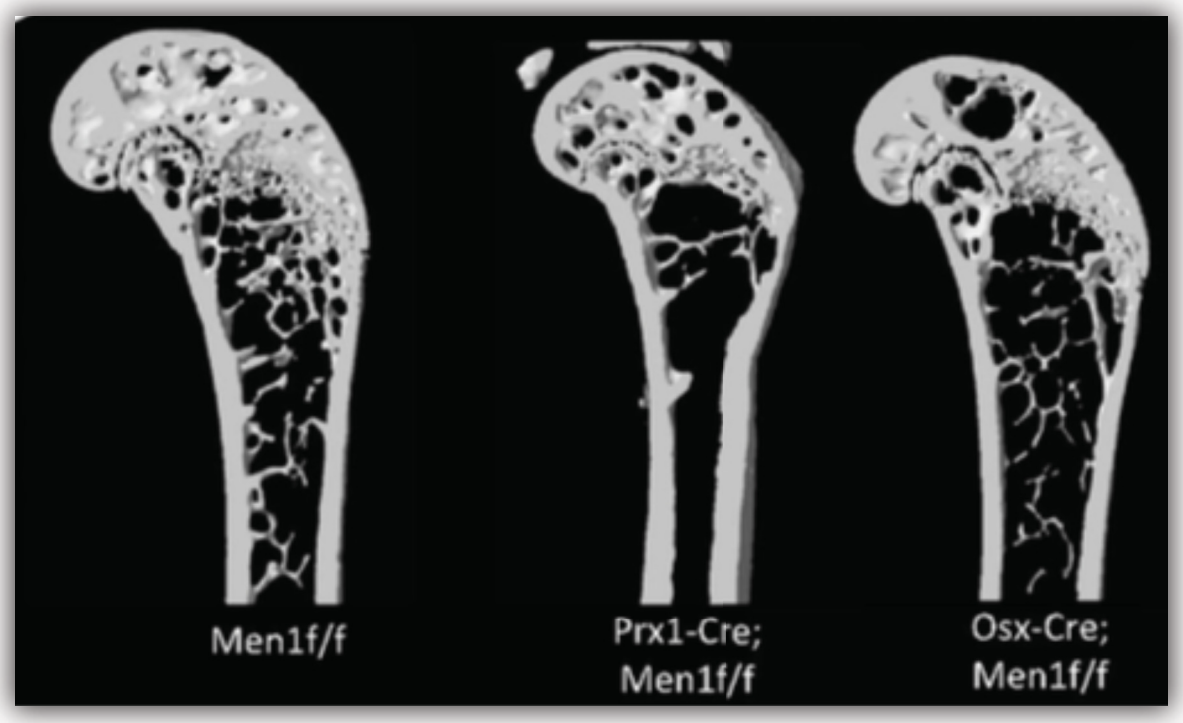

Figure 1.12: Representative images of mirco-CT analysis of the femurs of knockout mice. Total bone volume and trabecular bone volume of distal femurs from 6 month-old *Prx1-Cre; Men1f/f* and *Osx-Cre; Men1f/f* mice are significantly reduced in comparison to control *Men1f/f* mice (n=6).

Static and dynamic histomorphometry analyses were also performed in the current study (156). Parameters such as the bone structure, formation and resorption were measured in the distal femurs of both *Prx1-Cre; Men1f/f* and *Osx-Cre; Men1f/f* mice in comparison to their control wild-type *Men1f/f* littermates. The data obtained by our lab from these analyses revealed unchanged levels in terms of the number of osteoblasts and in the mineral apposition rates between knockout and wild-type mice. Interestingly, the number of osteoclasts and the percentage of erosion surface to bone surface were significantly increased (table 1.1). Hence, in the current study deleting menin early in the osteoblast lineage reduces bone mass, and this as a result of the increased bone resorption taking place.

Parameters	*Men1f/f* **Mean** ± SEM	*Osx-Cre;Men1f/f* **Mean** ± SEM
Bone Volume/ Total Volume (%)	8.24 ± 0.91	4.96 ± 0.67*
# Osteoblasts/Bone Perimeter (#/100mm)	375 ± 161	336 ±122
# Osteoclasts/Bone Perimeter (#/100mm)	65.9 ± 24.6	165.5 ± 23.7*
Mineral Apposition Rate (μm/day)	0.91 ± 0.08	1.02 ± 0.08
Erosion Surface/Bone Surface (%)	2.43 ± 0.75	5.83 ± 1.20*

Parameters	*Men1f/f* **Mean** ± SEM	*Prx1-Cre; Men1f/f* **Mean** ± SEM
Bone Volume/ Total Volume (%)	8.71 ± 0.56	6.05 ± 0.92*
# Osteoblasts/Bone Perimeter (#/100mm)	424.3 ± 71.8	376.6 ± 59.8
# Osteoclasts/Bone Perimeter (#/100mm)	96.7 ± 15.5	253.2 ± 42.4*
Mineral Apposition Rate (μm/day)	1.08 ± 0.08	1.02 ± 0.09
Erosion Surface/Bone Surface (%)	2.89 ± 0.35	7.01 ± 1.55*

Table 1.1: Dynamic and static histomorphometric analysis of the femurs of knockout mice. Parameters such as bone volume %, number of osteoblasts, number of osteoclasts, mineral apposition rate and erosion surface/bone surface (%) were assessed from femurs of 16 week-old *Prx1-Cre; Men1f/f* (n=10,11) and 14 week-old *Osx-Cre; Men1f/f* (n=7) mice. Significant increases in the number of osteoclasts and in the % of bone resorption are observed in knockout mice, indicating increased degree of osteoclastogenesis. * $P < 0.05$

CHAPTER 2: RATIONALE AND OBJECTIVES

Our lab has previously illustrated the importance of menin for proper functioning of mature osteoblasts and maintenance of bone mass in adult mice. More specifically, our group demonstrated that menin regulates osteoblast differentiation, mineralization and controls apoptosis of mature osteoblasts. These data were reported using *OC-Cre; Men1f/f* transgenic mice in which the *Men1* gene was specifically deleted in mature osteoblast. In the current study, the *in vivo* role that menin plays when it is expressed at earlier stages of osteoblast differentiation is being examined. For this, transgenic *Prx1-Cre; Men1f/f* and *Osx-Cre; Men1f/f* mice which represent specific knockout of the *Men1* gene at the level of the MSC and preosteoblast were generated. We hypothesized that the early expression of menin in the osteoblast lineage is essential for maintaining bone mass and for bone homeostasis. *In vivo* results that have been obtained by our lab through analysis of *Prx1-Cre; Men1f/f* and *Osx-Cre; Men1 f/f* mice show that BMD along with the total bone volume and trabecular bone volume of femurs are reduced when compared to wild-type littermates. Moreover, we observed unaltered changes in osteoblasts numbers *in vivo*, but significant increases in both osteoclast number and activity. To further pursue on these findings, my project objectives presented in this thesis were to:

1) Complete the skeletal phenotypic assessment of knockout mice by analyzing changes in bone quality and strength.
2) Characterize metabolic phenotypic changes taking place in transgenic mice when menin is deleted in osteoprogenitors.
3) Examine the *ex vivo* extent of proliferation, differentiation and mineralization of primary calvarial osteoblasts and bone marrow stromal cells (BMSCs) when menin is deleted early in the osteoblast lineage.

4) Examine the gene expression profile of cultures of primary calvarial osteoblasts and BMSCs.
5) Investigate the cause of the increase in osteoclast activity observed *in vivo*.

CHAPTER 3: MATERIALS & METHODS

3.1 Mice breeding

Men1$^{flox/flox}$ mice that possess loxP sites flanking exons 3-8 of the *Men1* gene and which were previously used by our lab were obtained from the Jackson Laboratory (155,157). *Pair-related homeobox gene 1-Cre* transgenic mice (*Prx1-Cre*$^{TG/+}$) and *Osterix-Cre* transgenic mice (*Osx-Cre*$^{TG/+}$) were also obtained from the Jackson Laboratory (158,159). For the generation of conditional knockout mice in which menin is specifically deleted at the level of the MSC, *Men1*$^{flox/flox}$ mice of an FVB background were first crossed with *Prx1-Cre*$^{TG/+}$ mice which were on a C57BL/6 background. The resulting *Prx1-Cre*$^{TG/+}$*; Men1*$^{+/flox}$ mice were then crossed with *Men1*$^{flox/flox}$ mice to generate *Prx1-Cre*$^{TG/+}$*/Men1*$^{flox/flox}$ mice. These were then crossed with *Men1*$^{flox/flox}$ to have litters where all mice have a floxed *Men1* gene, but where only half would express the Cre recombinase transgene. To maintain the mice colony *Prx1-Cre*$^{TG/+}$*; Men1*$^{flox/flox}$ mice were crossed with *Men1*$^{flox/flox}$ mice. The same above procedure was repeated with *Osx-Cre*$^{TG/+}$ mice for the generation of conditional knockout mice in which menin is specifically deleted at the level of the preosteoblast. The control littermate mice were designated as *Men1f/f* and knockout mice as *Prx1-Cre; Men1f/f* and *Osx-Cre; Men1f/f*.

3.2 Animals

Mice were maintained in a pathogen-free standard animal facility, and experimental procedures were performed following an animal use protocol approved by the animal Care and Use Committee of McGill University. This protocol is also conform to the ethical guidelines of the Canadian Council on Animal Care. Mice colonies were maintained on a 12-hour alternating light/dark cycle at 22-26^{0}C and fed a rodent chow diet (Envigo; Product# T.2918.15) containing 1.0% calcium, 0.7% phosphorus and 1.5 IU vitamin D_3/g.

3.3 Genotyping

Genomic DNA was obtained and isolated from *Men1f/f*, *Prx1-Cre; Men1f/f* and *Osx-Cre; Men1f/f* mice tail snips using the Quanta bioscience DNA extraction kit. The 2x green PCR Master-mix (ZmTech Scientifique, Qc, Canada) was used for polymerase chain reactions (PCR). Three different primers were employed for detecting the presence of either wild-type or floxed *Men1* alleles. Primer A (5' – CCCACATCCAGTCCCTCTTCAGCT - 3') is specific to exon 2 of the *Men1* gene. Primer B (5' - CCCTCTGGCTATTCAATGGCAGGG - 3') is specific to the wild-type sequence in intron 2 that is deleted in the cloning of the loxP sequence. Primer C (5'-CGGAGAAAGAGGTAATGAAATGGC - 3') is specific for the inserted loxP sequence. PCR with primers A and B generates a 300-bp amplicon, while PCR with primers A and C gives a 236-bp amplicon. $Men1^{flox/+}$ mice were identified as the ones having both the 300-bp and 236-bp amplicons, while $Men1^{flox/flox}$ mice would only show the 236-bp amplicon on an agarose gel. The 2x green PCR Master-mix (ZmTech Scientifique, Qc, Canada) was also used for detecting the presence of the Cre recombinase. The two primers used for detecting the Cre transgene were forward 5'–CTAGGCCACAGAATTGAAAGATCT-3' and reverse 5'-GTAGGTGGAAATTCTAGCATCATCC - 3'. The amplicon using these two primers corresponds to the internal positive control sequence that is put next to the Cre-recombinase transgene sequence in the transgenic mice provided by the Jackson Laboratory. $Prx1\text{-}Cre^{TG/+}$ and $Osx\text{-}Cre^{TG/+}$ mice were identified as those possessing a 100-bp amplicon, whereas $Prx1\text{-}Cre^{+/+}$ and $Osx\text{-}Cre^{+/+}$ mice, not expressing the Cre transgene, would show no PCR product when using these two primers.

For genotyping, the PCR conditions, using the T100^{TM} Thermal Cycler (Bio-Rad, California, USA), were as follows: 32 cycles of denaturation at 95^{o}C for 30s, annealing at 60^{o}C for 30s, and elongation at 72^{o}C for 1 minute. The PCR products were separated by gel

electrophoresis on a 2% agarose gel and were visualized using the Fluo-DNA/RNA gel staining solution (ZmTech Scientifique, Qc, Canada) with ultraviolet (UV) light using an electronic ultraviolet transilluminator (Alpha Innotech, California, USA).

3.4 Primary calvarial osteoblast isolation

Individual 5-6 month-old knockout mice and their control wild-type littermates were euthanized and their calvarias were isolated as previously described (160). Each calvaria were washed for 2 seconds in 70% ethanol and then rinsed with 1mL of PBS 1X. The calvarias were then dissected under sterile conditions in PBS 1X, making sure to remove sutures and soft tissues with a sterile scalpel. Each individual calvaria was chopped into small fragments of approximately 1-2 mm^2 and then transferred into a sterile conical in order to begin a series of enzymatic digests. One mL of freshly prepared solution I (10 mL α-MEM (Gibco, Life Technologies, USA), 125µL 0.25% trypsin (Wisent Inc.) + 5 µL collagenase P (Roche Diagnostics, Indianapolis, USA) (100mg/mL)) was then added in each conical and then incubated at 37°C for 15-20 minutes while shaking. Solution I was then discarded and replaced with 1mL of solution II (10 mL α-MEM (Gibco, Life Technologies, USA), 125 µL 0.25% trypsin (Wisent Inc.) + 10µL collagenase P (Roche Diagnostics, Indianapolis, USA) (100mg/mL)) at 37°C for 30 minutes while shaking. Lastly, solution II was aspirated and replaced with 1mL of solution III (10 mL α-MEM (Gibco, Life Technologies, USA), 125 µL 0.25% trypsin (Wisent Inc.) + 100uL collagenase II (Roche Diagnostics, Indianapolis, USA) (100mg/mL)) at 37°C for 60 minutes while shaking. For this last digestion, the tubes were shaken vigorously every 10 minutes. Solution III was then aspirated, and the fragments were washed with a solution of α-MEM (Gibco, Life technologies, USA) supplemented with 10% fetal bovine serum (FBS) (Wisent Inc.) and 1% penicillin-streptomycin

(Wisent Inc.). Calvaria fragments were then plated on a 10cm petri-dish and cultured for 5-7 days, until confluent, in α-MEM (Gibco, Life Technologies, USA) supplemented with 10% FBS (Wisent Inc.) and 1% penicillin-streptomycin (Wisent Inc.). After reaching adequate confluence, the cells were trypsinized with 0.25% trypsin/EDTA (Wisent Inc.) in order to detach the cells that migrated out of the calvaria fragments. For subsequent experiments, the bone cells were plated in differentiation medium containing 50μg/ml L-ascorbic acid (Sigma-Aldrich) and 10mM β-glycerophosphate (Sigma-Aldrich) at a density of 5 000 cells/cm^2, with the cell medium being freshly renewed 3 times each week.

3.5 Bone marrow stromal cell isolation

To isolate BMSCs, adult 5-6 month-old mice, including knockout from both the *Prx1* and *Osx* strains and their wild-type littermates, were euthanized and their femurs and tibias were carefully dissected under sterile conditions. Bones were washed for 2 seconds in 70% ethanol and then rinsed with 1 mL of sterile PBS 1X. Epiphyses of each bone were then removed and the marrow was harvested by inserting a syringe needle (27-gauge) into one end of the bone and flushed with αMEM (Gibco, Life technologies, USA) supplemented with 10% FBS (Wisent Inc.) and 1% penicillin-streptomycin (Wisent Inc.) into cell culture flasks. The next day, cells were washed three times with sterile PBS 1X in order to remove non-adherent cells. The adherent cell fraction was allowed to expand until 80% confluence and then passaged for differentiation assays. The cells were cultured in a 5% CO_2 incubator at 37°C and the cell medium was replaced every 2-3 days.

3.6 RNA isolation, RT-qPCR

For gene expression analyses of primary cell cultures, bones and brown fat tissues, quantitative reverse transcription PCR (RT-qPCR) was performed. Total RNA was extracted using the standard TRIzol reagent (Invitrogen, USA) method as recommended by the manufacturer.

For primary calvarial osteoblasts and BMSCs cultures, RNA was extracted with TRIzol reagent (Invitrogen, USA) after the cells were incubated for 14 days in an osteogenic medium containing 50μg/ml of L-ascorbic acid (Sigma-Aldrich) and 10mM of β-glycerophosphate (Sigma-Aldrich).

For brown fat tissues, after isolating them from mice, these were rapidly snap frozen in liquid nitrogen before placing them into chilled TRIzol reagent (Invitrogen, USA). The brown fat samples were subsequently homogenized using a Polytron PT 2500 E Homogenizer (Kinematica, Switzerland) and RNA isolated as per manufacturer's instructions using TRIzol reagent (Invitrogen, USA).

For the femurs and tibias, these were isolated from 5 month-old mice, making sure to quickly remove any attached tissues using a scalpel before placing them into RNAlater solution (ThermoFisher Scientific, USA) at 4^0C. To proceed with the RNA isolation, the epiphyses of both femurs and tibias were removed and the marrow flushed. The femurs and tibias were then cut into small pieces and placed into 1mL of TRIzol reagent that was kept on ice. The bone samples were then subsequently homogenized using a Polytron PT 2500 E Homogenizer (Kinematica, Switzerland) and RNA was isolated as per manufacturer's instructions using TRIzol reagent (Invitrogen, USA).

For each cell or tissue sample, 1-2 μg of total RNA was employed for the synthesis of single-stranded cDNA using the high capacity cDNA reverse transcription kit (Applied Biosystems, California, USA). RT-qPCR, using the Power SYBR Green PCR Master Mix (ThermoFisher Scientific, USA), was performed to estimate the abundance of specific mRNAs relative to GAPDH mRNA.

The following primers were used:

menin forward 5' – GTGGCCGACCTATCCATCATT – 3',

menin reverse 5' – GGCCCGGTCCTTGAAGTAG – 3'.

RUNX2 forward 5' – GCTCACGTCGCTCATCTTG – 3'

RUNX2 reverse 5' – TATGGCGTCAAACAGCCTCT – 3'

RANKL forward 5' – GCAGAAGGAACTGCAACACA – 3'

RANKL reverse 5' – TGATGGTGAGGTGTGCAAAT – 3'

OPG forward 5' – TGGAACCCCAGAGCGAAACA – 3'

OPG reverse 5' – GCAGGAGGCCAAATGTGCTG – 3'

OCN forward 5' – CAGACAAGTCCCACACAGCA – 3'

OCN reverse 5' – CTTGGCATCTGTGAGGTCAG – 3'

UCP-1 forward 5' – CACGGGGACCTACAATGCTT – 3'

UCP-1 reverse 5' – ACAGTAAATGGCAGGGGACG – 3'

PGC1-α forward 5' – TCTCAGTAAGGGGCTGGTTG – 3'

PGC1-α reverse 5' – TTCCGATTGGTCGCTACACC – 3'

ALP forward 5' – GGGAGATGGTATGGGCGTCT – 3'

ALP reverse 5' – AGGGCCACAAAGGGGAATTT – 3'

PPARγ forward 5' – AGCTGACCCAATGGTTGCTGA – 3'

PPARγ reverse 5' – GGCCATGAGGGAGTTAGAAGG – 3'

GAPDH forward 5' – CACCATCTTCCAGGAGCGAG – 3'

GAPDH reverse 5' – CCTTCTCCATGGTGGTGAAG – 3'

Annealing temperatures of each primer:

Menin: 58ºC

RUNX2: 58ºC

RANKL: 58ºC

OPG: 56ºC

OCN: 60ºC

UCP-1: 60ºC

PGC1-α: 60ºC

ALP: 60ºC

PPARγ: 60ºC

GAPDH: 56-60ºC

The PCR conditions, using the ViiA™ 7 Real-Time PCR (Applied Biosystems, USA), were as follows: 40 cycles of denaturation at 95ºC for 15s, annealing 56-60ºC for 45s, and elongation at 72ºC for 60s. All cDNA samples were ran in triplicate, averaged, and normalized to GAPDH, which was used as the housekeeping gene. The ΔΔCt method was used to assess changes in expression levels for each gene.

3.7 Differentiation and mineralization assays of primary cell cultures

After 14 and 21 days of culture in a differentiation medium containing 50μg/ml L-ascorbic acid (Sigma-Aldrich) and 10mM β-glycerophosphate (Sigma-Aldrich), primary calvarial osteoblasts and BMSCs were washed with PBS 1X and fixed with 100% ethanol for 15 minutes at room temperature.

For assessing calcium deposition, the cells were stained with 40mM alizarin Red-S (Sigma-Aldrich), pH 4.2 and incubated for 30 minutes at room temperature with gentle shaking. Mineral accumulation was quantified as followed: Alizarin Red-S was extracted by destainng with 10mM HCl in 70% ethanol and the intensities quantified at 520nm in 96-well plates using a plate reader (Synergy^{TM} H4 Hybrid Multi-Mode Microplate Reader, BioTek, USA).

ALP activity was determined by histochemical staining using NBT/BCIP tablets (Roche Diagnostics, Indianapolis, USA). Briefly, 1 tablet was dissolved in 10mL of distilled water and freshly prepared solution was used for staining. Prior to proceeding to the staining for ALP, primary cells were washed with PBS 1X and then fixed at room temperature for 10 minutes using 100% ethanol. After washing, freshly prepared solution of ALP was added onto fixed cells followed by direct incubation at 37^0C for 30 minutes in dark. Stained wells were washed with distilled water and air-dried. To quantify ALP staining, 10X microscopic images were taken using the Evos XL Core light microscope (Life Technologies, California, USA) and relative staining was determined by calculating the mean gray area using the ImageJ software (NIH).

3.8 Methyl Thiazolyl Tetrazolium (MTT) viability assay:

Primary calvarial osteoblasts and BMSCs were seeded at a density of 2-3 x 10^4 cells per well in 24-well tissue cultures plates and cultured with αMEM (Gibco, Life technologies, USA) supplemented with 10% FBS (Wisent Inc.) and 1% peninicllin/streptomycin (Wisent Inc.) at 37^0C in a 5% CO_2 incubator. 48 hours later, 20µl of MTT labeling reagent (Roche Diagnostics, Indianapolis, USA) was added, and incubation was continued for 4h at 37^0C. After incubation, purple crystals formed were eluted in 500µl of DMSO and absorbance was read at 570nm using a microplate reader (Synergy^{TM} H4 Hybrid Multi-Mode Microplate Reader, BioTek, USA).

3.9 3D Collagen scaffolds preparation

Plastically compressed collagen gels were used as 3D scaffolds and were prepared as previously described (161,162). Briefly, 4 mL of sterile rat-tail collagen type I (First Link Ltd, Wolverhampton, UK) at a protein concentration of 2 mg/mL in 0.6% acetic acid was mixed with 1mL of 10X DMEM (Sigma-Aldrich). Since this solution is acidic, it was neutralized by drop-wise addition of 5 M NaOH to pH ~ 7.4, or up until the color turns dark-red. After neutralization, primary calvarial osteoblasts from 6 month-old *Prx1-Cre; Men1f/f* and control *Men1f/f* mice were incorporated into the collagen solution at a cell density of 60 000 cells/mL. Directly after this, 1.5mL of this solution with the primary cells incorporated was added per well into 3 wells of a 48-well plate, followed by 30 minutes of incubation in a 5% CO_2 incubator at 37^oC.

After polymerization, highly hydrated hydrogels were placed on a stack of blotting paper, stainless mesh and nylon mesh. Another piece of nylon mesh was used to cover the gel from the top. A sterile 40g flat glass block was then put on top of the mesh of each gel for 1min30sec. Dense collagen scaffolds with more than 10 weight % fibrillary collagen density were produced by the

application of a compressive stress of 1 kPa to remove excess casting fluid (figure 3.1) (163). Each gel was then transferred into a 6-well plate to which 3 mL of αMEM medium (Gibco, Life technologies, USA) supplemented with 10% FBS (Wisent Inc.) and 1% penicillin/streptomycin (Wisent Inc.) was added. After a 48 hours recovery period, osteogenic differentiation with 50µg/ml L-ascorbic acid (Sigma -Aldrich) and 10mM β-glycerophosphate (Sigma-Aldrich) was initiated. The cell-seeded collagen gels were maintained in culture for up to 21 days in a 5% CO_2 incubator at 37^{o}C. The cell media was renewed 3 times a week.

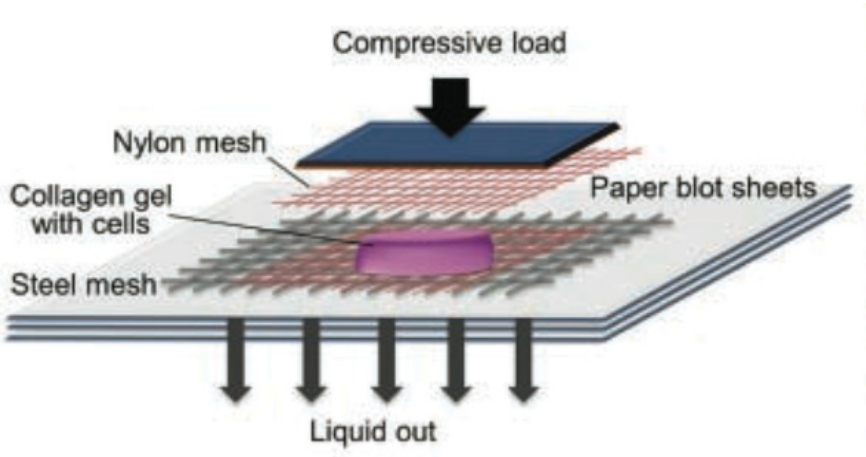

Figure 3.1: Schematic representation of the preparation of 3D collagen scaffolds. Hydrated collagen gels seeded with primary cells were put on a stack of blotting paper, nylon mesh and stainless steel mesh. Another piece of nylon mesh was used to cover the gels, and dense collagen scaffolds were obtained by plastic compression of the hydrated collagen gels using a 40g glass block. Reproduced with permission from Coyac BR, Chicatun F, Hoac B, Nelea V, Chaussain C, Nazhat SN, McKee MD. Mineralization of dense collagen hydrogel scaffolds by human pulp cells. *Journal of Dental Research*. 2013;92(7):648-54

3.10 Alamar blue assay

Cell metabolic activity among the dense collagen scaffolds was assessed using the alamar blue assay (ThermoFisher Scientific, USA) at days 2, 10, 15 and 21 of osteogenic differentiation. Briefly, 800µl of alamar blue solution was added and mixed with 8mL of osteogenic medium that

was pre-warmed in a 15 mL conical vial. 1mL of this solution was thereafter added per well to the cell-seeded collagen gels of a 6-well plate, and incubation was thereafter followed at 37^0C in a 5% CO_2 incubator for 3 hours. After the incubation period, three aliquots of 100µl of the alamar blue solution from each sample was transferred from the 6-well plate to a 96-well plate and the fluorescence was read using excitation and emission wavelengths of 530nm and 610nm with a microplate reader (Synergy™ H4 Hybrid Multi-Mode Microplate Reader, BioTek, USA).

3.11 Scanning Electron Microscopy (SEM)

Scanning electron microscopy (SEM) was performed on primary calvarial osteoblasts cell-seeded dense collagen gels from 6 month-old male *Prx1-Cre; Men1f/f* and control *Men1f/f* mice to analyze cell-mediated mineralization processes, scaffold microstructure and cellular morphology. Gels were fixed in 4% paraformaldehyde overnight, then rinsed with deionized water for 10 minutes and finally dehydrated through an ethanol gradient followed by immersion in 1,1,1,3,3,3-hexamethyldisilazane (Sigma-Aldrich). Dehydrated samples were coated with Pt using a Leica Microsystems EM ACE600 sputter coater (Austria). Images were acquired with a FEI Inspect F-50 FE-SEM (FEI Company, USA), at 5 kV.

3.12 Fourier Transform Infrared Spectroscopy (FTIR)

Infrared spectroscopy of primary calvarial osteoblast cell-seeded dense collagen gels from 6 month-old male *Prx1-Cre; Men1f/f* and control *Men1f/f* mice was performed with a Spectrum 400 (Perkin Elmer, USA) to characterize the mineralized scaffolds. Gels were fixed in 4% paraformaldehyde overnight, then rinsed with deionized water for 10 minutes and finally dehydrated through an ethanol gradient followed by immersion in 1,1,1,3,3,3-

hexamethyldisilazane (Sigma-Aldrich). Spectra were collected using a resolution of 2 cm^{-1}, an infrared range of 4000- 650 cm^{-1} and 64 scans. Spectra were then corrected with a linear baseline and normalized (absorbance of Amide I at 1643 cm-1 = 1.5) using Spectrum software (Perkin Elmer, USA).

3.13 Energy-Dispersive X-ray spectroscopy (EDS)

Energy-Dispersive x-ray spectroscopy (EDS) was used for chemical characterization of particles deposited in seeded gels. EDS was performed on primary calvarial osteoblasts cell-seeded dense collagen gels from 6 month-old male *Prx1-Cre; Men1f/f* and control *Men1f/f* mice. Briefly, gels were fixed in 4% paraformaldehyde overnight, then rinsed with deionized water for 10 minutes and finally dehydrated through an ethanol gradient followed by immersion in 1,1,1,3,3,3-hexamethyldisilazane (Sigma-Aldrich). Spectra were collected with a FEI Inspect F-50 FE-SEM (FEI Company, USA) at 10kV.

3.14 Forelimb grip strength test

A Grip Strength Meter (Bioseb, Chaville, France) was used to assess changes in skeletal muscle strength between knockout and wild-type control mice. Each individual mouse was lifted by its tail over the top of the grid so that it could grasp the grid platform with its front paws only. With its torso oriented in a horizontal position, the mouse was then gently pulled backward until it released the grid. The maximal force digitally displayed in grams on the grip strength meter applied by the mouse before releasing its grasp of the grid was recorded. The idea is that the mouse will keep holding onto the grid until it can no longer resist the increasing force being applied when pulling him backward. Genotype was blind to observer and the mean of ten consecutive trials was

taken as an index of forelimb grip strength. The bodyweight of each individual mice was measured at the end of the experiment to normalize the mean grip strength force to bodyweight.

3.15 Three-point bending test

To assess bone biomechanical changes, femurs from adult knockout mice and their control wild-type littermates were isolated. The right femora were used to perform the three-point bending test. Femurs were loaded to failure using an Instron model 5943 single column table frame machine (Instron, High Wycombe, UK). The experiments were performed in the posterior-to-anterior direction at a loading rate of 0.05 mm/s and using a support distance of 7 mm. The instrument produced load vs displacement curves for each test which were then subsequently used to determine individual bone structural properties. These were calculated in order to best characterize the specific aspects of the bone's mechanical behavior under load. Those properties included stiffness (N/mm), maximum load at failure (N), load at yield point (N) and the load at break (N).

3.16 Echo-MRI

Echo-MRI analysis was performed at the McGill Mouse Metabolic Platform on live animals using EchoMRI model ET-040, version 11,06,22 (EchoMRI LLC). Total body fat percentage was calculated as: [fat mass (g) / total bodyweight (g)] * 100% and total lean mass percentage as: [lean mass (g) / total bodyweight (g)] * 100%.

3.17 Tissue Analysis

Upon dissection, the weights of inguinal subcutaneous white fat pads and anterior interscapular brown fat pads were assessed. The right femurs of control and knockout mice were also carefully dissected, representative images were taken and their lengths measured using a high precision digital caliper.

3.18 Statistical analysis

All the results are expressed as a mean ± SEM. Statistical differences between groups were determined using the two-tailed unpaired Student's *t* test with the GraphPad Prism analysis software version 7.0 (GraphPad Software, Inc., San Diego, CA, USA). For all statistical tests, a *P* value of < 0.05 was considered statistically significant (*<0.05; **<0.01; ***<0.001; ****<0.0001).

CHAPTER 4: RESULTS

4.1 Deletion of the *Men1* gene is specific to bone

To confirm that the *Men1* gene deletion occurred only in the osteoblast lineage, DNA extracts analysis was performed as previously described by our group to ensure that the deletion was present only in bone of Cre-expressing mice (155). By PCR analysis, our group demonstrated in the current study that Cre-mediated recombination only occurred in the femur, tibia and calvaria tissues of *Prx1-Cre; Men1f/f* and *Osx-Cre; Men1f/f* mice, but not in wild-type control *Men1f/f* mice. Cre-mediated recombination was not present in the liver, kidney and heart tissues, which served as controls, of both knockout and wild-type mice.

4.2 Mice deficient for menin early in the osteoblast lineage have a reduced body size and show differences in whole body composition

Our study is looking into the effect of menin early deletion in the osteoblast lineage using conditional knockout mice. Given the recent emergence of bone as an endocrine organ and because osteoblasts are derived from multipotent MSCs which have the potential to commit to the adipocyte, chondrocyte and myocyte lineages, we decided to further investigate whether the early disruption of the *Men1* gene at the level of mesenchyme derived progenitors and osteoblast progenitors could also have an impact on whole body metabolism. To monitor the growth of our earlier menin knockout mice models, bodyweights of *Prx1-Cre; Men1f/f* and *Osx-Cre; Men1f/f* mice were measured every week. The weights of male and female *Prx1-Cre; Men1f/f* mice in comparison to control *Men1f/f* littermates were reduced between 8 and 21 weeks of age (figure 4.1 A-B). At 21 weeks of age, both male and female *Prx1-Cre; Men1f/f* mice demonstrated a significant decrease of ~13% in bodyweight in comparison to control mice (figure 4.1 A-B). The

bodyweight of male *Osx-Cre; Men1f/f* mice was reduced by approximately ~18% between 4 and 5 weeks, and by ~6-9% between 10 and 20 weeks of age (figure 4.1 C). *Osx-Cre; Men1f/f* females had marked decreases of ~18% in their bodyweight between 4 and 5 weeks (figure 4.1 D). Between 8 to 15 weeks the bodyweight of knockout *Osx* females was significantly reduced by approximately ~11-14% in comparison to the control mice (figure 4.1 D). Although their bodyweights were roughly similar between 17 to 20 weeks of age, their weights began to decrease at 21 weeks of age and showed marked differences at a more advanced age (figure 4.1 D).

Since all our knockout mice strains showed more pronounce decrease in bodyweight with advancing age, Echo-MRI analysis was performed in adult 10, 12 and 14 month-old animals. No significant changes in terms of the percentage of fat and lean mass content were observed in male *Prx1-Cre; Men1f/f* and *Osx-Cre; Men1f/f* mice at 12 and 10 months of age, respectively (figure 4.2 A-B). However, in both cases, the overall lean mass content was significantly decreased by ~8%, with the fat mass content of only male *Osx-Cre; Men1f/f* but not *Prx1-Cre; Men1f/f* mice being significantly reduced by ~20% (figure 4.2 A-B). Bodyweights of both male mice from the two knockout strains were also significantly decreased by approximately ~10-12% in comparison to age-matched *Men1f/f* controls (figure 4.2 A-B). Because no significant changes were perceived in the percentage of lean and fat mass in knockout adult male animals of the *Osx* and *Prx1* strains, one reason explaining the decrease in bodyweight could be due to an overall decrease in body size, potentially attributable to the marked changes seen in bone growth. Interestingly, the percentage of fat and lean masses between 14 month-old *Osx-Cre; Men1f/f* and control *Men1f/f* female mice were significantly lower by ~24% and higher by ~9%, respectively (figure 4.2 C). The total bodyweight of female *Osx-Cre; Men1f/f* was also significantly decreased by ~20% at 14 months of age in comparison to control mice (figure 4.2 C). Menin has been shown to interact with both

androgen and estrogen receptors, regulating their transcriptional activities (136,164,165). Thus, female mice might show a metabolic phenotype that is different from male mice at a more advanced age, which is what we observe here.

Taken together, these findings indicate that osteoblast menin is required for the normal growth of mice. Its early deletion at the level of the MSC and preosteoblast impacts the metabolism of both *Prx1-Cre; Men1f/f* and *Osx-Cre; Men1f/f* mice, as assessed here by the perceived changes in bodyweight and body composition between each group.

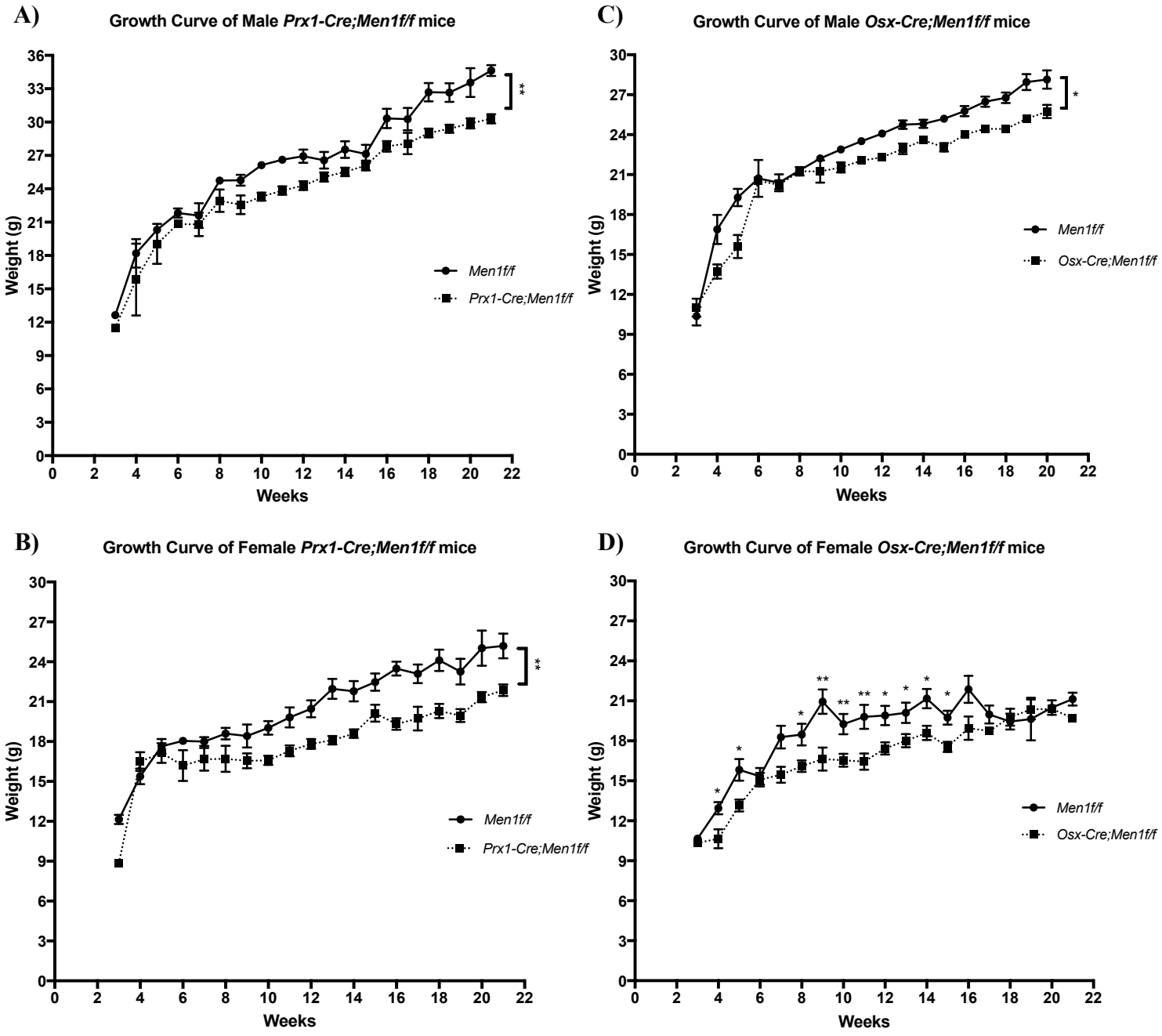

Figure 4.1. **Growth curves of *Prx1-Cre; Men1f/f* and *Osx-Cre; Men1f/f* mice during postnatal development.**

The growth curves of male and female transgenic mice of both strains were analyzed. Bodyweight changes from 3 weeks to 21 weeks of age in (A) male *Prx1-Cre; Men1f/f* (n=8), (B) female *Prx1-Cre; Men1f/f* (n=7), (C) male *Osx-Cre; Men1f/f* (n=6) and (D) female *Osx-Cre-; Men1f/f* (n=6) animals. ** $P < 0.05$, ** $P < 0.01$.*

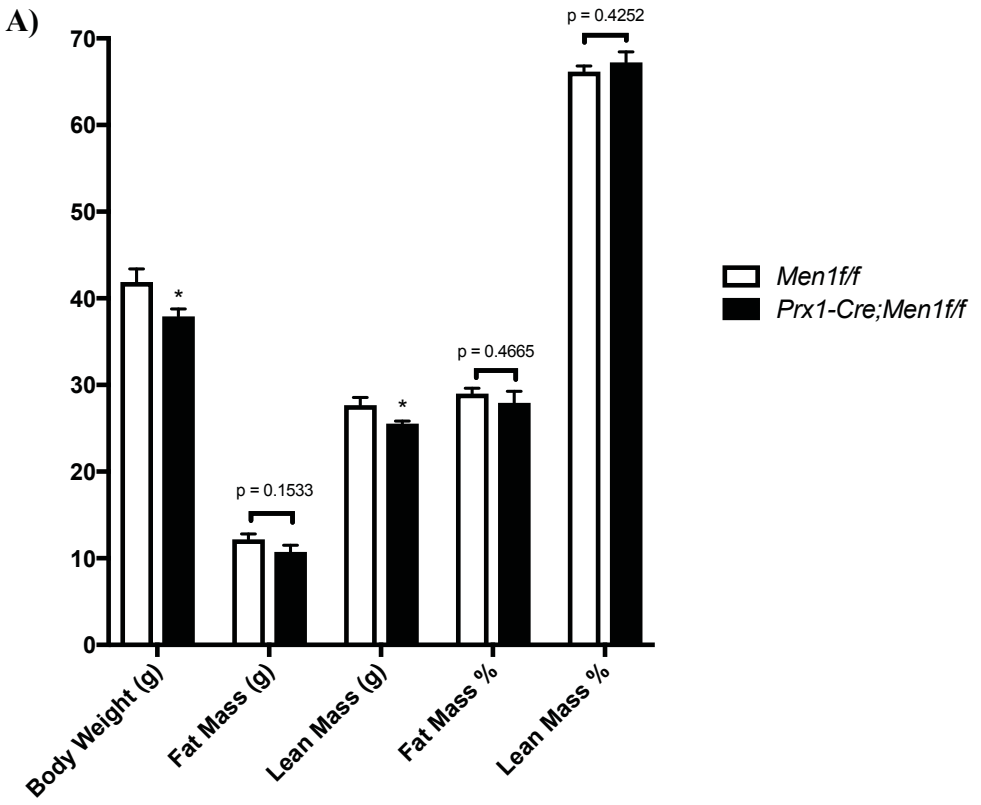
EchoMRI
Male 12 month-old
A)
70
60
50
40
30
20
10
0
p = 0.4252
p = 0.4665
p = 0.1533
*
*
Body Weight (g)
Fat Mass (g)
Lean Mass (g)
Fat Mass %
Lean Mass %
Men1f/f
Prx1-Cre;Men1f/f

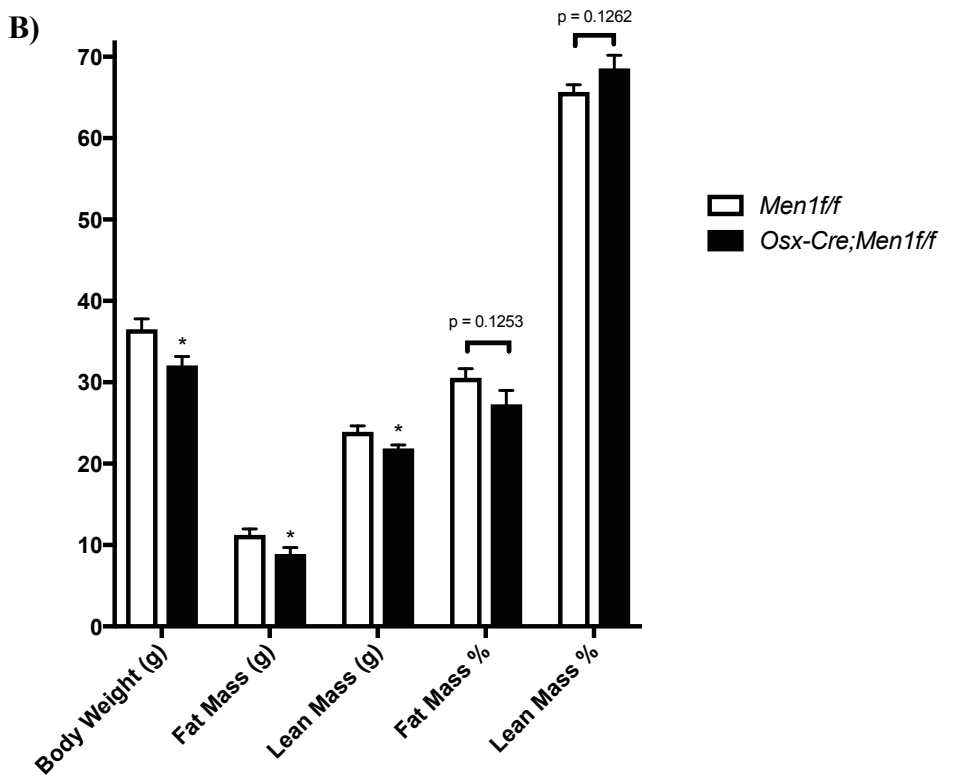
EchoMRI
Male 10 month-old
B)
70
60
50
40
30
20
10
0
p = 0.1262
p = 0.1253
*
*
*
Body Weight (g)
Fat Mass (g)
Lean Mass (g)
Fat Mass %
Lean Mass %
Men1f/f
Osx-Cre;Men1f/f

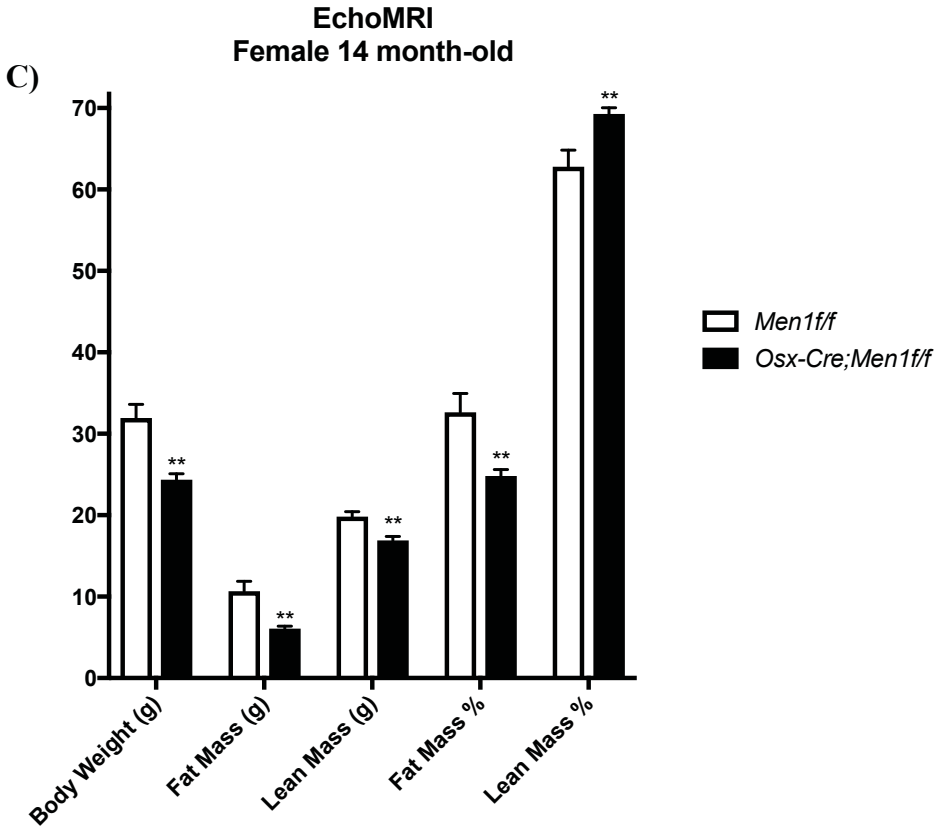

Figure 4.2. Body composition analysis of *Prx1-Cre; Men1f/f* and *Osx-Cre; Men1f/f* mice. Echo-MRI was performed on (A) 12 month-old male *Prx1-Cre; Men1f/f* (n=9,8), (B) 10 month-old male *Osx-Cre; Men1f/f* (n=10) and (C) 14 month-old female *Osx-Cre; Men1f/f* (n=9,12) mice. Echo-MRI components analyzed included the bodyweight, fat and lean mass body content, and the % of lean and fat mass relative to total bodyweight. * $P < 0.05$, ** $P < 0.01$.

4.3 Menin deletion in mesenchyme-derived progenitor cells alters brown adipose tissue activity.

Since Echo-MRI analysis revealed changes in the bodyweight, fat and lean mass content of knockout mice, fat deposits were further investigated. For this, the inguinal subcutaneous white adipose tissue (WAT) and the interscapular subcutaneous brown adipose tissue (BAT) were isolated from *Prx1-Cre; Men1f/f* and *Osx-Cre; Men1f/f* adult male mice and their control wild-type littermates. Nonstatistical tendencies of decrease in WAT and BAT weights were observed in *Prx1-Cre; Men1f/f* and *Osx-Cre; Men1f/f* adult male mice (figure 4.3 A-D). These results are consistent with the Echo-MRI analysis that shows a more significant reduction in the fat mass content of knockout mice.

In addition, total RNA was directly extracted from BAT tissues and the expression level of markers of energy metabolism, such as *Pgc1α* and *Ucp1*, along with the adipogenic marker, *PPARγ*, were analyzed. By RT-qPCR analysis, the expression level of *menin* was found to be similar between knockout and wild-type animals (figure 4.3 E). This reiterates results made by our group showing that deletion of the *Men1* gene in our conditional knockout mouse models is specific to bone tissues. Through RT-qPCR analysis, the relative expression level of *Ucp1* was approximately ~5-fold higher in *Prx1-Cre; Men1f/f* animals compared to controls (figure 4.3 G). Although not showing a significant statistical difference, the expression level of *Pgc1α* demonstrated a strong tendency of being ~2-fold reduced in male *Prx1-Cre; Men1f/f* animals (figure 4.3 H). Interestingly, the expression level of *PPARγ* was not significantly altered between knockout and wild-type animals (figure 4.3 F). Taken together, these data suggest that deleting menin early in the osteoblast lineage has profound effects on energy metabolism, in part by affecting BAT-dependent thermogenesis by altering expression levels of *Ucp1* and *Pgc1α*.

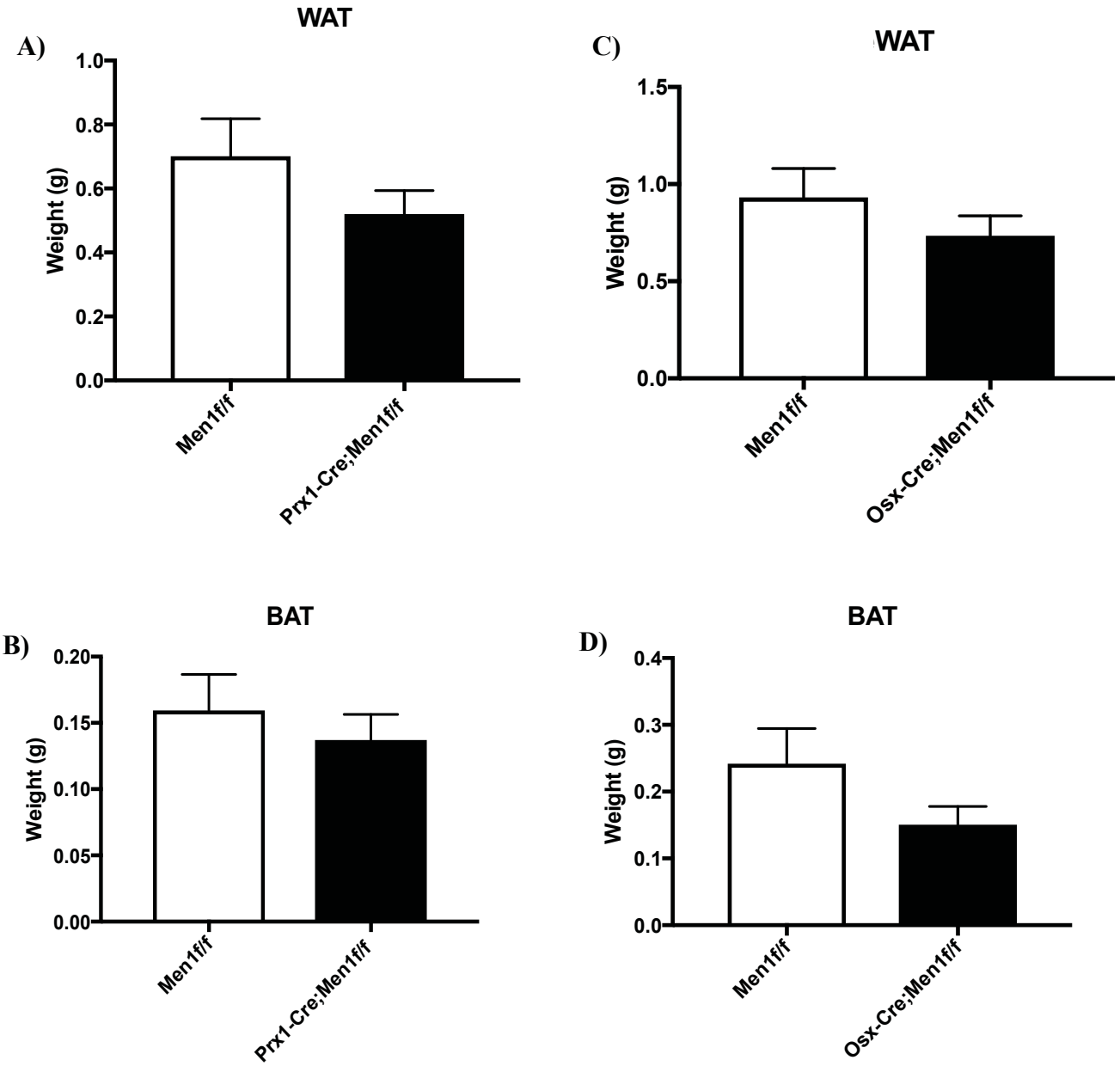
A)
WAT
Weight (g)
1.0
0.8
0.6
0.4
0.2
0.0
Men1f/f
Prx1-Cre;Men1f/f
C)
WAT
Weight (g)
1.5
1.0
0.5
0.0
Men1f/f
Osx-Cre;Men1f/f
B)
BAT
Weight (g)
0.20
0.15
0.10
0.05
0.00
Men1f/f
Prx1-Cre;Men1f/f
D)
BAT
Weight (g)
0.4
0.3
0.2
0.1
0.0
Men1f/f
Osx-Cre;Men1f/f

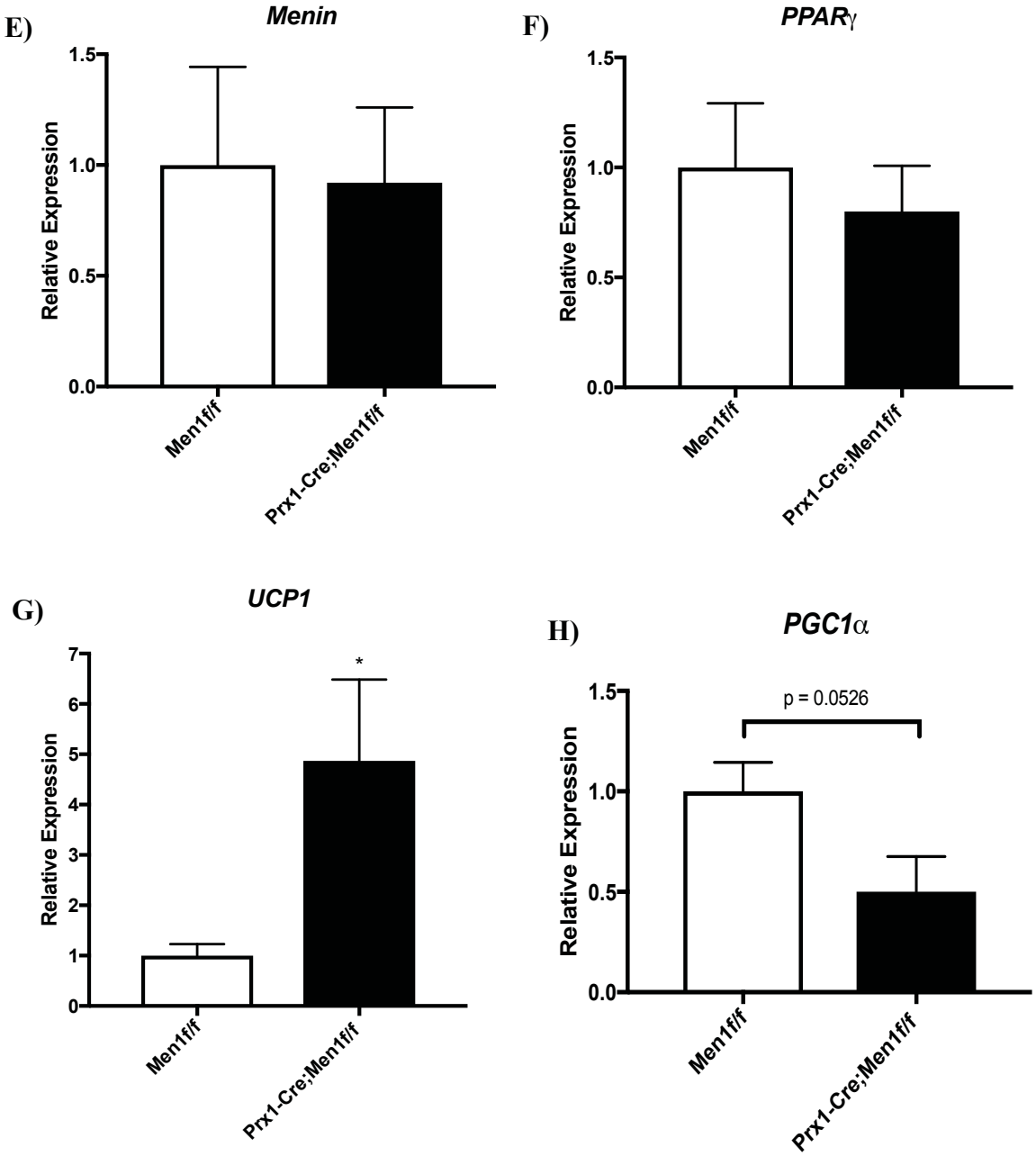

Figure 4.3. **BAT & WAT fat analysis.**
WAT and BAT organ weights for (A-B) 6 month-old male *Prx1-Cre; Men1f/f* (n=6) and (C-D) 9 month-old male *Osx-Cre; Men1f/f* (n=5) mice. The expression of (E) menin, (F) PPARγ, (G) Ucp1 and (H) Pgc1α from BAT tissues were analyzed by RT-qPCR. Gene expression was normalized to that of GAPDH, a housekeeping gene (n=6). * $P < 0.05$.

4.4 *Men1* knockout mice demonstrate altered forelimb grip strength abilities.

To determine whether changes observed in body metabolism and in lean mass content could affect the skeletal muscle strength of *Prx1-Cre; Men1f/f* and *Osx-Cre; Men1f/f* animals, the forelimb grip strength test was performed using adult mice from both knockout strains along with age-matched control littermates (figure 4.4 A).

6 month-old *Prx1-Cre; Men1f/f* male mice demonstrated a significant decrease of ~30% in forelimb grip strength in comparison to control *Men1f/f* animals (figure 4.4 C). Interestingly, the forelimb grip strength of 9 month-old male *Osx-Cre; Men1f/f* mice showed no statistical differences in comparison to control animals (figure 4.4 F). However, because bodyweights of both strains of knockout mice were significantly lower by approximately ~12-13% than control mice (figure 4.4 B, E), individual values obtained in grams from the grip strength test were normalized to each mouse total bodyweight. When normalizing individual grip strength measurements to the experimental mouse bodyweight, *Osx-Cre; Men1f/f* males demonstrated a marked increase of ~18% in the forelimb grip strength, while *Prx1-Cre; Men1f/f* animals still failed in grasping the grid bar with the same force as wild-type mice (figure 4.4 D, G). Because findings with the Echo-MRI analysis revealed an increase of ~9% in the percentage of lean mass in 14 month-old female *Osx-Cre; Menf/f* mice, the forelimb grip strength test was as well performed on the same animals. The forelimb grip strength of female knockout mice was similar to that of wild-type littermates (figure 4.4 I). When values were normalized to the bodyweight of each individual mice, the forelimb grip strength of female *Osx-Cre; Menf/f* mice was ~13% higher than control animals, which is consistent with the substantial increase in the percentage of lean mass that was previously demonstrated by Echo-MRI analysis (figure 4.4 H-J).

A)

♂

B)

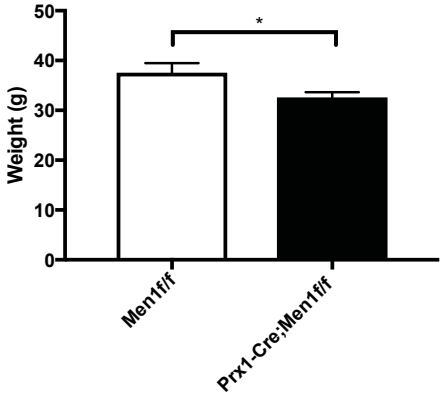
Weight (g)
50
40
30
20
10
0
*
Men1f/f
Prx1-Cre;Men1f/f

C)

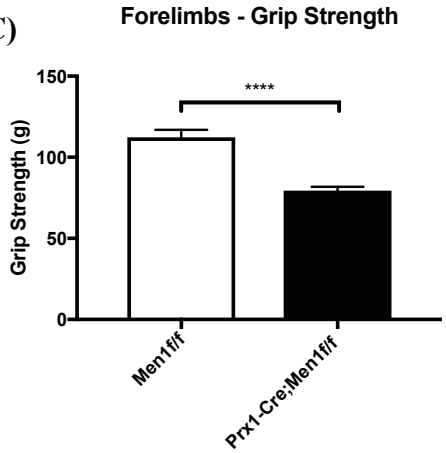
Forelimbs - Grip Strength
Grip Strength (g)
150
100
50
0
****
Men1f/f
Prx1-Cre;Men1f/f

D)

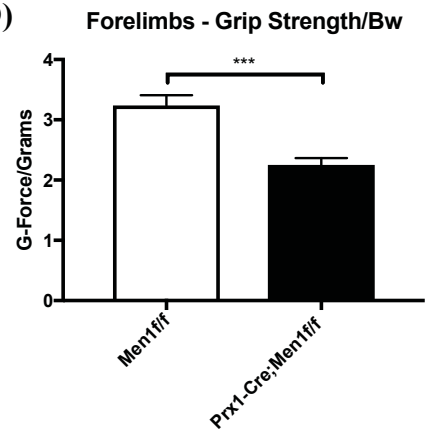
Forelimbs - Grip Strength/Bw
G-Force/Grams
4
3
2
1
0
***
Men1f/f
Prx1-Cre;Men1f/f

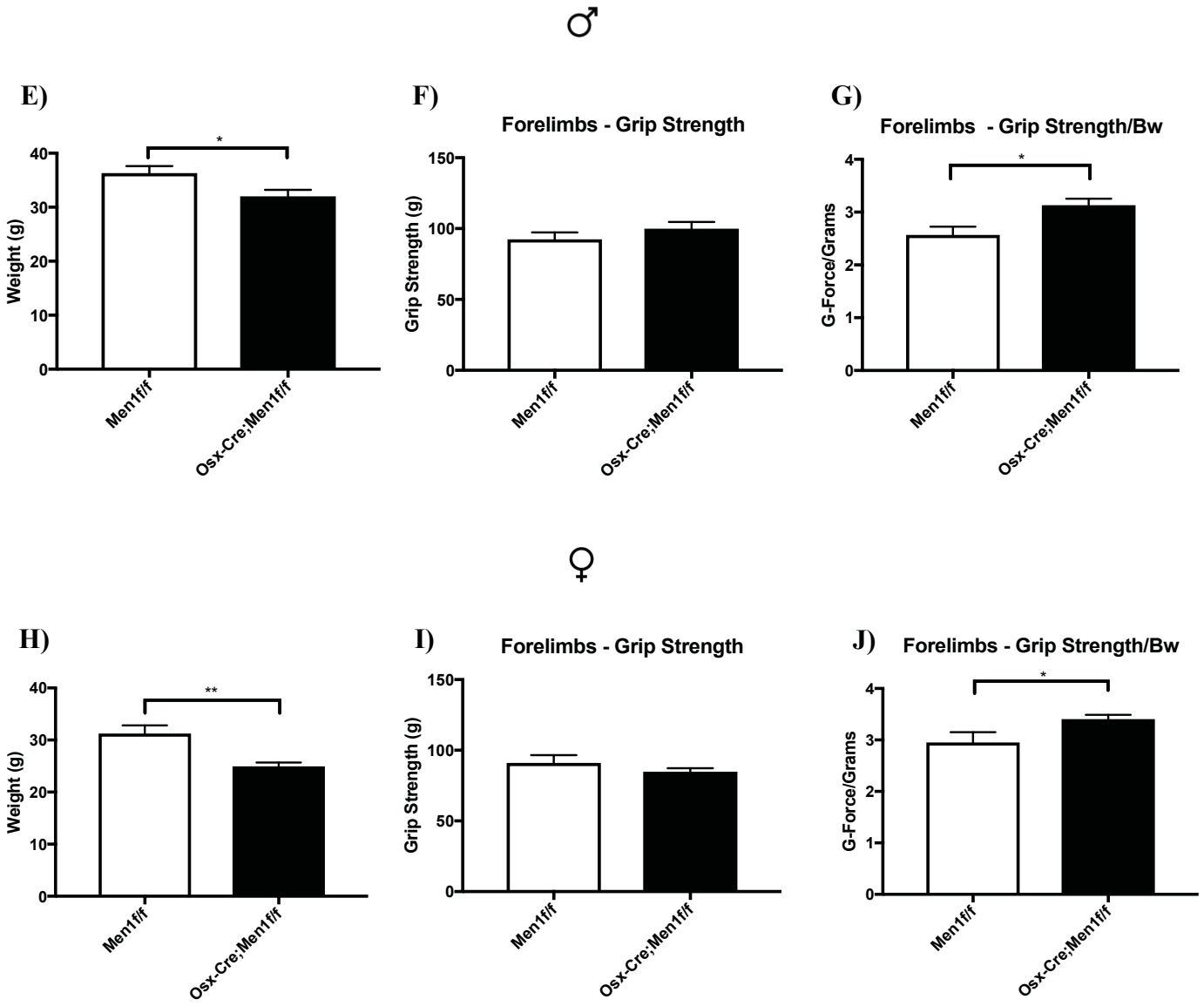

Figure 4.4: Forelimb grip strength test of *Prx1-Cre; Men1f/f* and *Osx-Cre; Men1f/f* mice.
(A) Grip strength of mouse forelimbs was measured by a grip strength meter by allowing individual mice to grip to a metal grid with only their forelimbs. The bodyweight and forelimb grip strength were measured using (B-C) 6 month-old male *Prx1-Cre; Men1f/f* (n=6), (E-F) 9 month-old male *Osx-Cre; Men1f/f* (n=10) and (H-I) 14 month-old female *Osx-Cre; Men1f/f* (n=10) mice. Grip strength values were normalized to bodyweight for each experiment (D,G,J). ** $P < 0.05$, ** $P < 0.01$, *** $P < 0.001$, **** $P < 0.0001$.*

4.5 Reduced femur length & bone strength are observed in *Men1* knockout femurs.

The substantial decreases seen in trabecular bone mass and in the BMD of 6 month-old *Prx1-Cre; Men1f/f* and *Osx-Cre; Men1f/f* mice suggest a mechanically weaker bone strength in these knockout mice. To confirm this hypothesis, the three-point bending test was conducted on both adult *Prx1-Cre; Men1f/f* and *Osx-Cre; Men1f/f* knockout femurs, and control *Men1f/f* femurs. Results from the 3-point bending test at the femur diaphysis indicated significant decreases in femur stiffness by ~26% , maximum load by ~30%, load at yield by ~35% and load at break by ~25% in *Prx1-Cre; Men1f/f* mice. The same parameters were also significantly reduced by approximately ~18%, ~18%, ~13% and ~14%, respectively, in *Osx-Cre; Men1f/f* knockout mice compared to control *Men1f/f* littermates (figure 4.5 E-L). These finding are consistent with the DXA, μCT and histomorphometric analyses that show a significant decrease in the bone volume density of knockout animals. Importantly, these results also reveal biomechanically weaker bones that are more prone to fracture when menin is deleted early in the osteoblast lineage. Knockout mice also demonstrate a low bone quality in comparison to control *Men1f/f* animals in this regard.

Femur lengths of adult *Prx1-Cre; Men1f/f* and *Osx-Cre; Men1f/f* mice were also significantly reduced by ~10% and ~4%, respectively, in comparison to wild-type mice, suggesting deficiencies not only in development, but as well in the growth of bones when menin is deleted at earlier stages of osteoblast differentiation (figure 4.5 A-D).

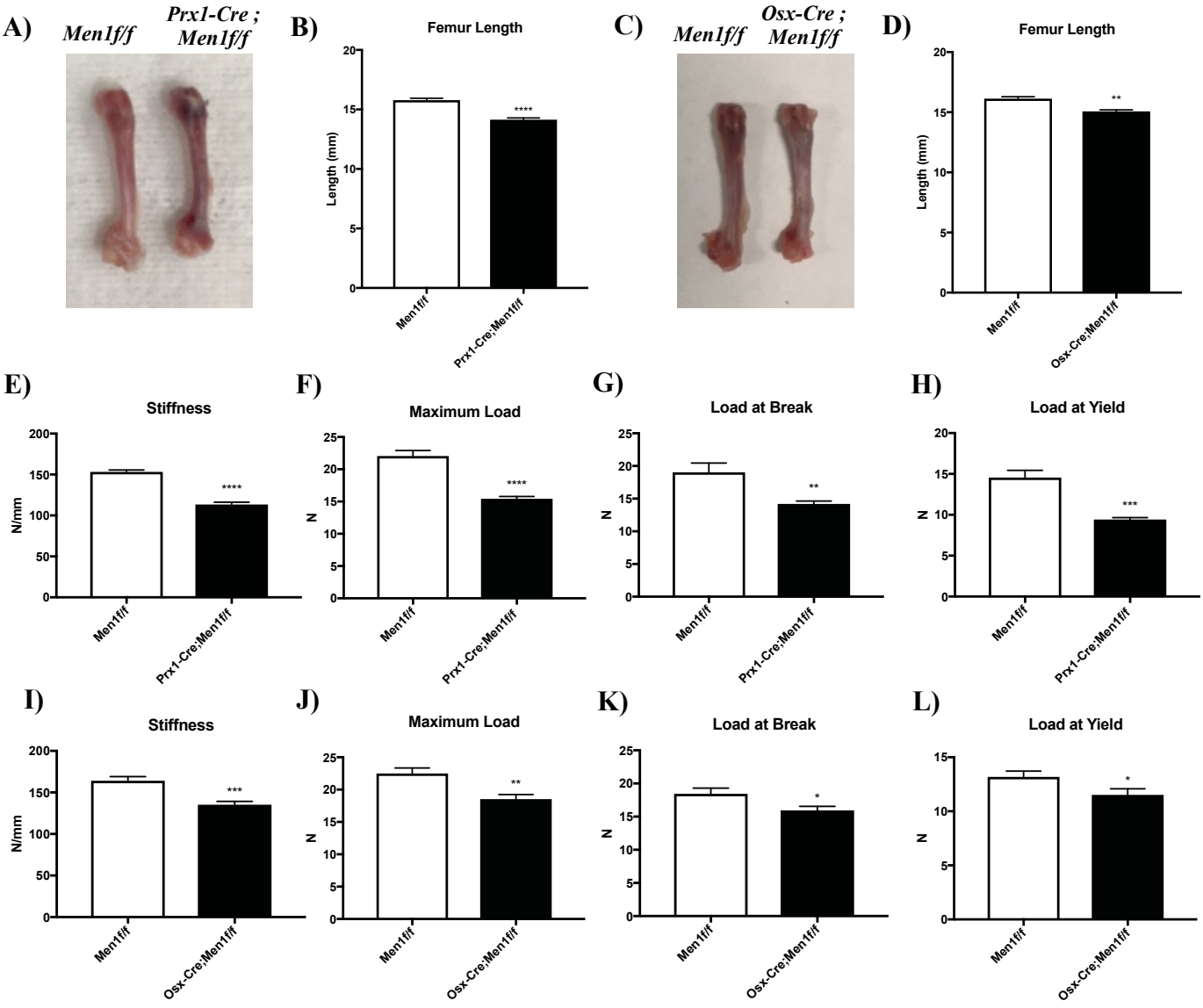

Figure 4.5: **Reduced femur length and bone biomechanical parameters in *Prx1-Cre; Men1f/f* and *Osx-Cre; Men1f/f* mice.**

Femur images and femur length of (A-B) 6 month-old male *Prx1-Cre; Men1f/f* and (C-D) *Osx-Cre; Men1f/f* mice (n=6). Three-point bending analysis of femurs from (E-H) 6 month-old male *Prx1-Cre; Men1f/f* (n=6) and (I-L) 9 month-old male *Osx-Cre; Men1f/f* mice (n=10). With the load vs displacement curves generated parameters such as the stiffness, maximum load, load at break and load at yield were measured. ** $P < 0.05$, ** $P < 0.01$, *** $P < 0.001$, **** $P < 0.0001$.*

4.6 Primary calvarial osteoblasts and BMSCs of the earlier menin knockout mice models demonstrate no changes in proliferation.

To further provide an explanation as to what causes the observed reduction in bone mass and strength in *Men1* knockout mice, primary cultures of calvarial osteoblasts and BMSCs from *Prx1-Cre; Men1f/f* and *Osx-Cre; Men1f/f* mice and their control wild-type littermates were analyzed. Microscopic images taken of both primary calvarial osteoblasts and BMSCs showed osteoblast-like cells similar in both knockout and wild-type cell cultures (figure 4.6 A-C), as well as elongated shape cells characteristic of BMSCs in primary cell cultures of knockout and wild-type mice (figure 4.6 D-F). No marked morphological differences were noted between primary cells derived from each mice strain.

Previous report by our group has shown that in mature osteoblasts menin controls proliferation events by preventing osteoblasts to enter premature apoptosis (125,126,155). Whether or not menin controls osteoblast proliferation when expressed at earlier stages of osteoblast differentiation was investigated in this study by performing the MTT cell viability assay. The MTT assay revealed no significant differences between primary calvarial osteoblasts and BMSCs isolated from *Prx1-Cre; Men1f/f*, *Osx-Cre; Men1f/f* and control *Men1f/f* mice 48 hours after the first passage of the isolated primary cells (figure 4.6 G-J).

These *in vitro* results indicate that the cell morphology of both calvarial osteoblasts and BMSCs, as well as their proliferative capabilities, are not affected when menin is deleted at earlier stages of the osteoblast lineage.

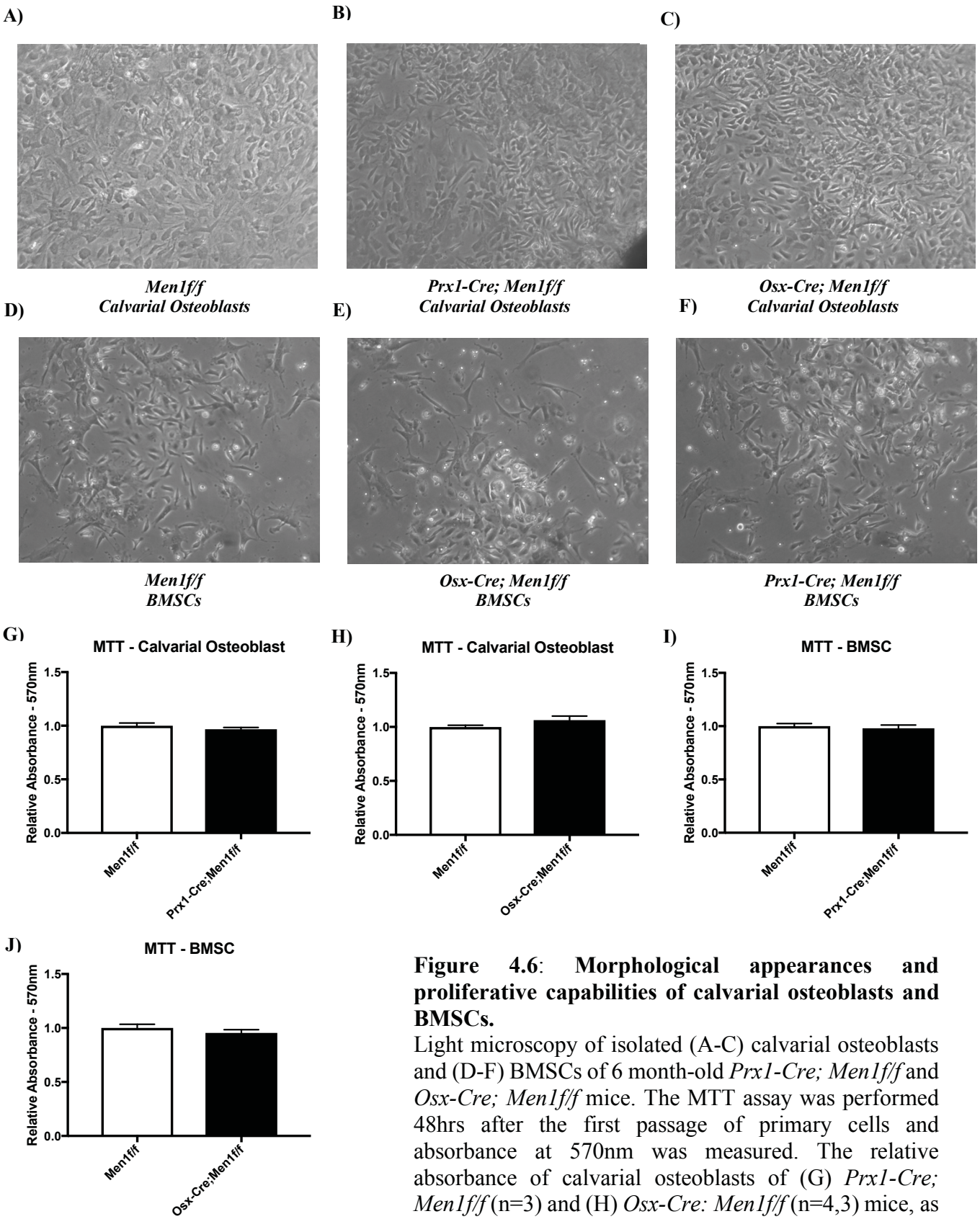

Figure 4.6: **Morphological appearances and proliferative capabilities of calvarial osteoblasts and BMSCs.**

Light microscopy of isolated (A-C) calvarial osteoblasts and (D-F) BMSCs of 6 month-old *Prx1-Cre; Men1f/f* and *Osx-Cre; Men1f/f* mice. The MTT assay was performed 48hrs after the first passage of primary cells and absorbance at 570nm was measured. The relative absorbance of calvarial osteoblasts of (G) *Prx1-Cre; Men1f/f* (n=3) and (H) *Osx-Cre: Men1f/f* (n=4,3) mice, as well as the relative absorbance of (I) BMSCs of *Prx1-Cre; Men1f/f* (n=6) and (J) *Osx-Cre: Men1f/f* (n=4,3) mice were calculated.

4.7 *In vitro* analysis of primary calvarial osteoblasts and BMSCs of *Men1* knockout mice shows altered mineralization capabilities but no change in alkaline phosphatase intensity.

Previous reports have demonstrated that menin can mediate osteoblast differentiation and mineralization by modulating BMP-2 and TGF-β signaling pathways (125,126,155). Hence, to further investigate the differentiation capabilities of primary calvarial osteoblasts and BMSCs when menin is specifically deleted early in the osteoblast lineage, these cells were cultured in an osteogenic medium containing L-ascorbic acid and β-glycerophosphate for 14 and 21 days, and stained for mineralized matrix formation with alizarin red, and for ALP. BMSCs isolated from *Prx1-Cre; Men1f/f* and *Osx-Cre; Men1f/f* animals and cultured in differentiation media for 14 days showed no differences in terms of the relative alizarin red staining in comparison to primary wild-type BMSCs (figure 4.7 A-F). Primary calvarial osteoblasts of *Prx1-Cre; Men1f/f* and *Osx-Cre; Men1f/f* mice both demonstrated reductions of approximately ~23-28% in terms of the extracellular calcium deposition, as assed by alizarin red staining at day 14 of osteogenic differentiation (figure 4.7 G-L). At day 21 of osteogenic differentiation, calvarial osteoblasts of *Prx1-Cre; Men1f/f* mice again showed a significant decrease of ~22% in calcium deposition in comparison to control *Men1f/f* calvarial osteoblasts (figure 4.7 M-O). ALP staining of primary calvarial osteoblasts and BMSCs cultured in an osteogenic medium revealed no changes in terms of the relative intensity between knockout and control primary cells (figure 4.7 A-O).

These results show that while levels and differentiation capabilities of primary calvarial osteoblasts and BMSCs, as assessed by ALP staining, between wild-type and knockout mice are no different, the mineralization capabilities of calvarial osteoblasts are however slightly reduced. This suggests that calvarial osteoblasts of knockout mice are defective in producing and secreting a mineralized ECM.

BMSCs

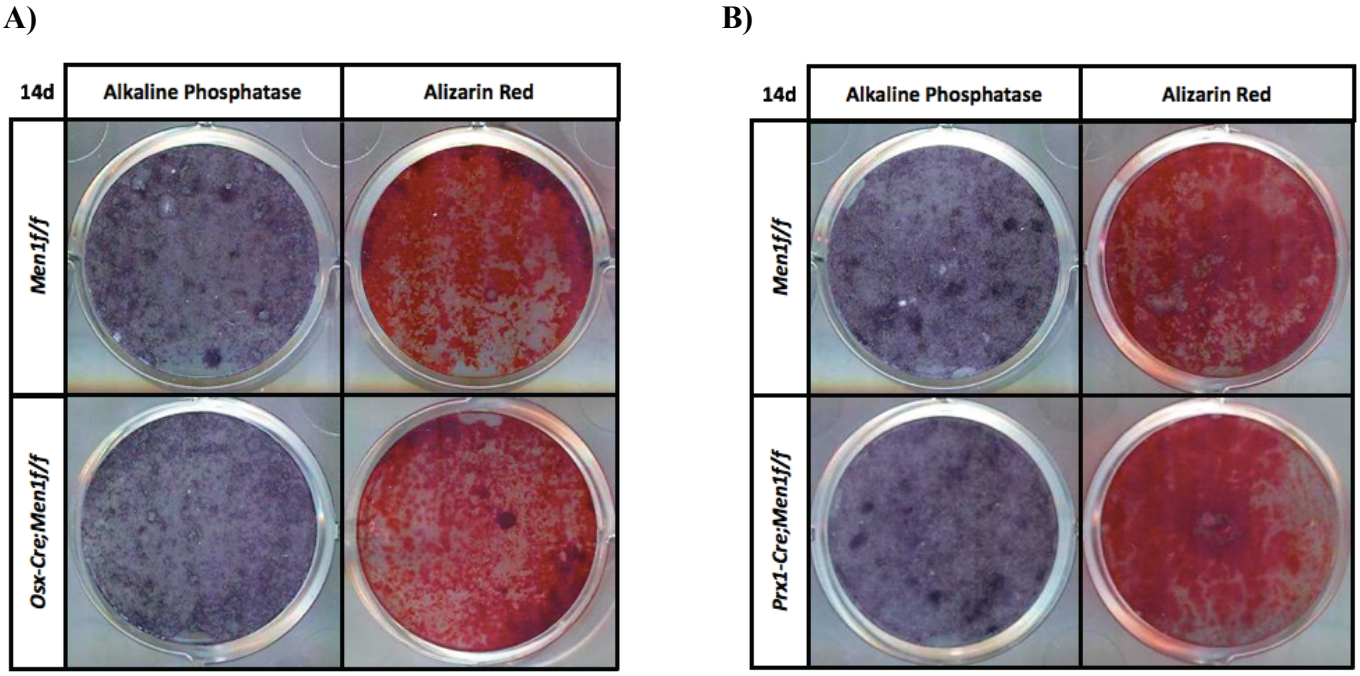
A)
14d
Alkaline Phosphatase
Alizarin Red
Men1f/f
Osx-Cre;Men1f/f
B)
14d
Alkaline Phosphatase
Alizarin Red
Men1f/f
Prx1-Cre;Men1f/f

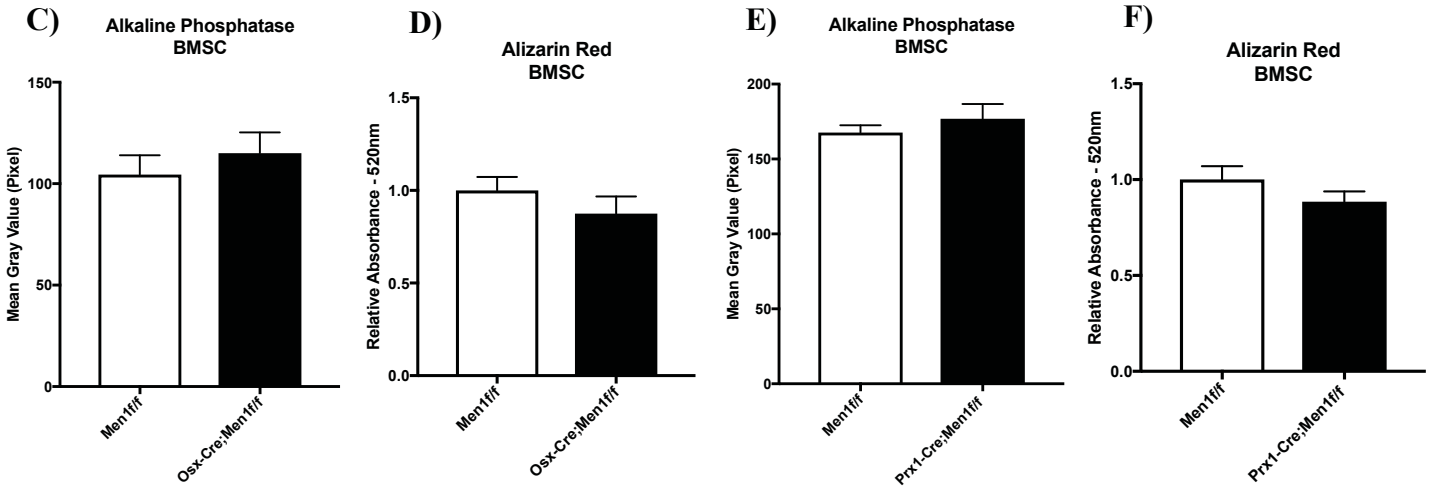
C)
Alkaline Phosphatase BMSC
Mean Gray Value (Pixel)
150
100
50
0
Men1f/f
Osx-Cre;Men1f/f
D)
Alizarin Red BMSC
Relative Absorbance - 520nm
1.5
1.0
0.5
0.0
Men1f/f
Osx-Cre;Men1f/f
E)
Alkaline Phosphatase BMSC
Mean Gray Value (Pixel)
200
150
100
50
0
Men1f/f
Prx1-Cre;Men1f/f
F)
Alizarin Red BMSC
Relative Absorbance - 520nm
1.5
1.0
0.5
0.0
Men1f/f
Prx1-Cre;Men1f/f

Calvarial Osteoblasts

G)

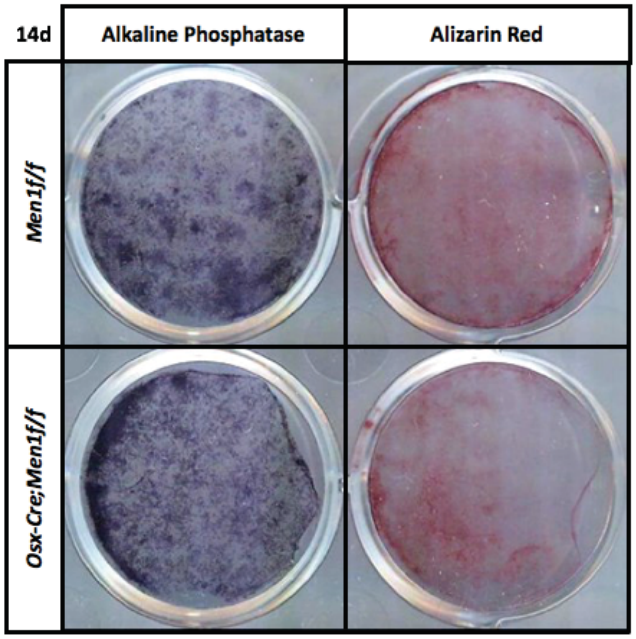

H)

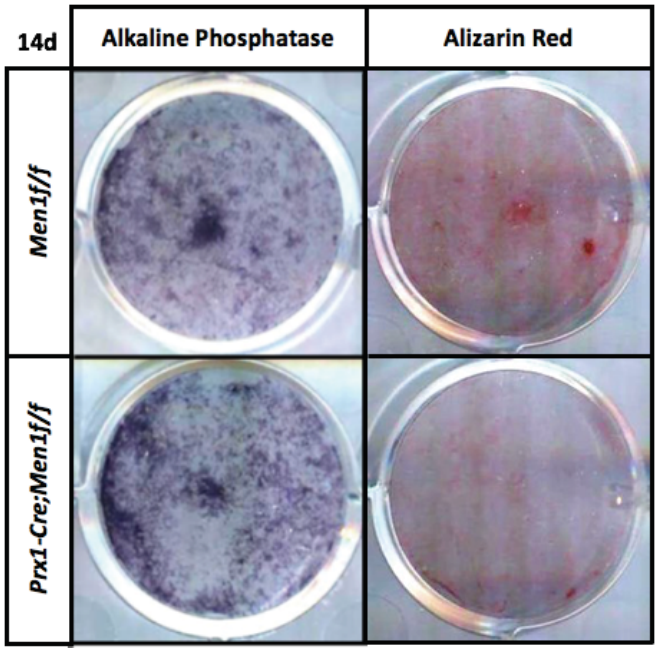

I)

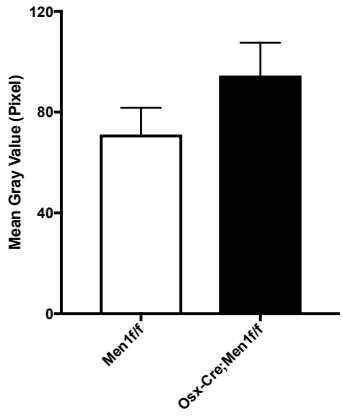

J)

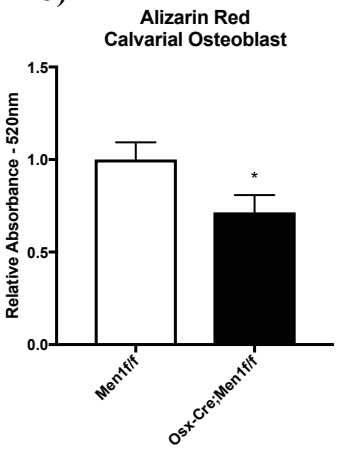

K)

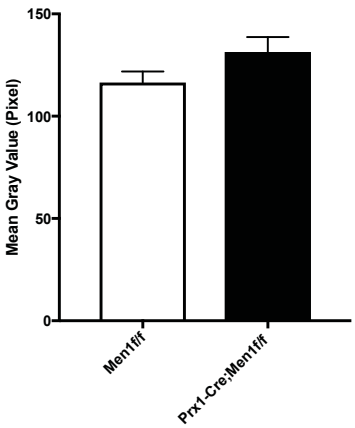

L)

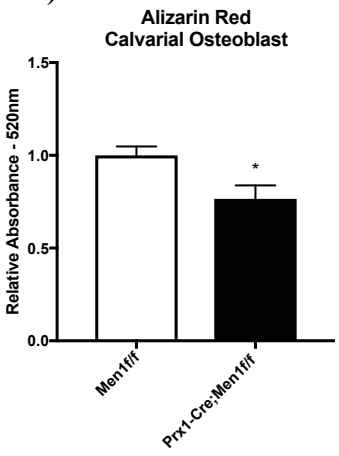

Calvarial Osteoblast

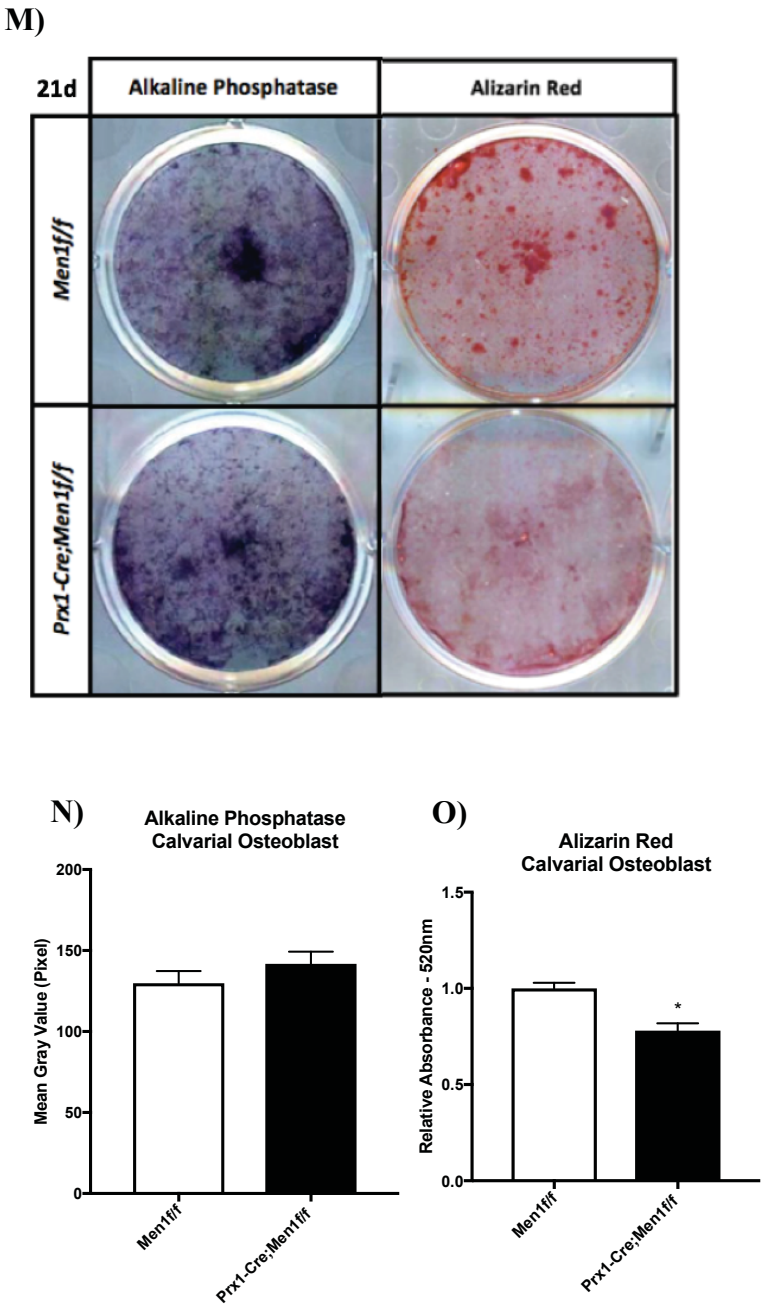

Figure 4.7: **Differentiation and mineralization assays for calvarial osteoblasts and BMSCs of *Prx1-Cre; Men1f/f* and *Osx-Cre; Men1f/f* mice.**
ALP and alizarin red staining with quantification of differentiated (A-F) BMSCs and (G-L) calvarial osteoblasts of 6 month-old *Prx1-Cre; Men1f/f* (n=3 for calvarial osteoblasts and n=6 for BMSCs) and *Osx-Cre; Men1f/f* (n=4,3) mice at day 14 of osteogenic differentiation. ALP and alizarin red staining with quantification of (M-O) calvarial osteoblasts of 6 month-old *Prx1-Cre; Men1f/f* mice at day 21 of osteogenic differentiation (n=3). * $P < 0.05$.

4.8 Disruption of the *Men1* gene early in the osteoblast lineage alters the *RANKL/OPG* ratio *in vitro*.

To investigate the molecular basis explaining the decrease in bone mass in our *Men1* knockout mice, gene expression analysis was made on calvarial osteoblasts and BMSCs isolated from *Prx1-Cre; Men1f/f* mice and control *Men1f/f* littermates. The isolated primary cells were further cultured for 14 days in an osteogenic medium containing L-ascorbic acid and β-glycerophosphate, and changes in mRNA levels of these cells analyzed by RT-qPCR.

RT-qPCR showed that the *Men1* gene expression was reduced by approximately 70% in isolated populations of calvarial osteoblasts and BMSCs from 6 month-old male *Prx1-Cre; Men1f/f* mice. RT qPCR also showed that the relative expression levels of *Runx2* and *OCN*, crucial osteoblastic markers, were not significantly altered in *Men1*$^{-/-}$ calvarial osteoblasts and BMSCs compared with that of control *Men1f/f* mice. Because histological sections showed a significant increase in the number and activity of osteoclasts, the expression levels of both *RANKL* and *OPG,* important markers for osteoclastogenesis, were analyzed. The relative expression level of *RANKL* was not found to be statistically different in primary cell cultures of calvarial osteoblasts and BMSCs of knockout and control mice. However, the expression of *OPG* was increased by ~2-3 fold in both cultures of calvarial osteoblasts and BMSCs of *Prx1-Cre; Men1f/f* mice. Hence, when the *RANKL/OPG* ratio was analyzed, it was reduced by ~70% in osteogenically induced cultures of BMSCs and calvarial osteoblasts from *Prx1-Cre; Men1f/f* mice. Interestingly, RT-qPCR showed that the expression level of *ALP* was ~2.5-fold higher in *Men1*$^{-/-}$ calvarial osteoblasts, whereas its expression in BMSCs isolated from *Prx1-Cre; Men1f/f* mice was not statistically different compared to control cells (Figure 4.8 A-B).

These findings suggest that deleting the *Men1* gene early in the osteoblast lineage does not alter the differentiation of osteoblasts, but rather attenuates their activity by altering *ALP* expression and changing the *RANKL/OPG* ratio.

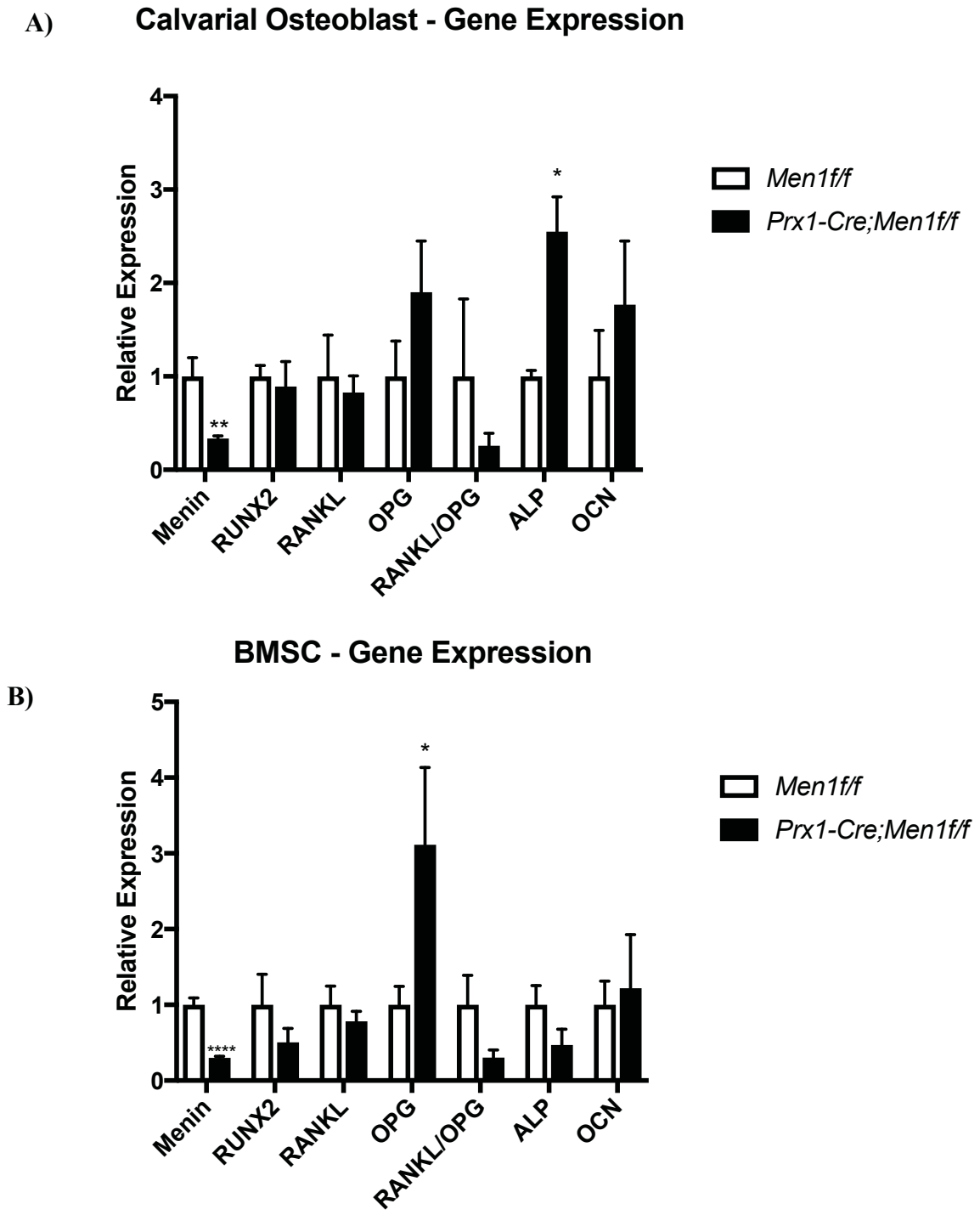

Figure 4.8: Gene expression profiles of isolated calvarial osteoblasts and BMSCs of *Prx1-Cre; Men1f/f* mice.

The expression of menin, Runx2, RANKL, OPG, ALP and OCN, along with variation in the RANKL/OPG ratio were examined by RT-qPCR in cultures of (A) calvarial osteoblasts (n=3) and (B) BMSCs (n=6) at day 14 of osteogenic differentiation. Gene expression was normalized to that of GAPDH, a housekeeping gene. White boxes indicate *Men1f/f* and black boxes indicated *Prx1-Cre; Men1f/f* mice. * *P < 0.05,* ** *P<0.01,* **** *P<0.0001.*

4.9 Osteoblast-specific early deletion of the *Men1* gene results in the increase of the *RANKL/OPG* ratio from bone RNA favoring osteoclastogenesis.

To evaluate what drives the increase in osteoclast numbers observed through our histomorphometric analysis, mRNA levels of osteoclast markers, such as *RANKL* and *OPG* were directly examined from the bones of knockout and wild-type animals. It is important to note that roughly 95% of total bone cells are osteocytes (23-25). Hence, the main type of cells we are looking at when extracting bone RNA are osteocytes, which are also known to be the main producers of *RANKL* in bone and important regulators of osteoclast differentiation.

RT-qPCR analysis of bone RNA isolated from the femur and tibia of 5 month-old *Prx1-Cre; Men1f/f* mice and their control wild-type littermates revealed a marked reduction of approximately 50-60% in *menin's* expression from the femur and tibia of knockout mice. This also shows that recombination of the *Men1* gene specifically occurs in bone tissues. RT-qPCR revealed no significant changes in the expression level of *Runx2* from both the femur and tibia RNA which is consistent with *in vitro* gene expression analysis. Trends of increase in *RANKL* expression levels were however observed from the tibia and femur of *Prx1-Cre; Men1f/f* mice. In contrast to *RANKL*, the expression level of *OPG* was reduced in knockout mice. This reduction was statistically significant in the tibia where it's expression was ~2-fold decreased in knockout mice. The femur on the other hand only showed a nonstatistical decrease of ~11% in the level of *OPG*. Nonetheless, when looking at the expression level of the *RANKL/OPG* ratio, this demonstrated an important trend of being increased by ~2-fold in both the femur and tibia of knockout mice (Figure 4.9 A-B).

The important increase in *RANKL/OPG* ratios observed from the femur and tibia bones suggests that deletion of menin early in the osteoblast lineage *in vivo* results in an elevated *RANKL/OPG* ratio from osteocytes that could induce osteoclastogenesis and promote bone resorption.

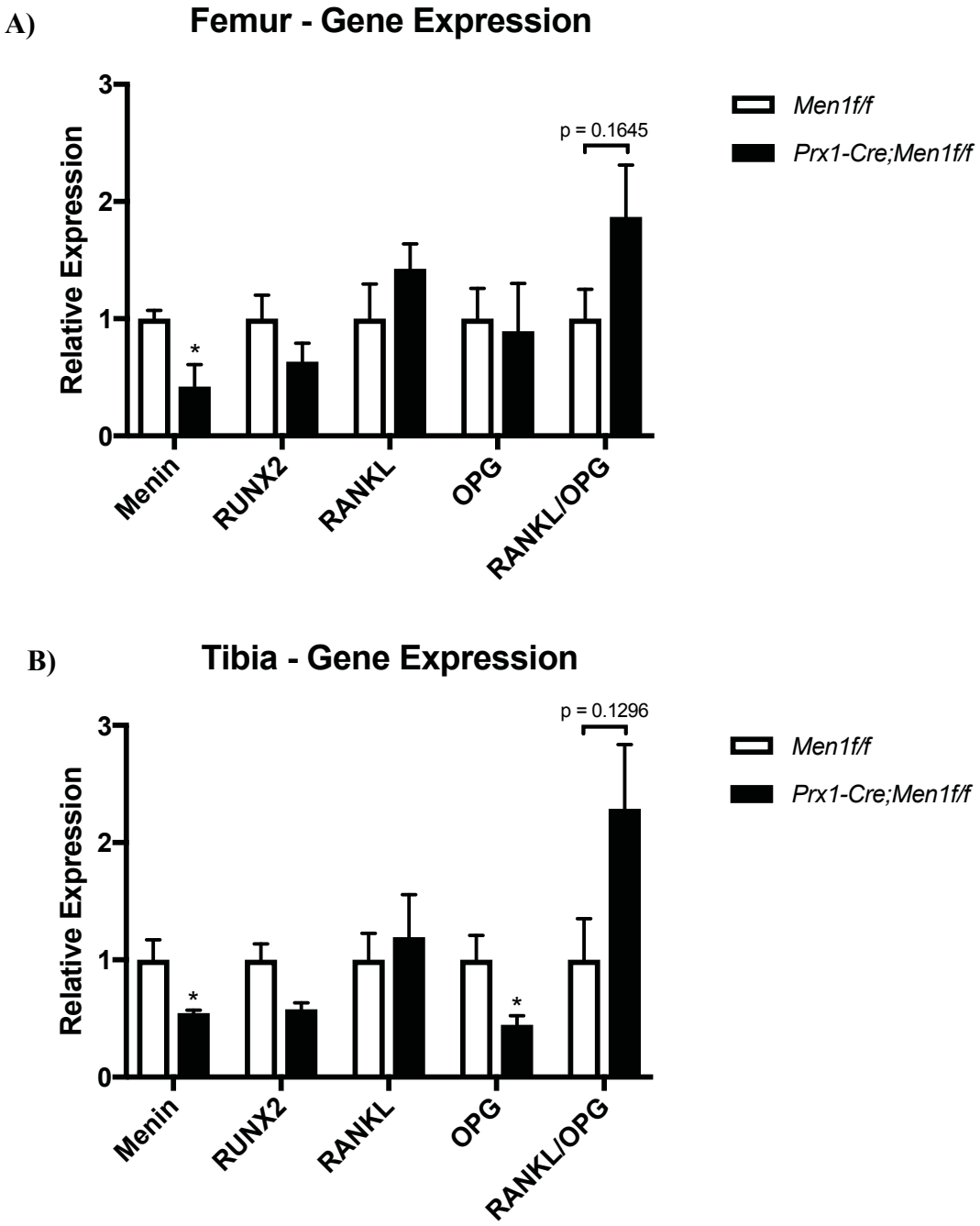

Figure 4.9: **Gene expression profiles of bone RNA of femurs and tibias of *Prx1-Cre; Men1f/f* mice.**
(A-B) The expression of menin, Runx2, RANKL and OPG, along with variation in the RANKL/OPG ratio were examined by RT-qPCR (n=4). Gene expression was normalized to that of GAPDH, a housekeeping gene. White boxes indicate *Men1f/f* and black boxes indicated *Prx1-Cre; Men1f/f* mice. * $P < 0.05$.

4.10 Primary calvarial osteoblasts of the early *Men1* knockout mice seeded within dense collagen gels show defective mineralization mediated processes.

The observed reduction in the mineralization capabilities of primary calvarial osteoblasts from knockout mice led us to further explore these changes. As opposed to two-dimensional (2D) cell-culture models done on plastic dish surfaces, dense collagen three-dimensional (3D) scaffolds better mimic the physiological bone microenvironment and also provide a more adequate natural matrix environment for mediating cellular differentiation and mineralization processes that are relevant to bone biology (166,167,168,169). As such, we decided to use 3D dense collagen hydrogel scaffolds as a cell-culture model to investigate the differentiation and mineralization capabilities of our primary osteoblast cell cultures. For this, primary calvarial osteoblasts isolated from 6 month-old control *Men1f/f* and knockout *Prx1-Cre; Men1f/f* mice were seeded into plastic compressed dense collagen gels and cultured for 21 days in an osteogenic medium to induce differentiation and mineralization.

Metabolic activity of calvarial osteoblasts seeded within dense collagen gels was monitored throughout the 21 days of osteogenic differentiation using the alamar blue assay. No significant changes were observed between wild-type and knockout derived calvarial osteoblasts at Day 2, 10, 15 and 21 of differentiation (figure 4.10 A). These findings are consistent with MTT results also revealing no marked changes in cell viability between calvarial osteoblasts derived from our knockout and control mice.

Scanning Electron Microscopy (SEM) was performed on collagen scaffolds seeded with primary calvarial osteoblasts derived from *Prx1-Cre; Men1f/f* and *Men1f/f* mice. SEM of cell-seeded scaffolds at day 21 of differentiation revealed the presence of a fine meshwork of collagen

fibrils constituting the scaffold and of osteoblast-like cells that were well dispersed within collagen fibrils (figure 4.10 B-C; E-F). Cell mediated mineralization at day 21 was as well observed in both *Men1f/f* and *Prx1-Cre; Men1f/f* samples (figure 4.10 D, G). However, in contrast to collagen gels seeded with wild-type primary calvarial osteoblasts (figure 4.10 D), collagen fibres of *Prx1-Cre; Men1f/f* seeded gels (figure 4.10 G) appeared covered by overall smaller calcium phosphate based mineral quantities, suggesting a different cell mediated mineralization process that is carried out by knockout cells in comparison to wild-type cells.

These marked qualitative differences observed in terms of the mineralization capabilities of primary knockout osteoblasts where menin is deleted, led us to further evaluate ionic composition changes of the extracellular mineralized matrix. Energy-dispersive x-ray (EDS) spectroscopy of day 21 mineralized collagen gels seeded with knockout and wild-type cells showed the presence of major spectral peaks for calcium (Ca) and phosphorus (P). As opposed to collagen gels seeded with *Men1f/f* calvarial osteoblasts, the intensity peaks for Ca and P in the collagen gels seeded with *Prx1-Cre; Men1f/f* calvarial osteoblasts were lower (figure 4.10 H-I).

Fourier Transform Infrared Spectroscopy (FTIR) analysis was performed on day 1, 15 and 21 cell-seeded samples. FTIR revealed characteristic peaks for collagen (amide I band at 1637cm^{1}, amide II band at 1544cm^{-1} and amide III band at 1237cm^{-1}) in day 1, 15 and 21 cell-seeded samples. Characteristic phosphate (PO_4^{3-}) and carbonate (CO_3^{2-}) absorbance peaks at 1020cm^{-1} and 872cm^{1}, respectively, were also observed in day 15 and 21 samples, but not in day 1 samples. The shape and value of the PO_4^{3-} band as well as the presence of a CO_3^{2-} peak suggest a mineral phase that is composed of carbonated apatite, the main component of hard bone tissues. Under osteogenic conditions, mineralization, assessed by the intensity of the PO_4^{3-} peak, of cell-seeded scaffolds gradually increased over time and reached the highest level at day 21 in both *Men1f/f* and *Prx1-*

Cre; Men1f/f cell-seeded gels. However, starting at day 15, the absorption band intensities attributable to phosphate and carbonate species of *Prx1-Cre; Men1f/f* cell-seeded gels appeared reduced in comparison to *Men1f/f* cell-seeded gels. This difference was found to be even more pronounced at day 21 (figure 4.11 A-B).

All together, these results indicate that using 3D dense collagen hydrogel scaffolds as an alternative to conventional 2D systems of primary cell cultures is both a better and more sensitive model for the study of cell-mediated mineralization processes. In our case, we also show here that early expression of menin is important for regulating osteoblast mineralization.

A)

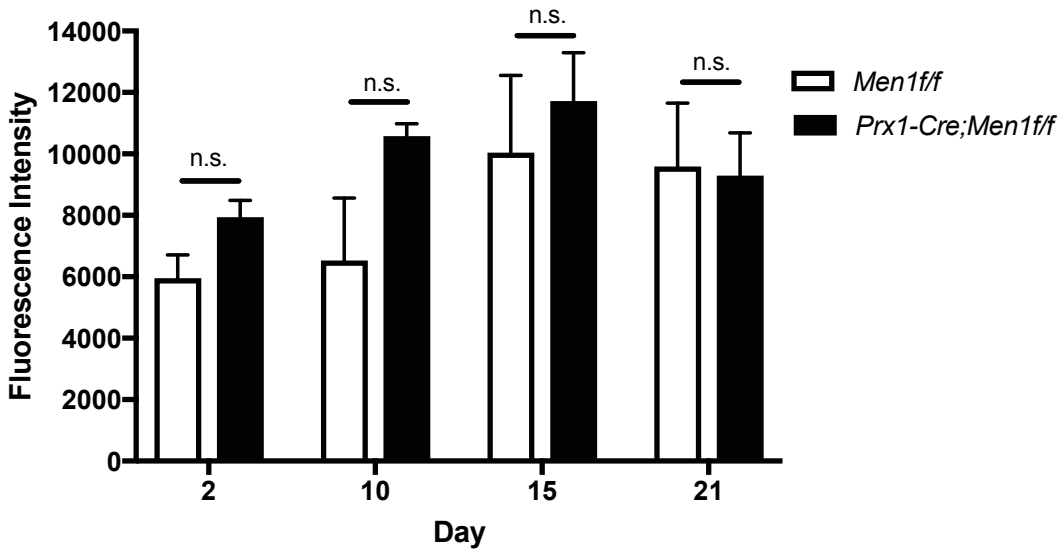
Alamar Blue Assay
Fluorescence Intensity
14000
12000
10000
8000
6000
4000
2000
0
n.s.
n.s.
n.s.
n.s.
2
10
15
21
Day
Men1f/f
Prx1-Cre;Men1f/f

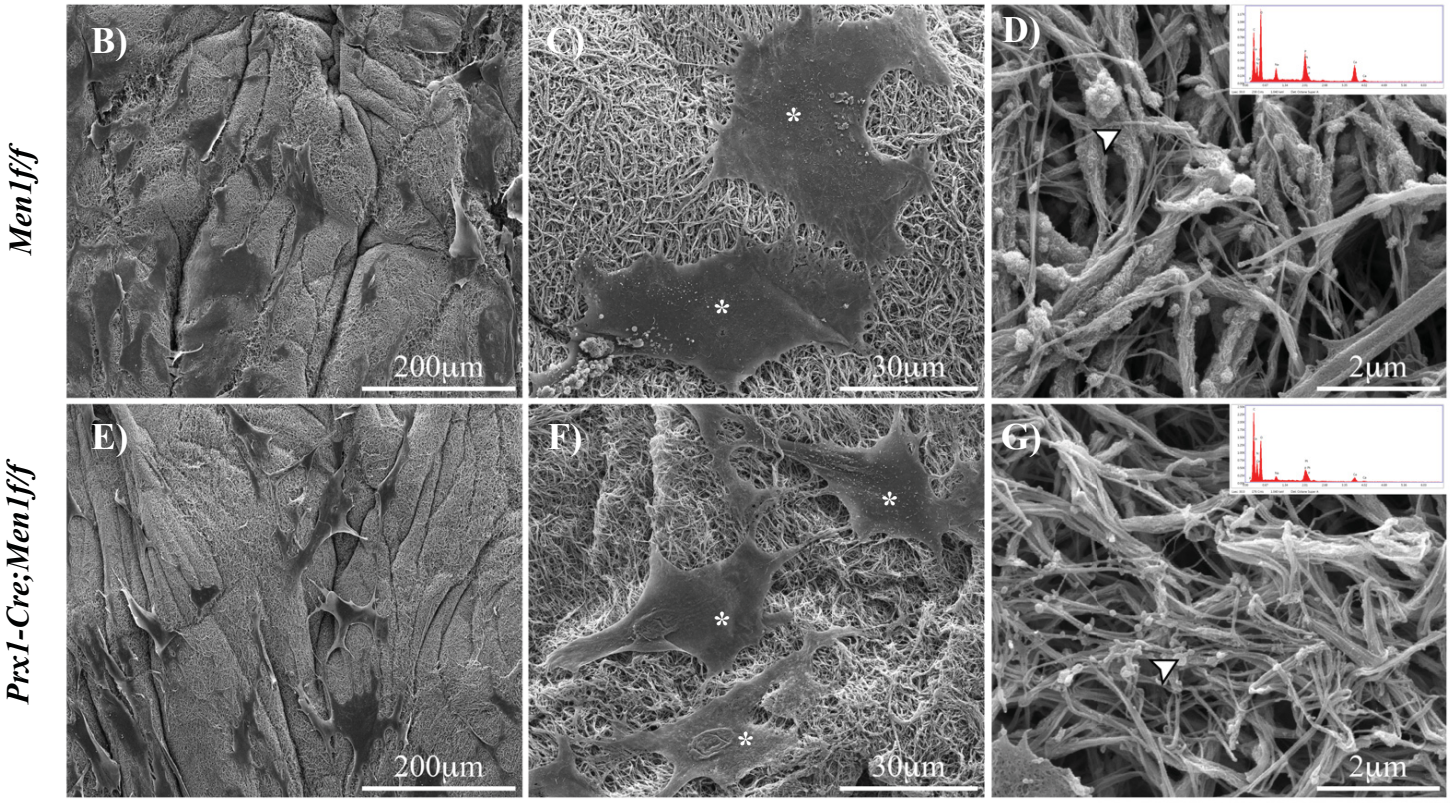
Men1f/f
Prx1-Cre;Men1f/f
B)
C)
D)
E)
F)
G)
200µm
30µm
2µm
200µm
30µm
2µm

H)

Men1f/f

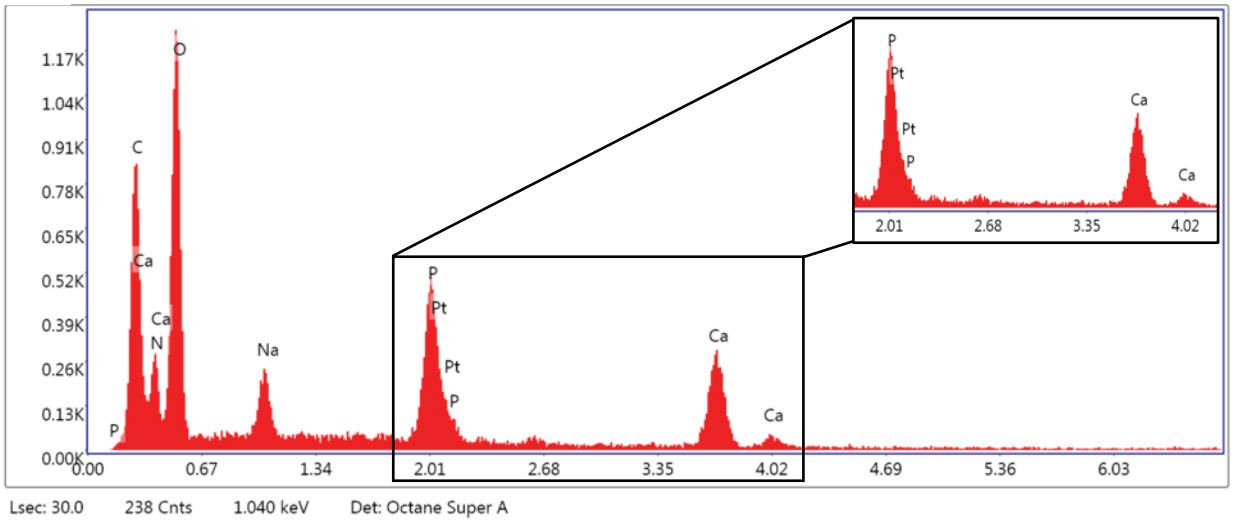

I)

Prx1-Cre; Men1f/f

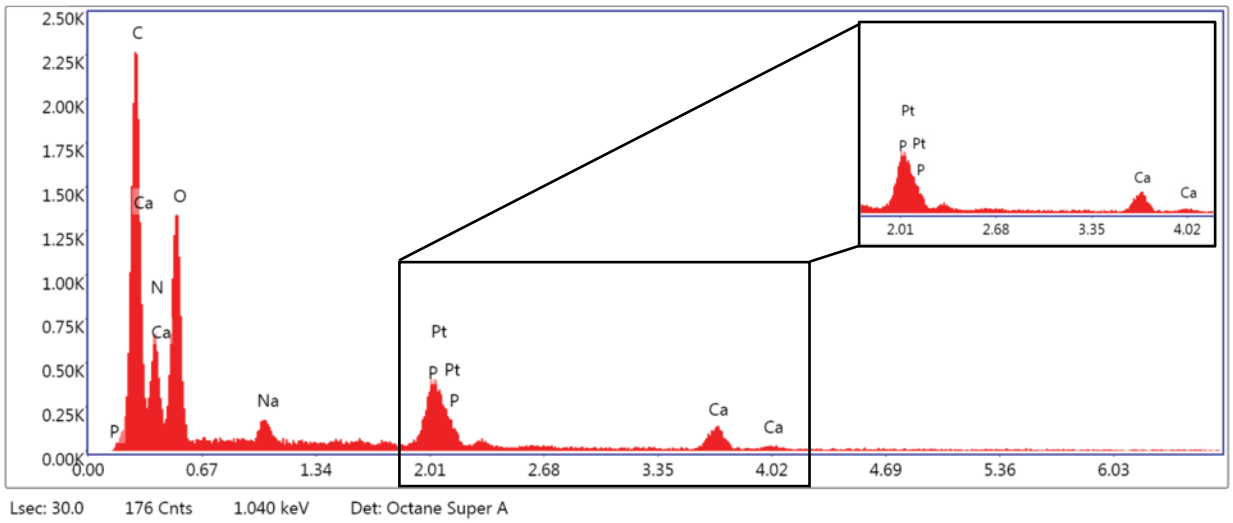

Figure 4.10: **Metabolic activity and microscopic analysis of primary calvarial osteoblast in dense collagen scaffolds under osteogenic conditions.**
(A) Alamar blue assay of cell-seeded gels of 6 month-old *Prx1-Cre; Men1f/f* and *Men1f/f* mice at day 2, 10, 15 and 21 of osteogenic differentiation (n=3). Scanning electron microscopy (SEM) micrographs of day 21 cell-seeded scaffolds with calvarial osteoblasts of 6 month-old (B-D) *Men1f/f* and (E-G) *Prx1-Cre; Men1f/f* mice (n=3). (C,F) Calvarial osteoblasts (asterisks) were evenly distributed within the collagen gels. Energy-dispersive x-ray (EDS) spectroscopy of day 21 mineralized collagen gels of (H) *Men1f/f* and (I) *Prx1-Cre; Men1f/f* samples reveals the major spectral peaks for phosphorus (P) and calcium (Ca) (n=3).

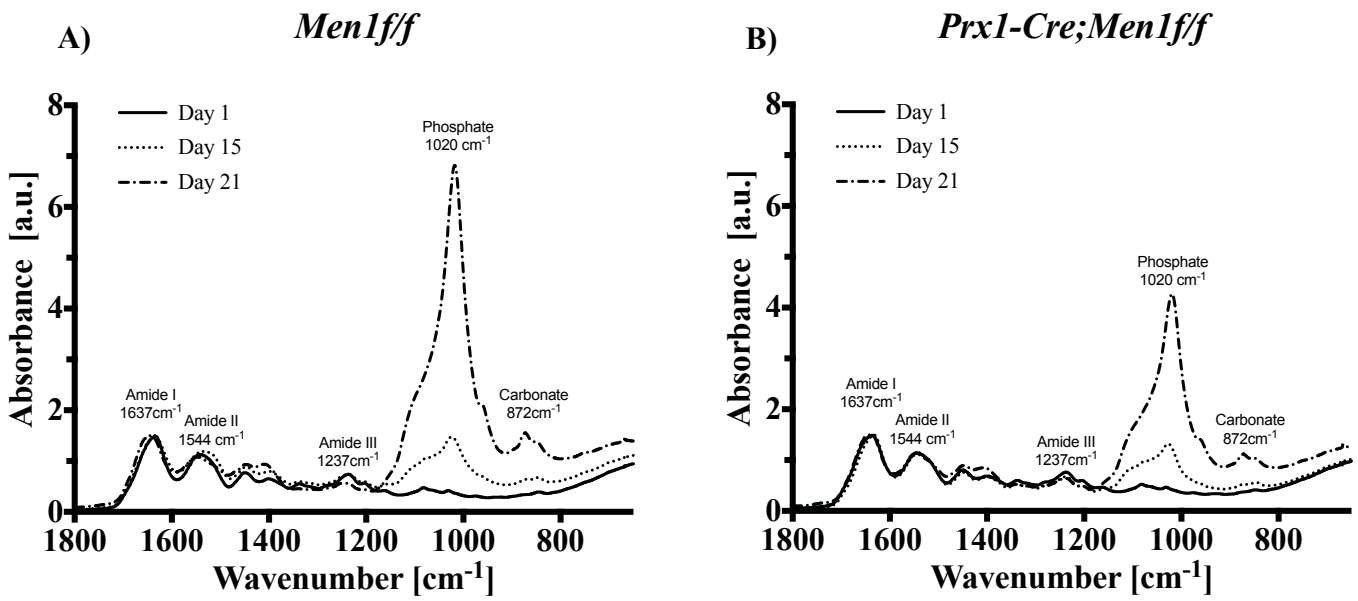

Figure 4.11: **FTIR analyses of mineralization of calvarial osteoblast-seeded dense collagen scaffolds under osteogenic differentiation.**
(A-B) FTIR spectra of cell-seeded gels of 6 month-old *Men1f/f* and *Prx1-Cre; Men1f/f* mice at day 1, 15 and 21 of osteogenic differentiation (n=3). Phosphate (1020 cm^{-1}) and carbonate (872 cm^{-1}) peaks characteristic of hydroxyapatite formation were identified at different wavelength.

CHAPTER 5: DISCUSSION

5.1 General discussion

In humans, bone is an important organ which besides providing support for other body organs plays essential roles in regulating metabolic processes (1,2). For the bone functions to be adequately maintained, bone itself must continuously be renewed. This is achieved by a mechanism called remodeling which persists throughout human life whereby old bone is degraded by osteoclasts and replaced with new bone via the action of osteoblasts (1,2). The processes of resorption and formation are maintained within a tightly regulated balance. Any imbalance in bone remodeling will cause metabolic bone disorders categorized through either loss (e.g. osteoporosis) or gain (e.g. osteopetrosis) in bone mass (1,2,46-48). Osteoporosis is the most prevalent metabolic bone disease characterized by a reduction in bone mass and deterioration of the overall bone microarchitecture. The causes of osteoporosis can be many, but generally speaking it is caused as a result of either low bone formation, increase bone resorption, or both (41,48,49). Therapeutically, anti-resorptive agents like bisphosphonates, which downregulate osteoclast activity, are often used after initial diagnosis of osteoporosis. However, their use does not increase bone mass or ameliorate the already damaged bone microarchitecture (49,56). Anabolic agents on the other hand can increase bone mass by stimulating bone formation. Presently, only teriparatide and abaloparatide, synthetic analogues of PTH and PTHrP, respectively, are approved for clinical use (56). In order to design new and better anabolic agents for treating low bone mass disorders such as osteoporosis, it is important to elucidate the functions of regulators affecting molecular pathways directly implicated in bone homeostasis.

Our group and others have identified the nuclear protein menin, encode by the *MEN1* gene, as an important mediator of osteoblast differentiation needed to maintain bone mass

(125,126,154,155). The first evidence of the implication of menin in bone development was suggested by studies by Crabtree *et al*, in 2001, and Bertolino *et al*, in 2003 (150,151). In these studies, using conventional knockout mouse models in which the *Men1* gene was constitutionally deleted, it was demonstrated that besides being embryonically lethal, homozygous *Men1*$^{-/-}$ fetuses exhibited important developmental delay, neural tube defects and craniofacial defects, suggesting the potential for menin to mediate intramembranous bone ossification. From these initial observations, other studies looked at the effects of osteoblast menin in mediating bone homeostasis. Our group has specifically shown that when expressed in osteoblast cell lines, menin regulates the TGF-β/BMP-2 signaling pathways which are important for osteoblast differentiation. In fact, menin associates with Smad1/5 and Smad3, crucial transducers of the BMP-2 and TGF-β signaling, respectively, in order to facilitate the commitment of MSCs to the osteoblast lineage and to control osteoblast apoptosis (125,126). These findings were demonstrated through *in vitro* studies, but were also recently confirmed by Kanazawa *et al*., in 2015 using primary calvarial osteoblast cultures from osteoblast-specific *Men1* knockout mice (155). Others have confirmed *in vivo* the important role that menin plays in bone development. Using neural crest-specific knockout mice whereby exons 3-8 of the *Men1* gene were deleted, Engleka *et al.,* illustrated the importance of menin for the adequate development of cranial and rib bones (154). From these results, it is clear that when expressed in neural crest cells or in mature osteoblasts, menin plays an important role in the development of bones and for maintaining bone mass *in vivo*. While menin modulates the TGF-β and BMP-2 signaling pathways in the mature osteoblast, it may be working through additional pathways when expressed at earlier stages of osteoblastogenesis, from the commitment of MSCs to the osteoblast lineage and later differentiation.

In the present study the role that menin plays early in the osteoblast lineage is being examined by conditionally disrupting the *Men1* gene at the level of the MSC (*Prx1-Cre; Men1f/f*) and osteoblast progenitor (*Osx-Cre; Men1f/f*). The hypothesis is that menin plays a crucial role in the early stages of osteoblast differentiation, and that its conditional knockout will be manifested as defects in bone development.

While osteoblast numbers, differentiation and proliferation were not altered between knockout and wild-type animals, results obtained have thus far clearly demonstrated that specific disruption of the *Men1* gene early in osteoblastogenesis significantly impacts bone development. In fact, skeletal phenotyping performed at 6 months of age showed significantly reduced BMD and bone volume in the *Prx1-Cre; Men1f/f* and *Osx-Cre; Men1f/f* knockout mice strains. Three-dimensional μCT imaging of both strains of knockout mice showed reduction in the trabecular bone volume and altered trabecular bone structure. The femur length of 6 month-old knockout mice of the *Prx1-Cre; Men1f/f* and *Osx-Cre; Men1f/f* strains was also found to be significantly reduced, indicating changes occurring not only in the development of bones, but as well as in their growth. Histomorphometric analyses showed an increase in osteoclast numbers and activity along with unaltered osteoblast numbers and bone formation rates in both strains of transgenic mice (156).

Analysis of the biomechanical properties by mechanical testing using the 3-point bending test demonstrated that the decrease in bone mass and microarchitecture after menin deletion in the osteoblast lineage also translated into substantial decreases in bone strength and stiffness. In fact, when assessing parameters such as the femur stiffness, maximum load, load at yield and load at

break, all were significantly reduced in adult *Prx1-Cre; Men1f/f* and *Osx-Cre; Men1f/f* mice. These results illustrate that the bones of knockout mice are more prone to fracture which is characteristic of low bone mass disorders, such as osteoporosis.

It is clear that disruption of the *Men1* gene both at the level of the MSC and osteoblast progenitor impacts bone development and formation. Based on the *in vivo* results so far presented the significant reduction in bone mass seems to be a priori a consequence of the marked increased in osteoclast number and activity favoring bone resorption. This is a striking feature that is different from when the *Men1* gene is deleted specifically at the level of the mature osteoblast *in vivo*, where the result is also a decrease in bone mass, but that is primarily attributable to a decrease in osteoblast differentiation and enhanced apoptosis rather than to an increase in osteoclast activity (155).

To unravel the cellular mechanisms that account for the low bone mass in our study, *in vitro* differentiation experiments with primary calvarial osteoblasts and BMSCs were performed. Assessment of the morphology, growth and differentiation capabilities of the primary cells isolated from 6 month-old knockout mice was made. The morphology as well as cell viability, assessed through the MTT assay, of both primary calvarial osteoblasts and BMSCs of *Prx1-Cre; Men1f/f* and *Osx-Cre; Men1f/f* mice were similar to the primary cells isolated from age- and sex-matched control mice. To investigate whether *Men1* disruption could influence osteoblast differentiation *in vitro,* primary calvarial osteoblasts and BMSCs were isolated and cultured in the presence of an osteogenic medium to induce cell differentiation. ALP and alizarin red histochemical staining were performed to assess changes in cell differentiation and mineralization, respectively.

ALP staining of primary calvarial osteoblasts and BMSCs isolated from 6 month-old *Prx1-Cre; Men1f/f* and *Osx-Cre; Men1f/f* mice and cultured in the presence of an osteogenic medium showed no significant changes in intensity in comparison to wild-type primary cells isolated from *Men1f/f* control mice. The metabolic activity of osteoblasts of knockout and control mice was monitored at weekly intervals throughout the 21 days in culture using the alamar blue cell viability assay, and revealed no significant changes at any time point. These results are consistent with *in vivo* static histomorphometric analysis that demonstrate no differences in the total osteoblast number per bone area in *Prx1-Cre; Men1f/f* and *Osx-Cre; Men1f/f* animals. Alizarin red staining, which shows the presence of calcium deposits in the extracellular matrix produced by differentiated osteoblasts, revealed a slight reduction in the mineralization capabilities of primary calvarial osteoblasts from both *Prx1-Cre; Men1f/f* and *Osx-Cre; Men1f/f* mice. However, BMSCs of knockout mice didn't demonstrate any marked changes in alizarin red staining in comparison to the control mice. These differences could be attributable to site-specific differences between calvarial osteoblasts and BMSCs, as well as to changes in the isolated cell type itself. In addition, it is important to note that calvarial bones are formed predominantly through intramembranous ossification whereas long bones, such as the tibia and femur, are formed through endochondral ossification (3-6). Hence, it is possible that osteoblasts derived from these two different sites have properties that differ as suggested by other studies (170).

Interestingly, the slight reduction observed *in vitro* in terms of the mineralization capabilities of the primary calvarial osteoblasts from knockout mice is in contrast to the *in vivo* dynamic histomorphometric analysis which do not show differences in both the bone formation

rate and mineral apposition rate between knockout and wild-type mice. Culturing the primary cells *ex vivo* in a cellular environment that does not precisely reflect the *in vivo* bone environment could be a reason explaining these differences. Hence, to address this particular question, we decided to culture primary calvarial osteoblasts in 3D-collagen gels which better mimic the bone microenvironment and provide a better alternative to 2D cell-culture models for the study of cellular differentiation and mineralization events (166-169). Such a technique also allows the observation of nanoscale changes in mineralization which can occur but that dynamic histomorphometry analysis won't necessarily reveal at the cellular level. In doing so, we found that the collagen fibres seeded with calvarial osteoblasts of *Prx1-Cre; Men1f/f* mice were covered by overall smaller calcium phosphate based mineral quantities than the collagen gels seeded with calvarial osteoblasts derived from *Men1f/f* control mice. This was confirmed by both SEM, FITR and EDS analysis, and is suggesting a different cell mediated mineralization process carried out by osteoblasts of knockout mice compared to wild-type. Overall, these results indicate that deletion of menin early in the osteoblast lineage affects the osteoblast-mediated mineralization of collagen fibrils (171).

In vitro gene expression profiling of RNA extracted from primary cultures of calvarial osteoblasts in our *Prx1-Cre; Men1f* mice revealed increases in the expression of *ALP* and decreases in the overall *RANKL/OPG* ratio. Clinically, bone-specific ALP can be used as a biochemical marker of bone formation and elevated levels generally indicate increased osteoblastic activity (172). It is also well established that high levels of bone specific *ALP* can lead to a higher probability of bone loss as a concurrent result of the high degree of bone resorption rate that is outweighing that of formation (173,174). Hence, the increased expression of *ALP* we observe from

our osteoblast cell cultures is consistent with the high osteoclastic activity we also observe *in vivo* in our knockout mice. While it is surprising to see that the levels of osteoblasts are not altered *in vitro* even though the increase in *ALP* expression, we do observe an increase in the levels of *OPG*. OPG is a protein that can be produced by osteoblast and acts as a decoy receptor to RANKL (32). The noted high osteoblastic activity could translate into osteoblast producing more OPG in order to compensate for the substantial increase in osteoclast activity concurrently happening in our mouse models where the *Men1* gene is disrupted early in the osteoblast lineage. It is also interesting to see that even though the activity of primary calvarial osteoblasts are elevated that there still is a slight reduction in their mineralization capabilities. In the literature, it has been reported that high bone turnover rate can lead to material and nanomehanical deformities in bone (175). In fact, compared to bones from patients with a normal turnover, bones from patients with a high turnover rate show lower mineralization as well as lower stiffness and hardness (175,176). These findings are consistent with our data, where we also demonstrate reductions in bone stiffness and strength as well as lower mineralization in the primary osteoblast of knockout mice. Hence, it is highly plausible that the observed increase in osteoblast activity, as a mean to produce more OPG to compensate for the elevated osteoclastic activity, alters their intrinsic functions leading to mineralization deficiencies and reduced overall bone quality.

The elevated numbers of osteoclasts observed *in vivo* along with the low RANKL/OPG ratio observed from primary osteoblast cell cultures *in vitro* led us to further investigate osteoclastic activity changes between knockout and wild-type mice by performing osteoclastogenesis experiments. Normal control osteoclastogenesis experiments consisting in exogenously stimulating osteoclast precursor cells with RANKL and M-CSF along with

osteoblast-osteoclast co-culture experiments using osteoblasts and osteoclast precursors from knockout and wild-type mice were performed in this regard. Surprisingly, significant increases in the numbers of osteoclasts were observed in osteoclastogenesis experiments with osteoclast precursors of both *Prx1-Cre; Men1f/f* and *Osx-Cre; Men1f/f* mice, while osteoblast-osteoclast co-culture experiments revealed no significant changes between knockout and wild-type mice (Data not shown) (177). This indicates an enhanced responsiveness of osteoclast precursors to RANKL and M-CSF, suggesting a priming effect occurring in the osteoclast precursors of knockout mice.

The lack of differences between knockout and control seen in co-culture experiments is intriguing considering the increase in osteoclastogenesis of knockout osteoclast precursors. These data are indicating that there could exist a mechanism by which osteoblasts could detect changes in osteoclastic activity and regulate it. Whether this would be at the level of differentiated osteoclasts or osteoclast precursors is unclear. The low RANKL/OPG ratio observed in primary osteoblasts of knockout mice is suggesting that such a mechanism could exist, whereby osteoblasts could detect the elevated differentiation capabilities of osteoclast precursors and regulate these levels to normal by lowering the RANKL/OPG ratio. In the literature, it is known that a possible means by which osteoblasts and osteoclasts could talk with each other is through the interplay of Ephrin receptor/ligand pathways (178). These are known to regulate important transcription factors involved in osteoclastogenesis, such as NFATc1 and c-Fos (178). Nonetheless, in our study, it is still surprising to see a low RANKL/OPG ratio considering the marked increase in osteoclast number and activity that are observed *in vivo*. From of these results, we believe that there must be another factor, other than RANKL and OPG produced and released by osteoblasts, that is mediating the increased osteoclastic activity in the knockout mice. In the literature, it is

known that other than osteoblasts, osteocytes are the most important source of RANKL and OPG (179,180). Recent studies have demonstrated that osteocytes are in fact the principal source of RANKL participating in the recruitment of osteoclasts and initiation of bone remodeling (179,181,182). Since the *Men1* gene is specifically disrupted early in the osteoblast lineage and osteocytes are mature osteoblasts trapped within the bone matrix, it could well be that factors released by osteocytes are promoting osteoclastic activity in our knockout mice models. To test this, we analyzed the expression levels of *RANKL* and *OPG* from RNA extracted directly from long bones, where ~95% of bone cells consist of osteocytes. Increases of ~2-fold in the expression of *RANKL/OPG* ratios from both the femur and tibia were found. Hence, increased osteoclast activity and bone resorption in our early menin knockout mice models could occur as a consequence of the higher RANKL/OPG ratio from osteocytes.

So far, we have established the role of menin in bone mass control through the study of *in vivo* mouse models. The recent emergence of the importance of bone as an endocrine organ led us to further investigate whether early deletion of menin in the osteoblast lineage also has a functional role in bone as a regulator of energy metabolism (59,63). For this, the bodyweights between both *Prx1-Cre; Men1f/f* and *Osx-Cre; Men1f/f* and their control wild-type littermates were measured. Significant decreases of approximately ~10-14% in bodyweights from both strains of knockout mice were observed in adult mice. Echo-MRI analysis showed changes in terms of the overall fat and lean mass content in adult mice from both strains of knockout animals, but when normalizing these values to total bodyweight, the percentage of fat and lean mass were not significantly altered in adult male mice. Since important differences in the bone phenotype of *Prx1-Cre; Men1f/f* and *Osx-Cre; Men1f/f* animals are seen, one reason could be that knockout animals have an overall

reduced body size as compared to wild-type controls. However, due to alterations in only lean mass and not fat mass content in *Prx1-Cre; Men1f/f* animals and due to significant changes in the percentage of fat and lean mass in female *Osx-Cre; Men1f/f* mice, there must be alterations other than the reduction of bone mass occurring by menin early deletion in the osteoblast lineage. Certain studies have demonstrated that menin is important for the commitment of MSCs to the adipogenic and myogenic lineages (138-140). These findings are of relevance to our study because we are specifically knocking-out menin in mesenchyme-derived progenitors, which could have resulted in the differentiation of MSCs to lineages other than osteoblasts being impacted upon. In addition to the decrease in bodyweight and changes in body composition, we find trends of reduction in WAT and BAT weights in our study. In mammals, BAT is known to regulate energy expenditure and thermogenesis (183). When looking at the expression levels of energy metabolism markers, such as *Pgc1α* and *Ucp1*, directly from BAT, the relative expression level of *Ucp1* was ~5-fold higher and the expression of *Pgc1α* ~2-fold reduced in *Prx1-Cre;Men1f/f* mice. These suggest that BAT could be a mediator of the effect of menin deletion in mesenchyme-derived progenitors on body metabolism.

Furthermore, reports have also well established that a positive correlation exists between BAT activity and bone mass. Studies using mouse models of either loss or gain of function in BAT have demonstrated that impairing BAT activity reduces bone mass, while inducing it has anabolic effects on the skeleton (184, 185). These findings have been further correlated with human studies showing that children and young non-obese women with higher BAT activity display an overall better maintenance of bone mass (186, 187). Uncoupling protein-1 (UCP1) is critical for the role of BAT to dissipate energy in the form of heat (188). Although the functions of BAT and UCP1

in energy homeostasis are well established, little is known about the precise mechanisms through which BAT activity mediated in part through UCP1 affects bone metabolism. A recent study by Nguyen *et al.*, looking into the effects of UCP1 ablation in bone homeostasis, demonstrated that UCP1 is important in protecting bone mass under thermal conditions when BAT UCP1 activation is needed for temperature control (189). This study further illustrated that one mechanism by which UCP1 could control bone mass was through mediating changes in hypothalamic neuropeptide Y (NPY) pathways that regulate the sympathetic nervous system (SNS) activity. To date, most of the studies looking at the effect of UCP1 and BAT activity in bone metabolism have been unidirectional in that only the consequences of BAT loss of function in bone homeostasis were investigated. Whether or not bone loss directly affects UCP1 mediated BAT functions is not known. In our study, we provide evidence to suggest that UCP1 could mediate a physiological response to the important loss of bone mass, which supports the findings made by Nguyen *et al*., of UCP1 being protective of bone mass. However, whether this is due to the inactivation of menin in mesenchyme-derived progenitors, to the osteoblast functions being altered or as a result of the substantial bone loss in our study needs to be further determined.

The tendency of ~2-fold decrease in *Pgc1α* expression in BAT was also an interesting finding. PGC1α is a transcriptional co-activator expressed in many tissues that plays crucial roles in mitochondrial biogenesis and in the regulation of genes involved in energy metabolism (190). While it is well known that dysregulation of PGC1α causes metabolic disorders such as obesity and diabetes, not much is known about the role of PGC1α in metabolic bone loss (190). The only reports of its effect on bone come from findings made by Khan *et al*, which demonstrated that PGC1α downregulation leads to osteoblast apoptosis and that its upregulation in osteoblasts

reverses type 2 diabetes-associated bone loss (191). In BAT, PGC1α can interact with the nuclear receptor PPARγ to regulate the transcription of thermogenic genes, such as *Ucp1*(192). Because the expression levels of both *menin* and *PPARγ*, a known molecular partner of menin, were unaffected in our knockout mice, this is suggesting that instead of menin, the observed changes in BAT activity might be mediated by a factor derived from *Men1*-deficient osteogenic cells which affects *Ucp1* transcriptional regulation through a transcriptional co-activator other than *Pgc1α*.

Another important finding made through assessing the metabolic phenotype of our knockout mice were the changes in lean mass content. It is well known that muscle and bone both functionally and mechanically interact together, and that muscle mass content generally positively correlates with bone mass (193). Hence, to determine whether the observed differences in bone and lean mass could affect the skeletal muscle strength of our transgenic mice strains, the grip strength test was performed. Interestingly, *Prx1-Cre; Men1f/f* male mice exhibited ~30% decrease in the forelimb grip strength, while both male and female *Osx-Cre; Men1f/f* mice showed ~13-18% increase in the forelimb grip strength when normalizing the grip strength values to each individual mice bodyweight. These findings are consistent with the Echo-MRI data revealing an important decrease of ~8% in the lean mass content of male *Prx1-Cre; Men1f/f* and increase of ~9% in the lean mass percentage of female *Osx-Cre; Men1f/f* mice. Although both male *Prx1-Cre; Men1f/f* and *Osx-Cre; Men1f/f* mice displayed significant decreases in lean mass content, male *Osx-Cre; Men1f/f* mice had decreases in both fat mass content by ~20% and lean mass content by ~9%, whereas male *Prx1-Cre; Men1f/f* mice only demonstrated a significant reduction in terms of their lean mass content, but not in fat mass content. Because bodyweights of both male *Prx1-Cre; Men1f/f* and *Osx-Cre; Men1f/f* mice were reduced by ~10-12%, we can assume that the decrease

in lean mass of ~8% in *Prx1-Cre; Men1f/f* male mice has a more severe effect than in *Osx-Cre; Men1f/f* mice as it is the main factor causing the reduction in bodyweight. A study by Aziz *et al*., has showed that menin potentiates TGF-β1 mediated Smad3 repression of myogenesis in the MSCs (140). The findings by Aziz *et al*., also illustrated that low expression of menin favors the differentiation of muscle cells and further demonstrated that knocking out menin specifically in neural crest cells *in vivo* increases intercostal muscle mass at birth (140). This would support the findings made with our female *Osx-Cre; Men1f/f* mice which showed a higher percentage of lean mass. Since *Prx1-Cre; Men1f/f* mice are deficient for menin at an earlier stage (MSC) than *Osx-Cre; Men1f/f* mice (osteoblast progenitor cells), it could be that *in vivo* menin might be needed for the initial commitment of MSCs to the myogenic lineage, but when muscle differentiation is induced menin's expression is downregulated. However, whether early deletion of menin in the osteoblast lineage directly affects myogenesis or not still remains to be elucidated in our study.

In summary, with the accumulated findings made so far, osteoblast menin plays a crucial role in bone development and maintenance of bone mass *in vivo*. With the mouse models presented herein, increased osteoclastogenesis and bone resorption, as a result of the elevated RANKL/OPG ratio from whole bone that includes osteocytes, are occurring in its absence. *In vitro*, menin deletion does not affect osteoblast differentiation but alters their activity by affecting mineralization. Early disruption of *Men1* gene in the osteoblast lineage also decreases body size, changes BAT functions and alters grip strength of the conditional knockout mice. Thus, menin's expression in mesenchyme-derived progenitors has overall important implications in body metabolism as well.

Like our current study, a recent publication by Liu *et al*., also analyzed the effects of loss of function of menin in the osteoblast lineage *in vivo*. The specific disruption of the *Men1* gene at the level of the osteoblast progenitors and osteocytes was achieved using *Runx2-Cre; Men1f/f Osx-Cre;Men1f/f* and *Dmp1-Cre; Men1f/f* mouse models, respectively (194). This study employed the Cre/LoxP recombination system for the generation of knockout animals. However, while the mouse models our group generated are deficient for exons 3-8 of the *Men1* gene, only exon 3 was deleted in all the mouse strains that Liu *et al*. examined (194).

In all of their *Men1*-deficient mouse models, they reported significant decreases in bone mass and trabecular bone volume. No significant changes in osteoblast numbers and bone formation rate were observed. The levels of osteoclasts and osteocytes were however significantly elevated. These results are similar to the findings made by our study when looking at the effects of menin at the level of the MSC and the osteoblast progenitor. While our study did not look into the role of menin specifically at the level of the osteocyte, findings made by Liu *et al*., seem to suggest that it acts similarly as to when it is expressed early in osteoblast lineage (194).

Interestingly, results reported in this study showed no differences in terms of alizarin red and ALP staining between *Men1*-deficient primary calvarial osteoblast and wild-type cells (194). In our study, we also show no changes in ALP staining, but slight reductions in the mineralization capabilities of the primary calvarial osteoblasts isolated from both *Prx1-Cre; Men1f/f* and *Osx-Cre; Men1f/f* mice. It is important to note that the results' assessment between the two studies is different. Our group directly cultured primary osteoblasts from knockout mice, whereas the experiments by Liu *et al*., consisted in isolating primary calvarial osteoblasts from *Rosa-Cre;*

Men1f/f mice and further inducing these cells with tamoxifen for three days to promote recombination of the *Men1* gene. As to why the authors of this study did not decide to investigate the effects of menin's deletion directly from primary cell cultures of the *Men1*-deficient mouse models from which they performed all their other *in vivo* analysis is unclear. In the literature it is also known that tamoxifen affects the cellular activities of osteoblasts, and its use could have had an impact in the differentiation process of the primary osteoblasts (195). The same method was used in their primary osteocyte cell cultures.

Nonetheless, similar to what our group is showing, Liu *et al*., also illustrate that the marked decreases in bone mass are primarily attributable to an increase in osteoclast number and activity leading to enhanced bone resorption. However, while we report elevated RANKL/OPG ratios from long bones, Liu *et al.*, note unchanged *RANKL* and *OPG* levels of expression in *DMP1-Cre; Men1f/f* mice (194). It is important to note that their analysis was performed on the calvarial bone of 3-day-old mice, while we performed ours from the femurs and tibias of 5 month-old mice. These results also only come from mice lacking menin at the level of the osteocyte and whether this trend also follows in their other transgenic mice model, where menin is deleted early in the osteoblast lineage, is not known. Interestingly, in their osteoclastogenesis co-culture experiments, the authors report unaltered levels of osteoclast when osteoclast precursors cells are co-cultured with osteoblast, but high osteoclast numbers when co-cultured with primary tamoxifen-induced osteocytes from *Rosa-Cre; Men1f/f* mice. This suggests that a factor released by osteocytes promotes osteoclast differentiation *in vitro* when menin is deleted. While the osteoblast-osteoclast co-culture results corroborate our findings, control osteoclastogenesis experiments with only osteoclast precursor cells were not reported. In our study we demonstrate an enhanced

responsiveness of osteoclast precursors to exogenous stimulation with RANKL and M-CSF, which is indicative of a priming effect occurring in the knockout mice. RANKL is a critical driver of osteoclastogenesis and it is well established that osteocytes are the major source of RANKL (179,181,182). It is thus strongly plausible that it is the high RANKL/OPG ratio we observe that is a driver of the elevated osteoclast activity in our early menin knockout mice model. While Liu *et al*., didn't precisely investigate these effects early in the osteoblast lineage, they did found a significant increase in the C-X-C motif chemokine 10 (CXCL10) expression in their isolated fractions of tamoxifen-induced *Rosa-Cre; Men1f/f* osteocytes (194). CXCL10 is a chemokine that binds to the CXCR3 receptor to illicit its biological activities which include but are not limited to supporting osteoclast differentiation (196). In Liu *et al*., paper this seems to be the main driver of osteoclastogenesis and bone resorption when menin is deleted in the osteoblast lineage. Whether CXCL10 or other chemokine factors known to modulate osteoclast differentiation, like CXCL12, remains to further investigated in our study (197, 198).

One important point which our study addresses is menin's implication in body metabolism. Our data along with results coming from other studies provide strong evidences to suggest that menin could be regulating the commitment of MSCs to other lineages, as well as having a role in mediating metabolic processes (138-140). Such effects of menin weren't further analyzed in Liu *et al.,* study. Nonetheless, Liu *et al*., results corroborate the data presented by our study in terms of the phenotypic bone parameter changes observed between transgenic mice lacking menin early in the osteoblast lineage and wild-type controls. Reviewing the mouse models used throughout the years to investigate the functions of the *Men1* gene product, menin, it has become clear that this nuclear protein is essential for the normal development of bones (Table 5.1). Menin plays a definite role as a regulator of molecular pathways involved in bone homeostasis *in vivo*.

Interestingly, another recent report by Lee *et al*., of the same German group as Liu *et al*., report mandibular ossifying fibroma occurring in aged (> 6 month-old) *Runx2-Cre; Men1f/f* and *Osx-Cre; Men1f/f* mice (199). Lee *et al.*, are in fact showing that loss of menin in craniofacial osteogenic cells results in increased proliferation rate of ossifying fibroma-derived mesenchymal stromal cells causing a benign bone neoplasm in mandibles that resembles ossifying fibroma seen in humans (199). This study suggests a potential role of menin for the formation of craniofacial bones, more specifically for mandible development. Other studies have also reported craniofacial defects with the deletion of the *Men1* gene, but the exact mechanism of actions leading to these abnormalities are unknown (150,151,154). This will be something to further investigate in our own study, although preliminary observations of 5 month-old mice do not reveal apparent irregularities between the mandibles of knockout and wild-type animals.

Table 5.1: *Men1* mouse models illustrating the role of menin in bone development

Mice Model	Heterozygous phenotype	Homozygous phenotype	References
Conventional knockout using *Men1* null mice	Tumors in the parathyroid, pancreas, pituitary, adrenals, gonads, thyroid; lipomas (age >12 months)	Embryonic lethal (E10.5-E14.5); developmental delay, craniofacial abnormalities, heart hypertrophy, haemorrhages, neural tube defects, abnormal liver organization	(150)*, (151)**, (152)***, (153)****
Neural crest-specific knockout using conditional *Pax3-Cre* and *Wnt1-Cre* transgenic mice	Intermediate increase in intercostal muscle mass at birth compared to the homozygous phenotype	Perinatal lethal; defects in palate, cranial bone, skeletal rib formation (E10.5-E17.5); Increased intercostal muscle mass at birth	(154)*, (140)*
Osteoblast-specific knockout using *OC-Cre* transgenic mice	ND	Decrease in bone mass and trabecular bone volume. Reduced osteoblast differentiation and high osteoblast apoptosis. Elevated levels of osteocytes. (9 month-old)	(155)*
Osteoprogenitor-specific knockout using *Runx2-Cre* and *Osx-Cre* transgenic mice	ND	Decrease in bone mass and trabecular bone volume. Increased bone resorption and osteoclast activity (12 week-old). Mandibular ossifying fibroma (> 12 months).	(194)**, (199)**
Osteocyte-specific knockout using *DMP1-Cre* transgenic mice	ND	Decrease in bone mass and trabecular bone volume. Increased bone resorption and osteoclast activity. High levels of osteocyte. (12 week -old)	(194)**
Mesenchyme-derived progenitor and osteoprogenitor-specific knockout using *Prx1-Cre* and *Osx-Cre* transgenic mice, respectively	Intermediate decrease in trabecular bone volume compared to the homozygous phenotype. (9 month-old)	Decrese in bone mass and trabecular bone volume. Increased bone resorption and osteoclast activity. Altered whole body composition and lean mass content. (6-12 month-old)	(156)*

*: Exons 3 - 8 of the *Men1* gene were deleted; **: Exon 3 of the *Men1* gene was deleted; ***: Exon 2 of the *Men1* gene was deleted; ****: Exons 1-2 of the *Men1* gene were deleted; ND: not determined.

5.2 Future work and perspectives

In this study, we established the importance of menin in maintaining bone mass as well as controlling metabolic processes. We show that loss of menin early in the osteoblast lineage increases bone resorption through the increase in the RANKL/OPG ratio from osteocytes resulting in low bone mass. We also demonstrated that osteoblast numbers and differentiation are not impaired by the disruption of the *Men1* gene in mesenchyme derived progenitors and in osteoblast progenitors. However, we found that osteoblast activity is altered with the early loss of menin in the osteoblast lineage. This was illustrated through our findings of high *ALP* and *OPG* expression from primary osteoblast cultures as well as with the reduced levels of mineralization. Characterizing the metabolic phenotype of our knockout mice, we found that menin deletion at the level of the MSCs reduces the body size and alters the BAT activity and *Ucp1* expression. We also demonstrated that menin has important implications in muscle strength that could well be explained through its known role in mediating the myogenic differentiation of MSCs (140).

The increase in bone specific *ALP* and *OPG* expression along with the elevated osteoclast activity and reduced osteoblast-mediated mineralization are indicative of a high bone turnover rate leading to deterioration of bone microarchitecture. Assessing changes in bone turnover through serum analysis of biochemical markers of bone formation and resorption would be relevant for our study. Serum procollagen type 1 amino-terminal propeptide (P1NP) and CTX have been recommended as reference markers of bone formation and resorption, respectively, by the International Osteoporosis Foundation (200). Besides measuring the levels of these two crucial markers of bone turnover, looking into changes in bone-specific ALP could provide further insight into the changes in osteoblast activity and mineralization we observe (201).

The increase trend in the RANKL/OPG ratio from bone RNA seems to be an important driver of osteoclastogenesis in our study. In this perspective, it would be important to increase the *n* number in order to see if with a larger sample size significance is reached, and also included RNA analysis from calvarial bone. It would also be important to perform osteocyte-osteoclast co-culture experiments to illustrate that a factor released by the osteocyte, which bones are primarily composed of, is promoting osteoclast differentiation. From the population of osteocyte cells isolated, analyzing expression changes in RANKL and OPG and demonstrating increases in RANKL/OPG ratio would confirm *in vivo* findings. We also plan on analyzing the expression of other factors that are released by osteocytes and that are known to modulate osteoclast differentiation such as CXCL10 and CXCL12 (196-198). The enhanced responsiveness of osteoclast precursors to RANKL stimulation is an interesting finding which is suggesting a priming effect. Such an effect could well be due to the high RANKL concentration relative to OPG which could prime osteoclast precursors to undergo differentiation more rapidly at a given concentration. For this our group plan on doing dose responsive osteoclastogenesis experiments with increasing RANKL concentrations, and measurement of the expression of the RANKL receptor, RANK, along with downstream transducers of the RANKL signaling, such as NFATc1.

Our study also reports an impairment in the capabilities of primary calvarial osteoblasts of knockout mice to mineralize. Culturing osteoblast in 3D collagen gels revealed differences in the mineral crystals as well as in the calcium and phosphate content of the formed extracellular mineral matrix. To further investigate the molecular basis of these differences we plan on analyzing the expression levels of important markers of mineralization that the loss of menin could attenuate.

Differences found in this perspective would unravel a novel mechanism through which menin could control osteoblast-mediated mineralization.

Elucidating the mechanism of action through which loss of menin leads to bone loss is important, and demonstrating the molecular pathway(s) affected upon menin deletion early in the osteoblast lineage is crucial for the design of pharmaceuticals that would target such pathways. For this our group plan on doing an unbiased RNAseq analysis to evaluate critical signaling pathways altered by the absence of menin in the osteoblast lineage. Because our group has already demonstrated that in the mature osteoblast menin promotes osteoblast function and bone formation by modulating the TGF-β/BMP-2 pathways, molecular components of this pathway will be investigated (125,126,155). However, when it is expressed early in the osteoblast lineage, menin's role seems to be that of a modulator of osteoclastogenesis. Hence, other molecular pathways impacted upon menin in the osteoblast lineage that are independent of the TGF-β/BMP-2 pathways must exist. An emphasis will particularly be put on the Wnt-β-catenin signaling pathway which plays a crucial role in the regulation of bone homeostasis by controlling osteoblastogenesis and osteoclastogenesis events (67). This pathway is of even more interest to us considering that our group has previously demonstrated *in vitro* that menin can interact physically and functionally with β-catenin in both MSCs and osteoblasts (123). Recent reports have shown that Wnt-β-catenin signaling in osteocytes and osteoblasts regulates osteoclast differentiation by repressing and promoting RANKL and OPG secretion, respectively (74,202,203). It has also been reported that the Wnt signaling can directly affect the differentiation and proliferation of osteoclast precursors (204). Taking all of these already established findings together, there is strong evidence to believe that the early loss of menin in the osteoblast lineage affects Wnt-β-catenin signaling, causing an

increase in the RANKL/OPG ratio from osteocytes as well as attenuating the responsiveness of osteoclast precursors to RANKL. Such a pathway is of even more relevance for our study considering other reports showing Wnt signaling supporting the maturation and mineralization of osteoblast (73).

In our study we also report metabolic changes as well as differences in whole body lean mass and skeletal muscle strength when menin is deleted in mesenchyme derived progenitors and in osteoblast progenitors. To further pursue these findings, it will be important to analyze serum OCN levels between knockout and wild-type mice. OCN is an osteoblast-derived hormone which can mediate important endocrine functions of bone, such as increasing energy expenditure and glucose tolerance (59,60,62). Analyzing circulating levels of OCN would reveal to us whether the noted metabolic changes are a consequence of the altered osteoblast activity we observe. The inter-functionality between muscle and bone has become evident in recent years, and factors released by muscle such as myostatin are known to impact osteoblast and osteocyte activity (205). To investigate whether loss of menin affects myogenesis, proceeding to the gene expression analysis of factors such as menin and myogenin, a crucial factor involved in skeletal muscle development (206), directly from muscle would reveal whether skeletal muscle changes are a consequence of the direct loss of menin and identify other factors impacted by the loss of menin that could have an effect on bone development. Lastly, histological analysis of fat and muscle would show whether changes are occurring in the development of these tissues when the *Men1* gene is disrupted early in the osteoblast lineage.

5.3 Conclusion

In light of this work, we can conclude that menin is important for the maintenance of bone mass. Mice deficient for menin specifically at the level of the MSCs and osteoblast progenitors show altered osteoblast activity and increase in the bone RANKL/OPG ratio which promotes osteoclastogenesis and bone resorption. This is different from when menin is deleted in mature osteoblasts, where reduced bone formation and enhanced osteoblast apoptosis are noted. These findings show the presence of different molecular pathways through which menin can mediate its functions during bone development. Such functions may vary depending on whether menin is expressed at an early or late stage of osteoblast differentiation. In our study, we also provide evidence of menin acting as a mediator of the functions of bone in regulating metabolic processes. We show reduced bodyweights and altered BAT activity changes in mice deficient for menin in mesenchyme-derived progenitors. We also demonstrate reduced skeletal muscle functions in our knockout mice, highlighting another important interplay of menin in mediating bone-muscle cross talk events. In conclusion, these studies demonstrate the crucial role that osteoblast menin and its interacting partners play in bone homeostasis, and also show the potential of menin being used as a molecular therapeutic target for treating disorders of low bone mass such as osteoporosis.

REFERENCES

1 : Gasser JA, Kneissel M. Chapter 2 - Bone Physiology and Biology. In : S.Y. Smith S, Varela A, Samadfam R. (eds), *Bone Toxicology*, Molecular and Integrative Toxicology. Springer, Cham 2017, pp. 27-94.

2 : Kini U. & Nandeesh BN. Physiology of bone formation, remodeling, and metabolism. In: *Radionuclide and Hybrid Bone Imaging*. 2012. I. Fogelman, G. Gnanasegaran, H. van der Wall (Eds). pp. 29-57.

3 : Gilbert S.F. Osteogenesis: The development of bones. *Dev Biol.* 2000. 6.

4 : Karaplis A.C. Chapter 3 – Embryonic development of bone and regulation of intramembranous and endochondral bone formation. *Principles of Bone Biol*. 2008. 3(1): 53-84.

5 : Berendsen AD, Olsen BR. Bone development. *Bone*. 2015. 80: 14-18.

6 : Long, F., & Ornitz, D. M. Development of the endochondral skeleton. *Cold Spring Harbor perspectives in biology*. 2013. 5(1), a008334.

7 : Clarke B. Normal bone anatomy and physiology. *Clin J Am Soc Nephrol*. 2008;3 Suppl 3:S131-9.

8 : Bonucci E. Bone mineralization. Front Biosci (Landmark Ed). 2012; 17:100-28.

9 : Boskey, AL. Bone Mineralization. In: Cowin, SC., editor. *Bone Biomechanics*. CRC Press; Boca Raton: 2001. p. 5.1-5.34. Ed 3.

10 : Boskey AL. Bone composition: relationship to bone fragility and antiosteoporotic drug effects. *Bonekey Rep*. 2013; 2:447.

11 : Fujisawa R, Tamura M. Acidic bone matrix proteins and their roles in calcification. *Front Biosci (Landmark Ed)*. 2012; 17:1891-903.

12 : Florencio-Silva R, Sasso GR, Sasso-Cerri E, Simoes MJ, Cerri PS. Biology of bone tissue: structure, function, and factors that influence bone cells. *Biomed Res Int*. 2015; 2015:421746.

13 : Beyer Nardi N, da Silva Meirelles L. Mesenchymal stem cells: isolation, in vitro expansion and characterization. *Handb Exp Pharmacol*. 2006(174):249-82.

14 : Hass R, Kasper C, Bohm S, Jacobs R. Different populations and sources of human mesenchymal stem cells (MSC): A comparison of adult and neonatal tissue-derived MSC. *Cell Commun Signal*. 2011; 9:12.

15 : Horwitz EM, Le Blanc K, Dominici M, Mueller I, Slaper-Cortenbach I, Marini FC, Deans RJ, Krause DS, Keating A, International Society for Cellular Therapy. Clarification of the nomenclature for MSC: The International Society for Cellular Therapy position statement. *Cytotherapy*. 2005;7(5):393-5.

16 : Keating A. Mesenchymal stromal cells. *Curr Opin Hematol*. 2006;13(6):419-25.

17 : Dominici M, Le Blanc K, Mueller I, Slaper-Cortenbach I, Marini F, Krause D, Deans R, Keating A, Prockop Dj, Horwitz E. Minimal criteria for defining multipotent mesenchymal stromal cells. The International Society for Cellular Therapy position statement. *Cytotherapy*. 2006; 8:315–317.

18 : Kim HJ, Park JS. Usage of Human Mesenchymal Stem Cells in Cell-based Therapy: Advantages and Disadvantages. *Dev Reprod*. 2017;21(1):1-10.

19 : Marks SC, Jr., Popoff SN. Bone cell biology: the regulation of development, structure, and function in the skeleton. *Am J Anat*. 1988;183(1):1-44.

20 : Jensen ED, Gopalakrishnan R, Westendorf JJ. Regulation of gene expression in osteoblasts. *Biofactors*. 2010;36(1):25-32.

21 : Yavropoulou MP, Yovos JG. Osteoclastogenesis--current knowledge and future perspectives. *J Musculoskelet Neuronal Interact*. 2008;8(3):204-16.

22 : Teitelbaum SL. Bone resorption by osteoclasts. *Science*. 2000;289(5484):1504-8.

23 : Rochefort GY, Pallu S, Benhamou CL. Osteocyte: the unrecognized side of bone tissue. *Osteoporos Int*. 2010;21(9):1457-69.

24 : Dallas SL, Prideaux M, Bonewald LF. The osteocyte: an endocrine cell ... and more. *Endocr Rev*. 2013;34(5):658-90.

25 : van Oers RF, Wang H, Bacabac RG. Osteocyte shape and mechanical loading. *Curr Osteoporos Rep*. 2015;13(2):61-6.

26 : Rutkovskiy A, Stenslokken KO, Vaage IJ. Osteoblast differentiation at a glance. *Med Sci Monit Basic Res*. 2016; 22:95-106.

27 : Stein GS, Lian JB, van Wijnen AJ, Stein JL, Montecino M, Javed A, Zaidi SK, Young DW, Choi JY, Pockwinse SM. Runx2 control of organization, assembly and activity of the regulatory machinery for skeletal gene expression. *Oncogene*. 2004;23(24):4315-29.

28 : Qi H, Aguiar DJ, Williams SM, La Pean A, Pan W, Verfaillie CM. Identification of genes responsible for osteoblast differentiation from human mesodermal progenitor cells. *Proc Natl Acad Sci U S A*. 2003;100(6):3305-10.

29 : Kwon OH, Lee CK, Lee YI, Paik SG, Lee HJ. The hematopoietic transcription factor PU.1 regulates RANK gene expression in myeloid progenitors. *Biochem Biophys Res Commun*. 2005;335(2):437-46.

30 : Ross FP. M-CSF, c-Fms, and signaling in osteoclasts and their precursors. *Ann N Y Acad Sci*. 2006; 1068:110-6.

31 : Matsumoto M, Kogawa M, Wada S, Takayanagi H, Tsujimoto M, Katayama S, Hisatake K, Nogi Y. Essential role of p38 mitogen-activated protein kinase in cathepsin K gene expression during osteoclastogenesis through association of NFATc1 and PU.1. *J Biol Chem*. 2004;279(44):45969-79.

32 : Boyce BF, Xing L. Functions of RANKL/RANK/OPG in bone modeling and remodeling. *Arch Biochem Biophys*. 2008;473(2):139-46.

33 : An J, Leeuwenburgh S, Wolke J, Jansen J. Chapter 4 – Mineralization processes in hard tissues: bone, in *Biomineralization & Biomaterials*. Woodhead Publishing. 2016. pp. 129-146.

34 : Bala Y, Farlay D, Boivin G. Bone mineralization: from tissue to crystal in normal and pathological contexts. *Osteoporos Int*. 2013;24(8):2153-66.

35 : Velleman SG. The role of the extracellular matrix in skeletal development. *Poult Sci*. 2000;79(7):985-9.

36 : Anderson HC. Matrix vesicles and calcification. *Curr Rheumatol Rep*. 2003;5(3):222-6.

37 : Anderson HC. Molecular biology of matrix vesicles. *Clin Orthop Relat Res*. 1995(314):266-80.

38 : Glimcher MJ. The nature of the mineral phase in bone. In : *Metabolic Bone Disease.* Academic Press, San Diego, CA, USA. 1998. pp. 23-50.

39 : Dean DD, Schwartz Z, Muniz OE, Gomez R, Swain LD, Howell DS, et al. Matrix vesicles are enriched in metalloproteinases that degrade proteoglycans. *Calcif Tissue Int*. 1992;50(4):342-9.

40 : Boivin G, Meunier PJ. The degree of mineralization of bone tissue measured by computerized quantitative contact microradiography. *Calcif Tissue Int*. 2002;70(6):503-11.

41 : Langdahl B, Ferrari S, Dempster DW. Bone modeling and remodeling: potential as therapeutic targets for the treatment of osteoporosis. *Ther Adv Musculoskelet Dis*. 2016;8(6):225-35.

42 : Kobayashi S, Takahashi HE, Ito A, Saito N, Nawata M, Horiuchi H, Ohta H, Ito A, Iorio R, Yamamoto N, Takaoka K. Trabecular minimodeling in human iliac bone. *Bone*. 2003;32(2):163-9.

43 : Manolagas S.C. Birth and Death of Bone Cells: Basic regulatory mechanisms and implications for the pathogenesis and treatment of osteoporosis. *Endocrine Reviews*. 2000. 21(2): 115-137.

44 : Jilka R. L. Biology of the basic multicellular unit and the pathophysiology of osteoporosis. *Medical and Pediatric Oncology*. 2003. 41:182–185.

45 : Sims N.A. & Martin T.J. Coupling the activities of bone formation and resorption a multitude of signals within the basic multicellular unit. *Bonekey Reports*. 2014. 3: 481.

46 : Hadjidakis D.J & Androulakis I.I. Bone remodeling. *Annals New York Academy of Sciences*. 2006. 1092 :385-396.

47 : Marin J.T., Bone biology and anabolic therapies for bone: current status and future prospects. *Journal of Bone Metabolism*. 2014. 21 :8-20.

48 : Feng X, McDonald JM. Disorders of bone remodeling. *Annu Rev Pathol*. 2011;6:121-45.

49 : Lin JT, Lane JM. Osteoporosis: a review. *Clin Orthop Relat Res*. 2004. (425):126-34.

50 : Johnell O, Kanis JA. An estimate of the worldwide prevalence and disability associated with osteoporotic fractures. *Osteoporos Int*. 2006;17(12):1726-33.

51 : Riggs BL, Khosla S, Melton LJ. The type I/typeII model for involutional osteoporosis. In: *Osteoporosis*, ed. Marcus R, Feldman D, Kelsey J. San Diego Academic. 2001. pp. 49-58.

52 : Takata S, Yasui N. Disuse osteoporosis. *J Med Invest*. 2001;48(3-4):147-56.

53 : Canalis E, Mazziotti G, Giustina A, Bilezikian JP. Glucocorticoid-induced osteoporosis: pathophysiology and therapy. *Osteoporos Int*. 2007;18(10):1319-28.

54 : Bernabei R, Martone AM, Ortolani E, Landi F, Marzetti E. Screening, diagnosis and treatment of osteoporosis: a brief review. *Clin Cases Miner Bone Metab*. 2014;11(3):201-7.

55 : Kennel KA, Drake MT. Adverse effects of bisphosphonates: implications for osteoporosis management. Mayo Clin Proc. 2009;84(7):632-7; quiz 8.

56 : Canalis E. Management of endocrine disease : Novel anabolic treatments for osteoporosis. *Eur J Endocrinol*. 2018;178(2):R33-R44.

57 : Shirley M. Abaloparatide: First Global Approval. *Drugs*. 2017;77(12):1363-8.

58 : Rosen CJ. Romosozumab - Promising or Practice Changing? *N Engl J Med*. 2017;377(15):1479-80.

59 : Karsenty G, Ferron M. The contribution of bone to whole-organism physiology. *Nature*. 2012;481(7381):314-20.

60 : Lombardi G, Perego S, Luzi L, Banfi G. A four-season molecule: osteocalcin. Updates in its physiological roles. *Endocrine*. 2015;48(2):394-404.

61 : Ferron M, Wei J, Yoshizawa T, Del Fattore A, DePinho RA, Teti A, Ducy P, Karsenty G. Insulin signaling in osteoblasts integrates bone remodeling and energy metabolism. *Cell*. 2010;142(2):296-308.

62 : Wei J, Karsenty G. An overview of the metabolic functions of osteocalcin. *Rev Endocr Metab Disord*. 2015;16(2):93-8.

63 : Lee NK, Sowa H, Hinoi E, Ferron M, Ahn JD, Confavreux C, Dacquin R, Mee PJ, McKee MD, Jung DY, Zhang Z, Kim JK, Mauvais-Jarvis F, Ducy P, Karsenty G. Endocrine regulation of energy metabolism by the skeleton. *Cell*. 2007;130(3):456-69.

64 : Mera P, Laue K, Wei J, Berger JM, Karsenty G. Osteocalcin is necessary and sufficient to maintain muscle mass in older mice. *Mol Metab*. 2016;5(10):1042-7.

65 : Ferron M, Hinoi E, Karsenty G, Ducy P. Osteocalcin differentially regulates beta cell and adipocyte gene expression and affects the development of metabolic diseases in wild-type mice. *Proc Natl Acad Sci U S A*. 2008;105(13):5266-70.

66 : Oury F, Ferron M, Huizhen W, Confavreux C, Xu L, Lacombe J, Srinivas P, Chamouni A, Lugani F, Lejeune H, Kumar TR, Plotton I, Karsenty G. Osteocalcin regulates murine and human fertility through a pancreas-bone-testis axis. *J Clin Invest*. 2013;123(6):2421-33.

67 : Baron R, Kneissel M. WNT signaling in bone homeostasis and disease: from human mutations to treatments. *Nat Med*. 2013;19(2):179-92.

68 : Day TF, Guo X, Garrett-Beal L, Yang Y. Wnt/beta-catenin signaling in mesenchymal progenitors controls osteoblast and chondrocyte differentiation during vertebrate skeletogenesis. *Dev Cell*. 2005;8(5):739-50.

69 : Kennell JA, MacDougald OA. Wnt signaling inhibits adipogenesis through beta-catenin-dependent and -independent mechanisms. *J Biol Chem*. 2005;280(25):24004-10.

70 : Hill TP, Spater D, Taketo MM, Birchmeier W, Hartmann C. Canonical Wnt/beta-catenin signaling prevents osteoblasts from differentiating into chondrocytes. *Dev Cell*. 2005;8(5):727-38.

71 : Hu H, Hilton MJ, Tu X, Yu K, Ornitz DM, Long F. Sequential roles of Hedgehog and Wnt signaling in osteoblast development. *Development*. 2005;132(1):49-60.

72 : Gaur T, Lengner CJ, Hovhannisyan H, Bhat RA, Bodine PV, Komm BS, Javed A, van Wijnen AJ, Stein JL, Stein GS, Lian JB. Canonical WNT signaling promotes osteogenesis by directly stimulating Runx2 gene expression. *J Biol Chem*. 2005;280(39):33132-40.

73 : Friedman MS, Oyserman SM, Hankenson KD. Wnt11 promotes osteoblast maturation and mineralization through R-spondin 2. *J Biol Chem*. 2009;284(21):14117-25.

74 : Glass DA, 2nd, Bialek P, Ahn JD, Starbuck M, Patel MS, Clevers H, Taketo MM, Long F, McMahon AP, Lang RA, Karsenty G. Canonical Wnt signaling in differentiated osteoblasts controls osteoclast differentiation. *Dev Cell*. 2005;8(5):751-64.

75 : Kawano Y, Kypta R. Secreted antagonists of the Wnt signalling pathway. *J Cell Sci*. 2003;116(Pt 13):2627-34.

76 : Li X, Ominsky MS, Niu QT, Sun N, Daugherty B, D'Agostin D, Kurahara C, Gao Y, Cao J, Gong J, Asuncion F, Barrero M, Warmington K, Dwyer D, Stolina M, Morony S, Sarosi I, Kostenuik PJ, Lacey DL, Simonet WS, Ke HZ, Paszty C. Targeted deletion of the sclerostin gene in mice results in increased bone formation and bone strength. *J Bone Miner Res*. 2008;23(6):860-9.

77 : Morvan F, Boulukos K, Clement-Lacroix P, Roman Roman S, Suc-Royer I, Vayssiere B, Ammann P, Martin P, Pinho S, Pognonec P, Mollat P, Niehrs C, Baron R, Rawadi G. Deletion of a single allele of the Dkk1 gene leads to an increase in bone formation and bone mass. *J Bone Miner Res*. 2006;21(6):934-45.

78 : Bodine PV, Stauffer B, Ponce-de-Leon H, Bhat RA, Mangine A, Seestaller-Wehr LM, Moran RA, Billiard J, Fukayama S, Komm BS, Pitts K, Krishnamurthy G, Gopalsamy A, Shi M, Kern JC, Commons TJ, Woodworth RP, Wilson MA, Wellmaker GS, Trybulski EJ, Moore WJ. A small molecule inhibitor of the Wnt antagonist secreted frizzled-related protein-1 stimulates bone formation. *Bone*. 2009;44(6):1063-8.

79 : Zuo C, Huang Y, Bajis R, Sahih M, Li YP, Dai K, Zhang X. Osteoblastogenesis regulation signals in bone remodeling. *Osteoporos Int*. 2012;23(6):1653-63.

80 : Chen G, Deng C, Li YP. TGF-beta and BMP signaling in osteoblast differentiation and bone formation. *Int J Biol Sci*. 2012;8(2):272-88.

81 : Guo X, Wang XF. Signaling cross-talk between TGF-beta/BMP and other pathways. *Cell Res*. 2009; 19:71-88.

82 : Shi Y, Massague J. Mechanisms of TGF-beta signaling from cell membrane to the nucleus. *Cell*. 2003;113(6):685-700

83 : Janssens K, ten Dijke P, Janssens S, Van Hul W. Transforming growth factor-beta1 to the bone. *Endocr Rev*. 2005;26(6):743-74.

84 : Hock JM, Canalis E, Centrella M. Transforming growth factor-beta stimulates bone matrix apposition and bone cell replication in cultured fetal rat calvariae. *Endocrinology*. 1990;126(1):421-6.

85 : Maeda S, Hayashi M, Komiya S, Imamura T, Miyazono K. Endogenous TGF-beta signaling suppresses maturation of osteoblastic mesenchymal cells. *EMBO J*. 2004;23(3):552-63.

86 : Tang Y, Wu X, Lei W, Pang L, Wan C, Shi Z, Zhao L, Nagy TR, Peng X, Hu J, Feng X, Van Hul W, Wan M, Cao X. TGF-beta1-induced migration of bone mesenchymal stem cells couples bone resorption with formation. *Nat Med*. 2009;15(7):757-65.

87 : Urist MR. Bone: formation by autoinduction. *Science*. 1965;150(3698):893-9.

88 : Wozney JM, Rosen V, Celeste AJ, Mitsock LM, Whitters MJ, Kriz RW, Hewick RM, Wang EA. Novel regulators of bone formation: molecular clones and activities. *Science*. 1988;242(4885):1528-34.

89 : Canalis E, Economides AN, Gazzerro E. Bone morphogenetic proteins, their antagonists, and the skeleton. *Endocr Rev*. 2003;24(2):218-35.

90 : Bandyopadhyay A, Tsuji K, Cox K, Harfe BD, Rosen V, Tabin CJ. Genetic analysis of the roles of BMP2, BMP4, and BMP7 in limb patterning and skeletogenesis. *PLoS Genet*. 2006;2(12): e216.

91 : Lin GL, Hankenson KD. Integration of BMP, Wnt, and notch signaling pathways in osteoblast differentiation. *J Cell Biochem*. 2011;112(12):3491-501.

92 : Chen D, Zhao M, Mundy GR. Bone morphogenetic proteins. *Growth Factors*. 2004;22(4):233-41.

93 : Hay E, Lemonnier J, Fromigue O, Marie PJ. Bone morphogenetic protein-2 promotes osteoblast apoptosis through a Smad- independent, protein kinase C-dependent signaling pathway. *J Biol Chem*. 2001. 276:29028 –29036

94 : Miyazawa K, Miyazono K. Regulation of TGF-beta Family Signaling by Inhibitory Smads. *Cold Spring Harb Perspect Biol*. 2017;9(3).

95 : Wu M, Chen G, Li YP. TGF-beta and BMP signaling in osteoblast, skeletal development, and bone formation, homeostasis and disease. *Bone Res*. 2016; 4:16009.

96 : Rahman MS, Akhtar N, Jamil HM, Banik RS, Asaduzzaman SM. TGF-beta/BMP signaling and other molecular events: regulation of osteoblastogenesis and bone formation. *Bone Res*. 2015; 3:15005.

97 : Chandrasekharappa SC, Guru SC, Manickam P, Olufemi SE, Collins FS, Emmert-Buck MR, Debelenko LV, Zhuang Z, Lubensky IA, Liotta LA, Crabtree JS, Wang Y, Roe BA, Weisemann J, Boguski MS, Agarwal SK, Kester MB, Kim YS, Heppner C, Dong Q, Spiegel AM, Burns AL, Marx SJ. Positional cloning of the gene for multiple endocrine neoplasia-type 1. *Science*. 1997;276(5311):404-7.

98 : Larsson C, Skogseid B, Oberg K, Nakamura Y, Nordenskjold M. Multiple endocrine neoplasia type 1 gene maps to chromosome 11 and is lost in insulinoma. *Nature*. 1988;332(6159):85-7.

99 : Stewart C, Parente F, Piehl F, Farnebo F, Quincey D, Silins G, Bergman L, Carle GF, Lemmens I, Grimmond S, Xian CZ, Khodei S, Teh BT, Lagercrantz J, Siggers P, Calender A, Van de Vem V, Kas K, Weber G, Hayward N, Gaudray P, Larsson C. Characterization of the mouse Men1 gene and its expression during development. *Oncogene*. 1998;17(19):2485-93.

100 : Thakker RV. Multiple endocrine neoplasia type 1 (MEN1). *Best Pract Res Clin Endocrinol Metab*. 2010;24(3):355-70.

101 : Lemmens I, Van de Ven WJ, Kas K, Zhang CX, Giraud S, Wautot V, Buisson N, De Witte K, Salandre J, Lenoir G, Pugeat M, Calender A, Parente F, Quincey D, Gaudray P, De Wit MJ, Lips CJ, Hoppener JW, Khodaei S, Grant AL, Weber G, Kytola S, Teh BT, Farnebo F, Thakker RV et al. Identification of the multiple endocrine neoplasia type 1 (MEN1) gene. The European Consortium on MEN1. *Hum Mol Genet*. 1997;6(7):1177-83.

102 : Marini F, Falchetti A, Luzi E, Tonelli F, Maria Luisa B. Multiple Endocrine Neoplasia Type 1 (MEN1) Syndrome. In: Riegert-Johnson DL, Boardman LA, Hefferon T, Roberts M, editors. Cancer Syndromes. Bethesda (MD)2009.

103 : Thakker RV, Newey PJ, Walls GV, Bilezikian J, Dralle H, Ebeling PR, Melmed S, Sakurai A, Tonelli F, Brandi ML, Endocrine Society. Clinical practice guidelines for multiple endocrine neoplasia type 1 (MEN1). *J Clin Endocrinol Metab*. 2012;97(9):2990-3011.

104 : Conemans EB, Nell S, Pieterman CRC, de Herder WW, Dekkers OM, Hermus AR, van der Horst-Schrivers AN, Bisschop PH, Havekes B, Drent ML, Vriens MR, Valk GD. Prognostic factors for survival of Men1 patients with duodenopancreatic tumors metastatic to the Liver: *Results from the Dmsg. Endocr Pract*. 2017;23(6):641-8.

105 : Guru SC, Goldsmith PK, Burns AL, Marx SJ, Spiegel AM, Collins FS, Chandrasekharappa SC. Menin, the product of the MEN1 gene, is a nuclear protein. *Proc Natl Acad Sci U S A*. 1998;95(4):1630-4.

106 : Dreijerink KMA, Timmers HTM, Brown M. Twenty years of menin: emerging opportunities for restoration of transcriptional regulation in MEN1. *Endocr Relat Cancer*. 2017;24(10):T135-T45.

107 : Hendy GN, Kaji H, Canaff L. Cellular functions of menin. *Adv Exp Med Biol*. 2009; 668:37-50.

108 : Murai MJ, Chruszcz M, Reddy G, Grembecka J, Cierpicki T. Crystal structure of menin reveals binding site for mixed lineage leukemia (MLL) protein. *J Biol Chem*. 2011;286(36):31742-8.

109 : Huang J, Gurung B, Wan B, Matkar S, Veniaminova NA, Wan K, Merchant JL, Hua X, Lei M. The same pocket in menin binds both MLL and JUND but has opposite effects on transcription. *Nature*. 2012;482(7386):542-6.

110 : Canaff L, Vanbellinghen JF, Kaji H, Goltzman D, Hendy GN. Impaired transforming growth factor-beta (TGF-beta) transcriptional activity and cell proliferation control of a menin in-frame deletion mutant associated with multiple endocrine neoplasia type 1 (MEN1). *J Biol Chem*. 2012;287(11):8584-97.

111 : Karin M, Liu Z, Zandi E. AP-1 function and regulation. *Curr Opin Cell Biol*. 1997;9(2):240-6.

112: Jochum W, Passegue E, Wagner EF. AP-1 in mouse development and tumorigenesis. *Oncogene*. 2001;20(19):2401-12.

113 : Agarwal SK, Guru SC, Heppner C, Erdos MR, Collins RM, Park SY, Saggar S, Chandrasekharappa SC, Collins FS, Spiegel AM, Marx SJ, Burns AL. Menin interacts with the AP1 transcription factor JunD and represses JunD-activated transcription. *Cell*. 1999;96(1):143-52.

114 : Gobl AE, Berg M, Lopez-Egido JR, Oberg K, Skogseid B, Westin G. Menin represses JunD-activated transcription by a histone deacetylase-dependent mechanism. *Biochim Biophys Acta*. 1999;1447(1):51-6.

115 : Kim H, Lee JE, Cho EJ, Liu JO, Youn HD. Menin, a tumor suppressor, represses JunD-mediated transcriptional activity by association with an mSin3A-histone deacetylase complex. *Cancer Res*. 2003;63(19):6135-9.

116 : Hess JL. MLL: a histone methyltransferase disrupted in leukemia. *Trends Mol Med*. 2004;10(10):500-7.

117 : Hughes CM, Rozenblatt-Rosen O, Milne TA, Copeland TD, Levine SS, Lee JC, Hayes DN, Shanmugam KS, Bhattacharjee A, Biondi CA, Kay GF, Hayward NK, Hess JL, Meyerson M. Menin associates with a trithorax family histone methyltransferase complex and with the hoxc8 locus. *Mol Cell*. 2004;13(4):587-97.

118 : Milne TA, Hughes CM, Lloyd R, Yang Z, Rozenblatt-Rosen O, Dou Y, Schnepp RW, Krankel C, Livolsi VA, Gibbs D, Hua X, Roeder RG, Meyerson M, Hess JL. Menin and MLL cooperatively regulate expression of cyclin-dependent kinase inhibitors. *Proc Natl Acad Sci U S A*. 2005;102(3):749-54.

119 : Yokoyama A, Wang Z, Wysocka J, Sanyal M, Aufiero DJ, Kitabayashi I, Herr W, Cleary ML. Leukemia proto-oncoprotein MLL forms a SET1-like histone methyltransferase complex with menin to regulate Hox gene expression. *Mol Cell Biol*. 2004;24(13):5639-49.

120 : Karnik SK, Hughes CM, Gu X, Rozenblatt-Rosen O, McLean GW, Xiong Y, Meyerson M, Kim SK. Menin regulates pancreatic islet growth by promoting histone methylation and expression of genes encoding p27Kip1 and p18INK4c. *Proc Natl Acad Sci U S A*. 2005;102(41):14659-64.

121 : Chen G, A J, Wang M, Farley S, Lee LY, Lee LC, Sawicki MP. Menin promotes the Wnt signaling pathway in pancreatic endocrine cells. *Mol Cancer Res*. 2008;6(12):1894-907.

122 : Cao Y, Liu R, Jiang X, Lu J, Jiang J, Zhang C, Li X, Ning G. Nuclear-cytoplasmic shuttling of menin regulates nuclear translocation of {beta}-catenin. *Mol Cell Biol*. 2009;29(20):5477-87.

123 : Inoue Y, Hendy GN, Canaff L, Seino S, Kaji H. Menin interacts with beta-catenin in osteoblast differentiation. *Horm Metab Res*. 2011;43(3):183-7.

124 : Jiang X, Cao Y, Li F, Su Y, Li Y, Peng Y, Cheng Y, Zhang C, Wang W, Ning G. Targeting beta-catenin signaling for therapeutic intervention in MEN1-deficient pancreatic neuroendocrine tumours. *Nat Commun*. 2014; 5:5809.

125 : Sowa H, Kaji H, Canaff L, Hendy GN, Tsukamoto T, Yamaguchi T, Miyazono K, Sugimoto T, Chihara K. Inactivation of menin, the product of the multiple endocrine neoplasia type 1 gene, inhibits the commitment of multipotential mesenchymal stem cells into the osteoblast lineage. *J Biol Chem*. 2003;278(23):21058-69.

126 : Sowa H, Kaji H, Hendy GN, Canaff L, Komori T, Sugimoto T, Chihara K. Menin is required for bone morphogenetic protein 2- and transforming growth factor beta-regulated osteoblastic differentiation through interaction with Smads and Runx2. *J Biol Chem*. 2004;279(39):40267-75.

127 : Kaji H, Canaff L, Lebrun JJ, Goltzman D, Hendy GN. Inactivation of menin, a Smad3-interacting protein, blocks transforming growth factor type beta signaling. *Proc Natl Acad Sci U S A*. 2001;98(7):3837-42.

128 : Hendy GN, Kaji H, Sowa H, Lebrun JJ, Canaff L. Menin and TGF-beta superfamily member signaling via the Smad pathway in pituitary, parathyroid and osteoblast. *Horm Metab Res*. 2005;37(6):375-9.

129 : Lacerte A, Lee EH, Reynaud R, Canaff L, De Guise C, Devost D, Ali S, Hendy GN, Lebrun JJ. Activin inhibits pituitary prolactin expression and cell growth through Smads, Pit-1 and menin. *Mol Endocrinol*. 2004;18(6):1558-69.

130 : Sowa H, Kaji H, Kitazawa R, Kitazawa S, Tsukamoto T, Yano S, Tsukada T, Canaff L, Hendy GN, Sugimoto T, Chihara K. Menin inactivation leads to loss of transforming growth factor beta inhibition of parathyroid cell proliferation and parathyroid hormone secretion. *Cancer Res*. 2004;64(6):2222-8.

131 : Naito J, Kaji H, Sowa H, Kitazawa R, Kitazawa S, Tsukada T, Hendy GN, Sugimoto T, Chihara K. Expression and functional analysis of menin in a multiple endocrine neoplasia type 1 (MEN1) patient with somatic loss of heterozygosity in chromosome 11q13 and unidentified germline mutation of the MEN1 gene. *Endocrine*. 2006;29(3):485-90.

132 : Jin S, Mao H, Schnepp RW, Sykes SM, Silva AC, D'Andrea AD, Hua X. Menin associates with FANCD2, a protein involved in repair of DNA damage. *Cancer Res*. 2003;63(14):4204-10.

133 : Busygina V, Kottemann MC, Scott KL, Plon SE, Bale AE. Multiple endocrine neoplasia type 1 interacts with forkhead transcription factor CHES1 in DNA damage response. *Cancer Res*. 2006;66(17):8397-403.

134 : Obungu VH, Lee Burns A, Agarwal SK, Chandrasekharapa SC, Adelstein RS, Marx SJ. Menin, a tumor suppressor, associates with nonmuscle myosin II-A heavy chain. *Oncogene*. 2003;22(41):6347-58.

135 : Lopez-Egido J, Cunningham J, Berg M, Oberg K, Bongcam-Rudloff E, Gobl A. Menin's interaction with glial fibrillary acidic protein and vimentin suggests a role for the intermediate filament network in regulating menin activity. *Exp Cell Res*. 2002;278(2):175-83.

136 : Dreijerink KM, Mulder KW, Winkler GS, Hoppener JW, Lips CJ, Timmers HT. Menin links estrogen receptor activation to histone H3K4 trimethylation. *Cancer Res*. 2006;66(9):4929-35.

137 : Dreijerink KM, Varier RA, van Nuland R, Broekhuizen R, Valk GD, van der Wal JE, Lips CJ, Kummer JA, Timmers HT. Regulation of vitamin D receptor function in MEN1-related parathyroid adenomas. *Mol Cell Endocrinol*. 2009;313(1-2):1-8.

138 : Dreijerink KM, Varier RA, van Beekum O, Jeninga EH, Hoppener JW, Lips CJ, Kummer JA, Kalkhoven E, Timmers HT. The multiple endocrine neoplasia type 1 (MEN1) tumor suppressor regulates peroxisome proliferator-activated receptor gamma-dependent adipocyte differentiation. *Mol Cell Biol*. 2009;29(18):5060-9.

139 : Parekh VI, Modali SD, Desai SS, Agarwal SK. Consequence of menin deficiency in mouse adipocytes derived by in vitro differentiation. *Int J Endocrinol*. 2015; 2015:149826.

140 : Aziz A, Miyake T, Engleka KA, Epstein JA, McDermott JC. Menin expression modulates mesenchymal cell commitment to the myogenic and osteogenic lineages. *Dev Biol*. 2009;332(1):116-30.

141 : Lee KS, Kim HJ, Li QL, Chi XZ, Ueta C, Komori T, Wozney JM, Kim EG, Choi JY, Ryoo HM, Bae SC. Runx2 is a common target of transforming growth factor beta1 and bone morphogenetic protein 2, and cooperation between Runx2 and Smad5 induces osteoblast-specific gene expression in the pluripotent mesenchymal precursor cell line C2C12. *Mol Cell Biol*. 2000;20(23):8783-92.

142 : Liu D, Black BL, Derynck R. TGF-beta inhibits muscle differentiation through functional repression of myogenic transcription factors by Smad3. *Genes Dev*. 2001;15(22):2950-66.

143 : Darling TN, Skarulis MC, Steinberg SM, Marx SJ, Spiegel AM, Turner M. Multiple facial angiofibromas and collagenomas in patients with multiple endocrine neoplasia type 1. *Arch Dermatol*. 1997;133(7):853-7.

144 : Semple RK, Chatterjee VK, O'Rahilly S. PPAR gamma and human metabolic disease. *J Clin Invest*. 2006;116(3):581-9

145 : Heaney AP, Fernando M, Melmed S. PPAR-gamma receptor ligands : novel therapy for pituitary adenomas. *J Clin Invest*. 2003;111(9):1381-8.

146 : Messager M, Carriere C, Bertagna X, de Keyzer Y. RT-PCR analysis of corticotroph-associated genes expression in carcinoid tumours in the ectopic-ACTH syndrome. *Eur J Endocrinol*. 2006;154(1):159-66.

147 : Jochum W, Passegue E, Wagner EF. AP-1 in mouse development and tumorigenesis. *Oncogene*. 2001;20(19):2401-12.

148 : Naito J, Kaji H, Sowa H, Hendy GN, Sugimoto T, Chihara K. Menin suppresses osteoblast differentiation by antagonizing the AP-1 factor, JunD. *J Biol Chem*. 2005;280(6):4785-91.

149 : Krishnan V, Bryant HU, Macdougald OA. Regulation of bone mass by Wnt signaling. *J Clin Invest*. 2006;116(5):1202-9.

150 : Crabtree JS, Scacheri PC, Ward JM, Garrett-Beal L, Emmert-Buck MR, Edgemon KA, Lorang D, Libutti SK, Chandrasekharappa SC, Marx SJ, Spiegel AM, Collins FS. A mouse model of multiple endocrine neoplasia, type 1, develops multiple endocrine tumors. *Proc Natl Acad Sci U S A*. 2001;98(3):1118-23.

151 : Bertolino P, Radovanovic I, Casse H, Aguzzi A, Wang ZQ, Zhang CX. Genetic ablation of the tumor suppressor menin causes lethality at mid-gestation with defects in multiple organs. *Mech Dev*. 2003;120(5):549-60.

152 : Loffler KA, Biondi CA, Gartside M, Waring P, Stark M, Serewko-Auret MM, Muller HK, Hayward NK, Kay, GF. Broad tumor spectrum in a mouse model of multiple endocrine neoplasia type 1. *Int J Cancer*. 2007;120(2):259-67.

153 : Harding B, Lemos MC, Reed AA, Walls GV, Jeyabalan J, Bowl MR, Tateossian H, Sullivan N, Hough T, Fraser WD, Ansorge O, Cheeseman MT, Thakker RV. Multiple endocrine neoplasia type 1

knockout mice develop parathyroid, pancreatic, pituitary and adrenal tumours with hypercalcaemia, hypophosphataemia and hypercorticosteronaemia. *Endocr Relat Cancer*. 2009;16(4):1313-27.

154 : Engleka KA, Wu M, Zhang M, Antonucci NB, Epstein JA. Menin is required in cranial neural crest for palatogenesis and perinatal viability. *Dev Biol*. 2007;311(2):524-37.

155 : Kanazawa I, Canaff L, Abi Rafeh J, Angrula A, Li J, Riddle RC, Boraschi-Diaz I, Komarova SV, Clemens TL, Murshed M, Hendy GN. Osteoblast menin regulates bone mass in vivo. *J Biol Chem*. 2015;290(7):3910-24.

156 : Hendy, G.N., Abi-Rafeh, J., Canaff, L. & Troka, I. Osteoblast Menin and Bone Mass: Studies in Conditional Knockout Mice. *Osteoporosis International.* **28** (Suppl.1) p. S366; P593 (2017).

157 : 129S(FVB)Men1tm1.2Ctre/J.(n.d.). Retrieved April 5th 2018 from https://www.jax.org/strain/005109

158 : B6.Cg-Tg(Prrx1-Cre)1Cjt/J. (n.d.) Retrieved April 5th 2018 from https://www.jax.org/strain/005584

159 : B6.Cg-Tg(Sp7-tTA,tet0-EGFP/cre)1Amc/J. (n.d.) Retrieved April 5th 2018 from https://www.jax.org/strain/006361

160 : Bakker AD, Klein-Nulend J. Osteoblast isolation from murine calvaria and long bones. *Methods Mol Biol*. 2012; 816:19-29.

161 : Brown RA, Wiseman M, Chuo CB, Cheema U, Nazhat SN. Ultrarapid engineering of biomimetic materials and tissues: fabrication of nano- and microstructures by plastic compression. *Advanced Functional Mater.* 2005; 15:1762-1770.

162 : Abou Neel EA, Cheema U, Knowles JC, Brown RA, Nazhat SN. Use of multiple unconfined compression for control of collagen gel scaffold density and mechanical properties. *Soft Matter*. 2006; 2:986-992.

163 : Coyac BR, Chicatun F, Hoac B, Nelea V, Chaussain C, Nazhat SN, McKee MD. Mineralization of dense collagen hydrogel scaffolds by human pulp cells. *J Dent Res*. 2013;92(7):648-54.

164 : Dreijerink KMA, Groner AC, Vos ESM, Font-Tello A, Gu L, Chi D, Reyes J, Cook J, Lim E, Lin CY, de Laat W, Rao PK, Long HW, Brown M. Enhancer-mediated oncogenic function of the menin tumor suppressor in breast cancer. *Cell Rep*. 2017;18(10):2359-72.

165 : Malik R, Khan AP, Asangani IA, Cieslik M, Prensner JR, Wang X, Iyer MK, Jiang X, Borkin D, Escara-Wilke J, Stender R, Wu YM, Niknafs YS, Jing X, Qiao Y, Palanisamy N, Kunju LP, Krishnamurthy PM, Yocum AK, Mellacheruvu D, Nesvizhskii AI, Cao X, Dhanasekaran SM, Feng FY, Grembecka J, Cierpicki T, Chinnaiyan AM. Targeting the MLL complex in castration-resistant prostate cancer. *Nat Med*. 2015;21(4):344-52.

166 : Bitar M, Brown RA, Salih V, Kidane AG, Knowles JC, Nazhat SN. Effect of cell density on osteoblastic differentiation and matrix degradation of biomimetic dense collagen scaffolds. *Biomacromolecules*. 2008;9(1):129-35.

167 : Buxton PG, Bitar M, Gellynck K, Parkar M, Brown RA, Young AM, Knowles JC, Nazhat SN. Dense collagen matrix accelerates osteogenic differentiation and rescues the apoptotic response to MMP inhibition. *Bone*. 2008;43(2):377-85.

168 : Chicatun F, Pedraza CE, Ghezzi CE, Marelli B, Kaartinen MT, McKee MD, Nazhat SN. Osteoid-mimicking dense collagen/chitosan hybrid gels. *Biomacromolecules*. 2011;12(8):2946-56.

169 : Pedraza CE, Marelli B, Chicatun F, McKee MD, Nazhat SN. An in vitro assessment of a cell-containing collagenous extracellular matrix-like scaffold for bone tissue engineering. *Tissue Eng Part A*. 2010;16(3):781-93.

170 : van den Bos T, Speijer D, Bank RA, Bromme D, Everts V. Differences in matrix composition between calvaria and long bone in mice suggest differences in biomechanical properties and resorption: Special emphasis on collagen. *Bone*. 2008;43(3):459-68.

171 : Troka I, Griffanti G, Nazhat SN, Hendy GN. Deletion of Menin Early in the Osteoblast Lineage Affects Mineralization of Dense Collagen Gels by Primary Osteoblasts. [abstract]. In: 24th Canadian Connective Tissue Conference; 23-25 May, 2018; Toronto ON.

172 : Sarac F. & Saygili F. Causes of high bone alkaline phosphatase. *Biotechnology & Biotechnological Equipment*. 2007; 21:2 194-197.

173 : Ross PD, Knowlton W. Rapid bone loss is associated with increased levels of biochemical markers. *J Bone Miner Res*. 1998;13(2):297-302.

174 : Sonia A Talwar. Bone Markers in Osteoporosis. In: Medscape – Drugs & Diseases. 2017. Retrieved April 5th from https://emedicine.medscape.com/article/128567-overview

175 : Malluche HH, Porter DS, Monier-Faugere MC, Mawad H, Pienkowski D. Differences in bone quality in low- and high-turnover renal osteodystrophy. *J Am Soc Nephrol*. 2012;23(3):525-32.

176 : Ng AH, Hercz G, Kandel R, Grynpas MD. Association between fluoride, magnesium, aluminum and bone quality in renal osteodystrophy. *Bone*. 2004;34(1):216-24.

177 : Troka I, Abi-Rafeh J, Canaff L, Boraschi-Diaz I, Komarova S, Hendy GN. Effect of menin early deletion in the osteoblast lineage in conditional knockout mice. [abstract]. In: 2018 Metabolic Disorders and Complications Research Day; 29 March, 2018; Montreal Qc.

178 : Teti A. Mechanisms of osteoclast-dependent bone formation. *Bonekey Rep*. 2013;2:449.

179 : Bellido T. Osteocyte-driven bone remodeling. *Calcif Tissue Int*. 2014;94(1):25-34.

180 : Wright HL, McCarthy HS, Middleton J, Marshall MJ. RANK, RANKL and osteoprotegerin in bone biology and disease. *Curr Rev Musculoskelet Med*. 2009;2(1):56-64.

181 : Nakashima T, Hayashi M, Fukunaga T, Kurata K, Oh-Hora M, Feng JQ, Bonewald LF, Kodama T, Wutz A, Wagner EF, Penninger JM, Takayanagi H. Evidence for osteocyte regulation of bone homeostasis through RANKL expression. *Nat Med*. 2011;17(10):1231-4.

182 : Xiong J, Onal M, Jilka RL, Weinstein RS, Manolagas SC, O'Brien CA. Matrix-embedded cells control osteoclast formation. *Nat Med*. 2011;17(10):1235-41.

183 : Gesta S, Tseng YH, Kahn CR. Developmental origin of fat: tracking obesity to its source. *Cell*. 2007;131(2):242-56.

184 : Rahman S, Lu Y, Czernik PJ, Rosen CJ, Enerback S, Lecka-Czernik B. Inducible brown adipose tissue, or beige fat, is anabolic for the skeleton. *Endocrinology*. 2013;154(8):2687-701.

185 : Motyl KJ, Bishop KA, DeMambro VE, Bornstein SA, Le P, Kawai M, Lotinun S, Horowitz MC, Baron R, Bouxsein ML, Rosen CJ. Altered thermogenesis and impaired bone remodeling in Misty mice. *J Bone Miner Res*. 2013;28(9):1885-97.

186 : Ponrartana S, Aggabao PC, Hu HH, Aldrovandi GM, Wren TA, Gilsanz V. Brown adipose tissue and its relationship to bone structure in pediatric patients. *J Clin Endocrinol Metab*. 2012;97(8):2693-8.

187 : Bredella MA, Fazeli PK, Freedman LM, Calder G, Lee H, Rosen CJ, Kilbanski A. Young women with cold-activated brown adipose tissue have higher bone mineral density and lower Pref-1 than women without brown adipose tissue: a study in women with anorexia nervosa, women recovered from anorexia nervosa, and normal-weight women. *J Clin Endocrinol Metab*. 2012;97(4): E584-90.

188 : Nedergaard J, Golozoubova V, Matthias A, Asadi A, Jacobsson A, Cannon B. UCP1: the only protein able to mediate adaptive non-shivering thermogenesis and metabolic inefficiency. *Biochim Biophys Acta*. 2001;1504(1):82-106.

189 : Nguyen AD, Lee NJ, Wee NKY, Zhang L, Enriquez RF, Khor EC, Nie T, Wu D, Sainsbury A, Baldock PA, Herzog H. Uncoupling protein-1 is protective of bone mass under mild cold stress conditions. *Bone*. 2018; 106:167-78.

190 : Liang H, Ward WF. PGC-1alpha: a key regulator of energy metabolism. *Adv Physiol Educ*. 2006;30(4):145-51.

191 : Khan MP, Singh AK, Joharapurkar AA, Yadav M, Shree S, Kumar H, Gurjar A, Mishra JS, Tiwari MC, Nagar GK, Kumar S, Ramachandran R, Sharan A, Jain MR, Trivedi AK, Maurya R, Godbole MM, Gayen JR, Sanyal S, Chattopadhyay N. Pathophysiological Mechanism of Bone Loss in Type 2 Diabetes Involves Inverse Regulation of Osteoblast Function by PGC-1alpha and Skeletal Muscle Atrogenes: AdipoR1 as a Potential Target for Reversing Diabetes-Induced Osteopenia. *Diabetes*. 2015;64(7):2609-23.

192 : Seale P. Transcriptional Regulatory Circuits Controlling Brown Fat Development and Activation. *Diabetes*. 2015;64(7):2369-75.

193 : Kaji H. Interaction between Muscle and Bone. *J Bone Metab*. 2014;21(1):29-40.

194 : Liu P, Lee S, Knoll J, Rauch A, Ostermay S, Luther J, Malkusch N, Lerner UH, Zaiss MM, Neven M, Wittig R, Rauner M, David JP, Bertolino P, Zhang CX, Tuckermann JP. Loss of menin in osteoblast lineage affects osteocyte-osteoclast crosstalk causing osteoporosis. *Cell Death Differ*. 2017;24(4):672-82.

195 : Miki Y, Suzuki T, Nagasaki S, Hata S, Akahira J, Sasano H. Comparative effects of raloxifene, tamoxifen and estradiol on human osteoblasts in vitro : estrogen receptor dependent or independent pathways of raloxifene. *J Steroid Biochem Mol Biol*. 2009;113(3-5):281-9.

196 : Lee JH, Kim HN, Kim KO, Jin WJ, Lee S, Kim HH, Jin WJ, Lee S, Kim HH, Ha H, Lee ZH. CXCL10 promotes osteolytic bone metastasis by enhancing cancer outgrowth and osteoclastogenesis. *Cancer Res*. 2012;72(13):3175-86.

197 : Shahnazari M, Chu V, Wronski TJ, Nissenson RA, Halloran BP. CXCL12/CXCR4 signaling in the osteoblast regulates the mesenchymal stem cell and osteoclast lineage populations. *FASEB J*. 2013;27(9):3505-13.

198 : Grassi F, Cristino S, Toneguzzi S, Piacentini A, Facchini A, Lisignoli G. CXCL12 chemokine up-regulates bone resorption and MMP-9 release by human osteoclasts: CXCL12 levels are increased in synovial and bone tissue of rheumatoid arthritis patients. *J Cell Physiol*. 2004;199(2):244-51.

199 : Lee S, Liu P, Teinturier R, Jakob J, Tschaffon M, Tasdogan A, Wittig R, Hoeller S, Baumhoer D, Frappart L, Vettorazzi S, Bertolino P, Zhang C, Tuckermann J. Deletion of Menin in craniofacial osteogenic cells in mice elicits development of mandibular ossifying fibroma. *Oncogene*. 2018 ;37(5):616-26.

200 : Vasikaran S, Eastell R, Bruyere O, Foldes AJ, Garnero P, Griesmacher A, McClung M, Morris HA, Silverman S, Trenti T, Wahl DA, Cooper C, Kanis JA. Markers of bone turnover for the prediction of fracture risk and monitoring of osteoporosis treatment: a need for international reference standards. *Osteoporos Int*. 2011;22(2):391-420.

201 Shetty S, Kapoor N, Bondu JD, Thomas N, Paul TV. Bone turnover markers: Emerging tool in the management of osteoporosis. *Indian J Endocrinol Metab*. 2016;20(6):846-52.

202 : Holmen SL, Zylstra CR, Mukherjee A, Sigler RE, Faugere MC, Bouxsein ML, Deng L, Clemens TL, Williams BO. Essential role of beta-catenin in postnatal bone acquisition. *J Biol Chem*. 2005;280(22):21162-8.

203 : Kramer I, Halleux C, Keller H, Pegurri M, Gooi JH, Weber PB, Feng JQ, Bonewald LF, Kneissel M. Osteocyte Wnt/beta-catenin signaling is required for normal bone homeostasis. *Mol Cell Biol*. 2010;30(12):3071-85.

204 : Pederson L, Ruan M, Westendorf JJ, Khosla S, Oursler MJ. Regulation of bone formation by osteoclasts involves Wnt/BMP signaling and the chemokine sphingosine-1-phosphate. *Proc Natl Acad Sci U S A*. 2008;105(52):20764-9.

205 : Qin Y, Peng Y, Zhao W, Pan J, Ksiezak-Reding H, Cardozo C, Wu Y, Divieti Pajevic P, Bonewald LF, Bauman WA, Qin W. Myostatin inhibits osteoblastic differentiation by suppressing osteocyte-derived exosomal microRNA-218 : A novel mechanism in muscle-bone communication. *J Biol Chem*. 2017;292(26):11021-33.

206 : Venuti JM, Morris JH, Vivian JL, Olson EN, Klein WH. Myogenin is required for late but not early aspects of myogenesis during mouse development. *J Cell Biol*. 1995;128(4):563-76.